

ADVANCING PHOTO-CLICK CHEMISTRY TOWARDS MACROCYCLIZATION AND SEQUENCE-DEFINED OLIGOMERS

by

SHUBHAM SHARMA

(Under the Direction of VLADIMIR POPIK AND SERGIY MINKO)

ABSTRACT

Nature uses sequence-defined (having a precise sequence of units) monodisperse (same molecular weight) polymers for the data storage and transfer (DNA, RNA), for the control of properties and structure (proteins), for the efficient catalysis of various reactions (enzymes), and many more. However, these bio-macromolecules have limited stability and lack chemical and structural diversity. We have developed photo-SPAAC ligation approach to the bulk synthesis of sequence-defined polymers. The trifunctional monomer, containing photo-caged cyclooctyne, azide group, and a moiety allowing the attachment of various functionalities (e.g., dye, catalysts, enzymes, etc.). Photo-activation of the cyclooctyne at the terminus of the growing chain allows for the attachment of the next monomer via quantitative and fast SPAAC reaction. We have demonstrated the purification-free synthesis of two pentamers sequences.

INDEX WORDS: photo-SPAAC, SPAAC, Cyclooctynes, Sequence defined oligomers

**ADVANCING PHOTO-CLICK CHEMISTRY TOWARDS
MACROCYCLIZATION AND SEQUENCE-DEFINED OLIGOMERS**

by

SHUBHAM SHARMA

BS-MS, IISER BHOPAL, INDIA 2014

A Dissertation Submitted to the Graduate Faculty of The University of Georgia in Partial
Fulfillment of the Requirements for the Degree

DOCTOR OF PHILOSOPHY

ATHENS, GEORGIA

2022

© 2022

SHUBHAM SHARMA

All Rights Reserved

**ADVANCING PHOTO-CLICK CHEMISTRY TOWARDS
MACROCYCLIZATION AND SEQUENCE-DEFINED OLIGOMERS**

by

SHUBHAM SHARMA

Major Professor:	Vladimir Popik Sergiy Minko
Committee:	Eric Ferreira Robert Phillips

Electronic Version Approved:

Ron Walcott
Vice Provost for Graduate Education and Dean of the Graduate School
The University of Georgia
August 2022

DEDICATION

I dedicate my dissertation to my mother, Mrs. Saroj Sharma

TABLE OF CONTENTS

	Page
CHAPTER	
1 Literature Review.....	1
1.1 Light Induced Click Reactions.....	1
1.2 Introduction to Sequence Defined Oligomers.....	5
1.3 Introduction to Macrocyclization.....	12
2 Synthesis of Macrocycles via PhotoClick Chemistry	15
2.1 Results and Discussion	15
3 Synthesis of Sequence Defined Oligomers via Photo-Click Chemistry	21
3.1 Results and Discussion	21
4 Experimental Data	30
4.1 Synthesis	30
4.2 Kinetics data.....	41
4.3 NMR Data	43
4.4 Mass Data	69
REFERENCES	82

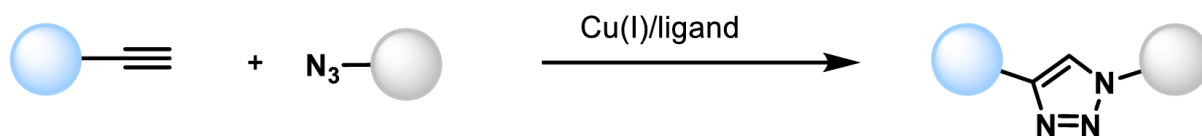
CHAPTER 1

LITERATURE REVIEW

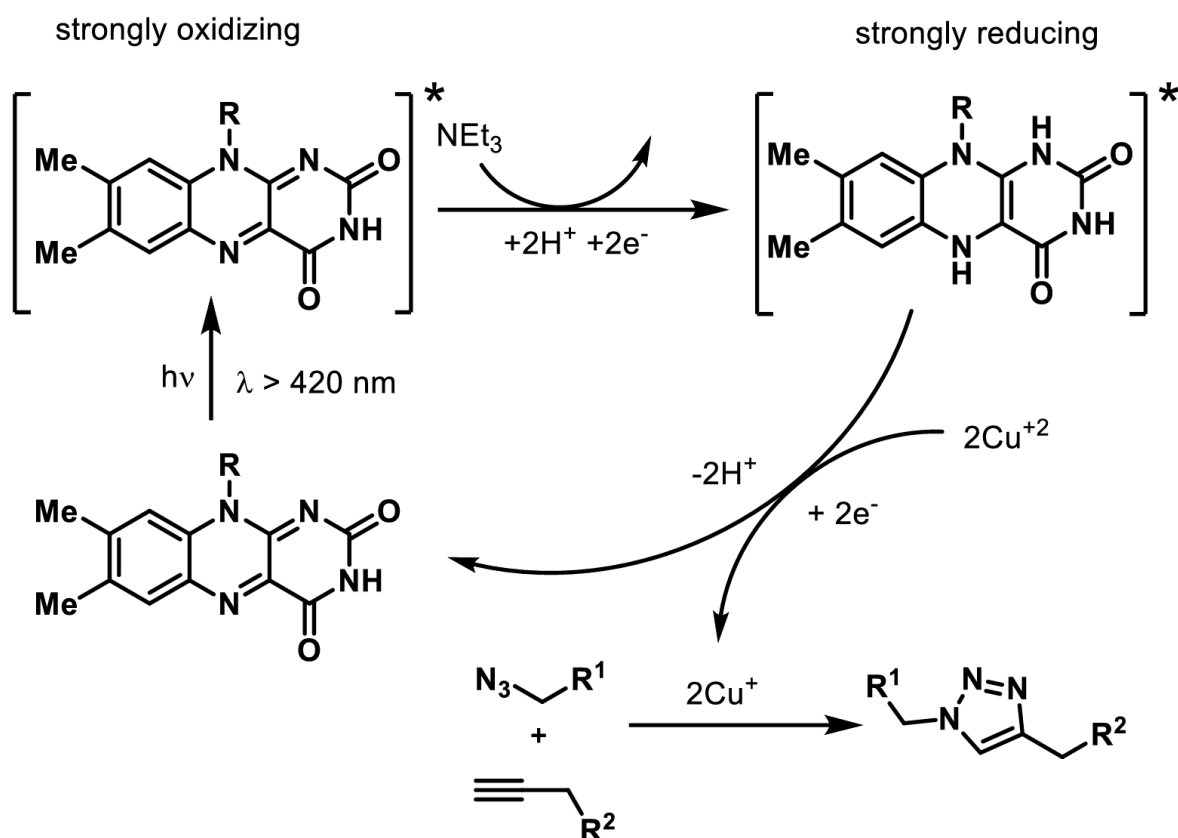
1.1 Light Induced Click Reactions

The Cu(I)-catalyzed azide–alkyne cycloaddition (CuAAC) discovered by Sharpless¹ and Meldal² has shown its application in biomolecular ligation, combinatorial synthesis, medicinal chemistry, surface functionalization, and polymer synthesis. Cu(I) catalyzes CuAACs, which is generally produced from Cu(II) salts through, reduction, electrochemical generation^{3, 4} and photochemical approaches⁵ along with reducing agents as Cu(I) is not very stable. Photochemical generation of Cu(I) provides more control over reaction as reaction can be stopped anytime by bubbling air to oxidize Cu(I) into Cu(II). Photochemical generation of Cu(I) can be done by direct photolysis of Cu(II) catalytic system or indirectly via photochemically generation of reducing agent. The first example of photo CuAAC was shown through indirect approach by photoirradiation of riboflavin tetraacetate in the presence of Et₃N to convert into flavin, which reduces Cu(II) to Cu(I).⁵ The first example of direct approach was shown by UV/vis irradiation of CuCl₂ in the presence of the PMDETA ligand by Yagci and co-workers.⁶ After that huge array of copper catalysts including CuCl₂·2H₂O/sodium benzoate⁷, copper(II)(tris(2-aminoethyl)-amine) ketoprofenate^{8, 9}, copper(II)(N,N'-dimethylethylenediamine) ketoprofenate¹⁰, and others^{11, 12} are developed for photoinduced CuAAC. These catalysts can be deactivated by bubbling air and can be reactivated by bubbling inert gas (by removing oxygen). The reversible nature of these catalyst gave this reaction a temporal control and found many applications in material chemistry.

a)



b)



c)

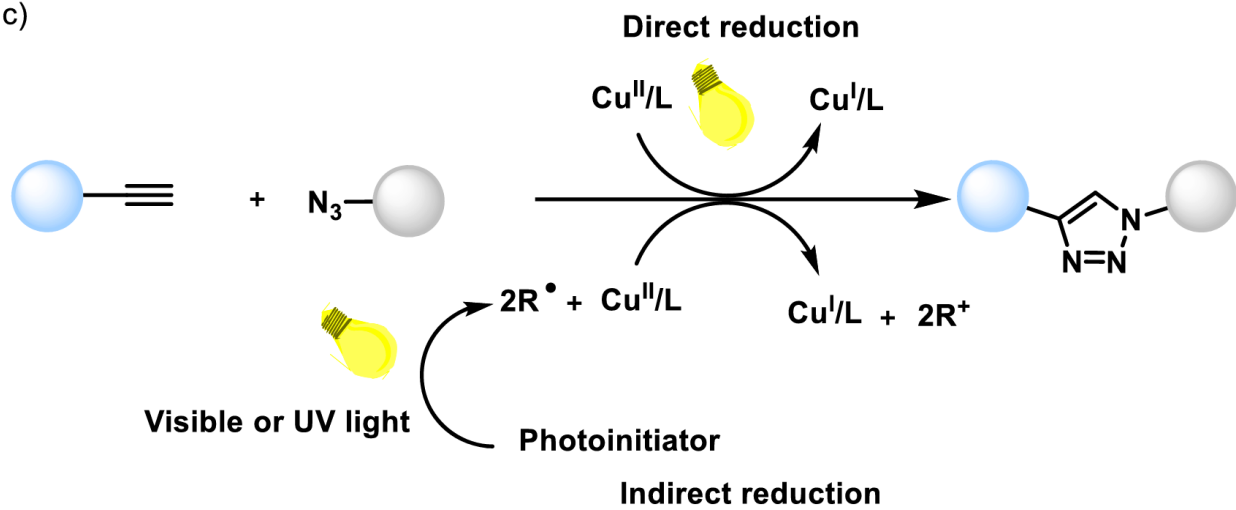


Figure 1. a) Schematic of CuAAC, b) photo-CuAAC via indirect approach using riboflavin⁵, c)
photo-CuAAC via direct approach¹³

However, the toxicity of copper and catalyst removal from the polymer system possess a challenge to use CuAAC reaction in many applications. To tackle this problem strain promoted azide–alkyne cycloaddition (SPAAC) reaction was developed as it doesn't need any catalyst. The first example was shown by Bertozzi and coworkers using cyclooctyne and azide.¹⁴ Due to the importance of SPAAC reaction, many strained cyclooctynes were developed including fluorinated cyclooctynes, dibenzocyclooctynes (DIBO), and thiacycloalkynes.¹⁵⁻¹⁷

First report of photo-SPAAC was reported by Popik and co-workers by developing photo protected DIBO precursors using cyclopropanones.^{18, 19} These strained cyclopropanone protected dibenzocyclooctynes (photo-DIBO) showed excellent thermal stability and survives boiling water and doesn't react with azides. Deprotection of photo-DIBO can be easily done by irradiating it with 350 nm light and then DIBO reacts with azides to form triazole product. Photo-DIBO has been successfully employed in biological environment such as glycan labeling, cell labeling, and cell sorting.²⁰⁻²² This reaction has shown its importance in material chemistry as it has been applied to brush polymers, surface functionalization, hydrogel derivatization and nanoparticles derivatization.²³⁻²⁶

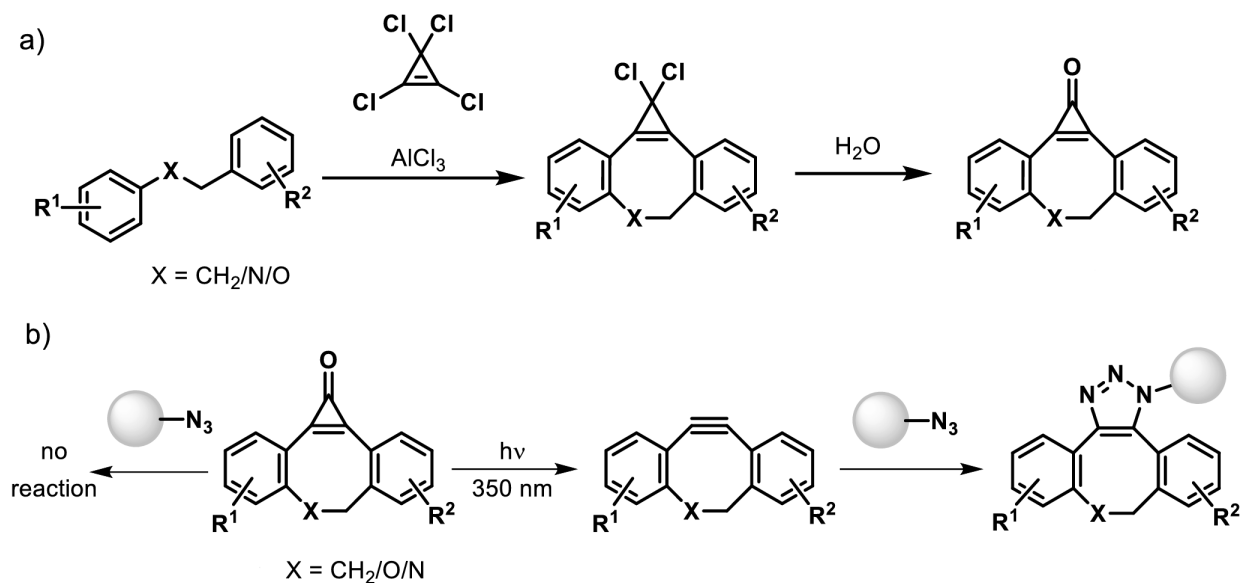


Figure 2. a) Synthesis of cyclopropenone masked strained cyclooctyne, b) photo-DIBO azide reaction scheme¹³

Another important substrate for photo-SPAAC reaction was developed by Popik group using DIBOD. DIBOD is a bis-alkyne crosslinker and can be used for double SPAAC reactions.²⁷ It has limited aqueous stability hence limited applications. Popik and co workers protected both alkynes of DIBOD with cyclopropenones and developed a new reagent, photo-DIBOD with excellent stability even with an anti-aromatic structure.²⁸ Moreover, cyclopropenones can sequentially be removed from photo-DIBOD to crosslink two different azides.²⁹ This significantly broadens the utility of photo-DIBOD as compared to DIBOD.

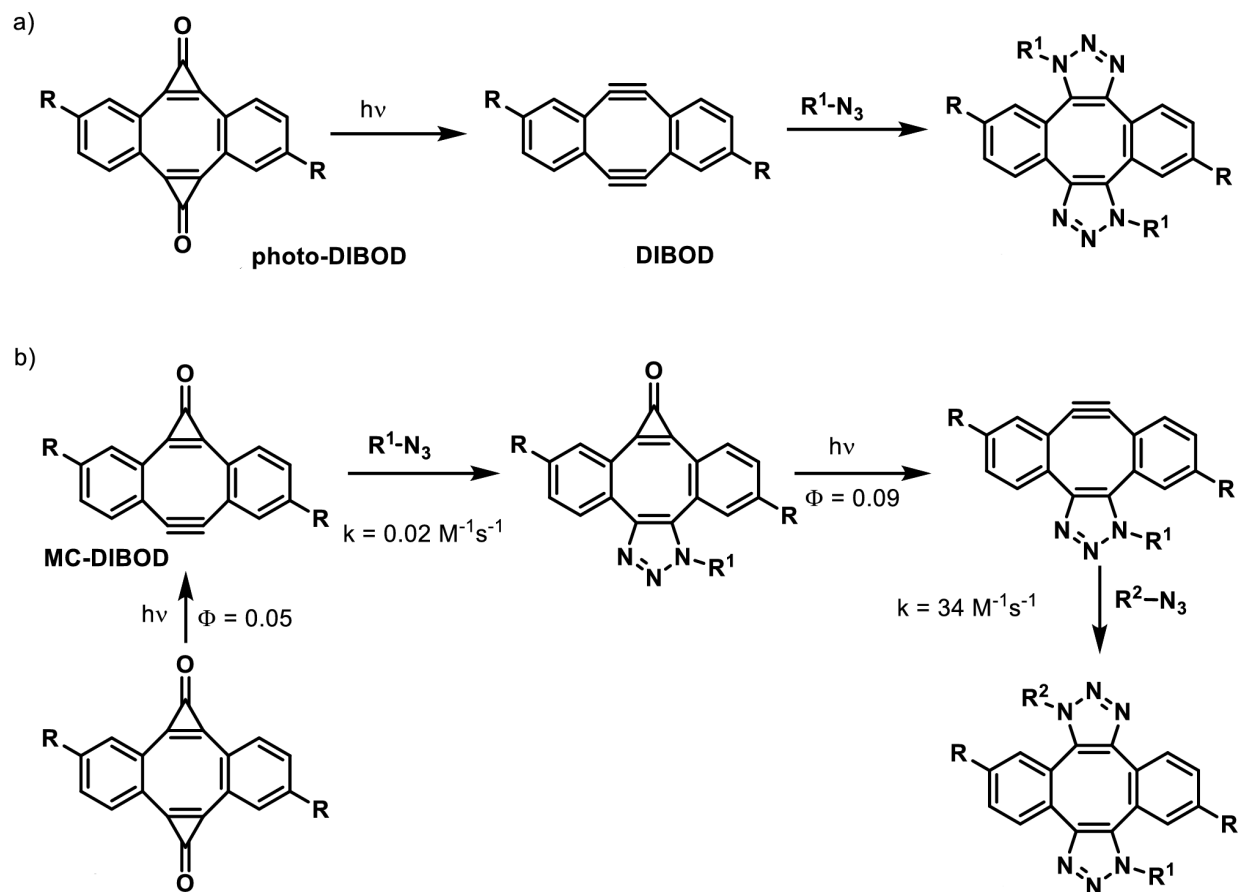


Figure 3. a) photo-DIBOD to DIBOD, b) photo-DIBOD to MC-DIBOD¹³

1.2 Introduction to Sequence Defined Oligomers

Over the last decade, a new class of polymers called sequence-controlled polymers has emerged with the advent of controlled/living radical polymerization. These polymers have a specific sequence repeated multiple times with high precision. The simplest example is a block copolymer which has a repeated unit of two monomers. Due to sequence incorporation, the polymer was able to combine different functionalities which made them a material with distinct physical and chemical properties. These new properties open a range of applications in materials engineering for coatings, sensors, separation technologies, catalysis, medical applications, and many more applications.³⁰ However, these materials have not yet reached the potential of their biological

counterparts. Nature uses sequence-defined polymers for data storage and transfer (DNA, RNA), for controlling properties and structure (proteins), and for the efficient catalysis of various reactions (enzymes).

To bridge the gap between biomacromolecules and synthetic macromolecules, several different approaches were developed to synthesize monodisperse material, known as sequence-defined (SD) oligomers. The most common strategy is to build the sequence step by step. This strategy was used to build oligopeptides, but the complexity of purifications increased with chain length. Also, the yield of the macromolecule decreased with the growing sequence. The discovery of solid-phase synthesis greatly simplified the purification method³¹ and automation of this technique has reduced the cost of synthesis to make oligopeptides readily available.³² A similar approach has been successfully implemented for DNA and RNA synthesis.³³ However, bio-macromolecules have limited stability as proteins can be degraded by change in temperature, pH and by oxidative reactions.³⁴ Also, biomacromolecules have limited chemical diversity as protein has 20 amino acids and DNA has just 4 bases. Developing methods to synthesize SD oligomers/polymers which can incorporate diverse chemical and physical properties can generate novel materials with tunable properties. SD oligomers can have several potential applications in catalysis, data storage, energy and medicine. Several novel approaches using liquid phase and solid support synthesis based on fast and high yield chemical reactions were reported for the synthesis of SD oligomers.

Thomas Junkers et al. reported a photo-induced copper mediated radical polymerization (photoCMP) single unit monomer insertion (SUMI) reaction-based strategy.² They used methyl acrylate (MA) as monomer and ethyl 2-bromoisobutyrate (EBiB) as initiator. First methyl acrylate was inserted into a ethyl 2-bromoisobutyrate (EBiB) initiator and then for all further SUMI reactions, the following molar ratios were applied: $[M] : [I] : [CuBr_2] : [ME6TREN] =$

1 : 1 : 0.012 : 0.084. They were able to generate a library of pentamers with yield ranging from 2-10% as shown in figure 4. Due to the use of copper catalyst and ligand, they needed to purify at each step, which decreased the yield and increased the work and cost of this material.³⁵

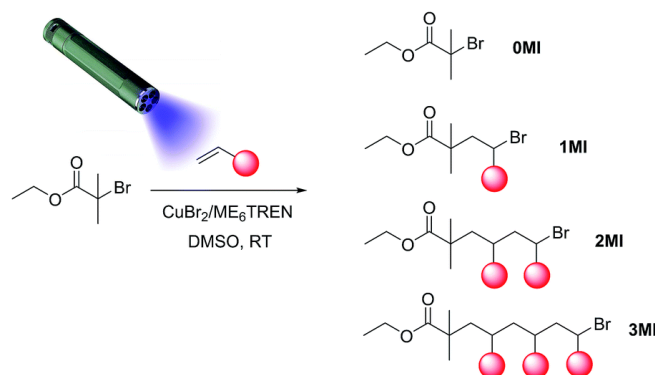


Figure 4. Sequence defined oligomerization using photoCMP SUMI reaction

Several liquid phase-based approaches were reported by using multicomponent reactions Ugi³⁶ and Passernini^{37, 38}, and fluorine tagged hydroxyproline building block and purification by fluorous silica gel³⁹. To simplify the purification, solid support bound thio-acetone based monomer with two iterative process is shown to synthesize SD oligomers.⁴⁰ 2-chlorotrityl chloride resin was loaded with a cyclic thioester linker bearing carboxylic acid to form the initiator for the iterative process. The initiator was reacted with 50 eq of amine to put the functional handle on the sequence and for chain extension, 10 eq of thioester linker was added in the reaction mixture as shown in Figure 5.

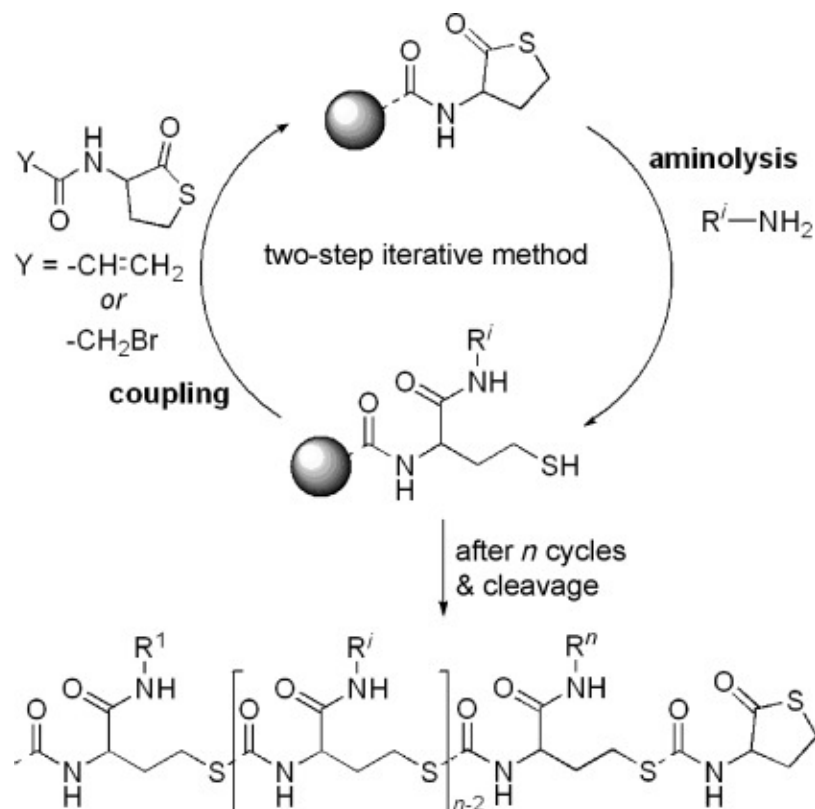


Figure 5. Resin-bound thioacetone based approach for Sequence defined oligomers

This method was used to build sequences till pentamer without any protecting group. One of the problems encountered was the formation of disulfide bonds after aminolysis which terminated the chain extension. Disulfide bonds were partially reduced by using dimethylphenylphosphine. By proving the potential of thioester-based chemistry for the formation of SD oligomers, they developed an automated synthesis procedure by tweaking their strategy to build longer chains. Ethanolamine was used to open the thioester ring and the released thiol was reacted with functionalized acrylate to introduce the functional group in the oligomers as shown in Figure 6.⁴¹

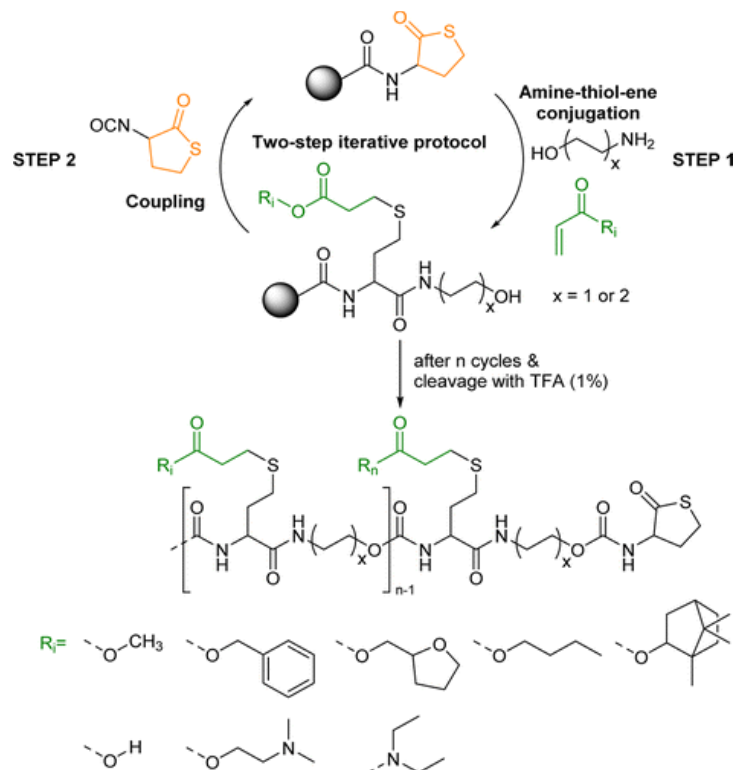


Figure 6. Automated synthesis of sequence defined oligomers

They were able to successfully synthesize five decamer sequences by using 10 eq of ethanolamine and 20 eq of acrylate at every step to derive their reaction to completion. Click Chemistry has also been used to synthesize SD oligomers particularly Copper-catalyzed azide-alkyne cycloaddition (CuAAC). Dr. Luftz has used AB + CD approach where A = acid, B = alkyne, C = amine, D = azide. The sequence was elongated by using copper click chemistry and amide bond formation. They were able to synthesize eight trimers by using the iterative synthesis as shown below in Figure 7.⁴² These monomers can be used for data storing as they can be interfered by mass spectrometry.

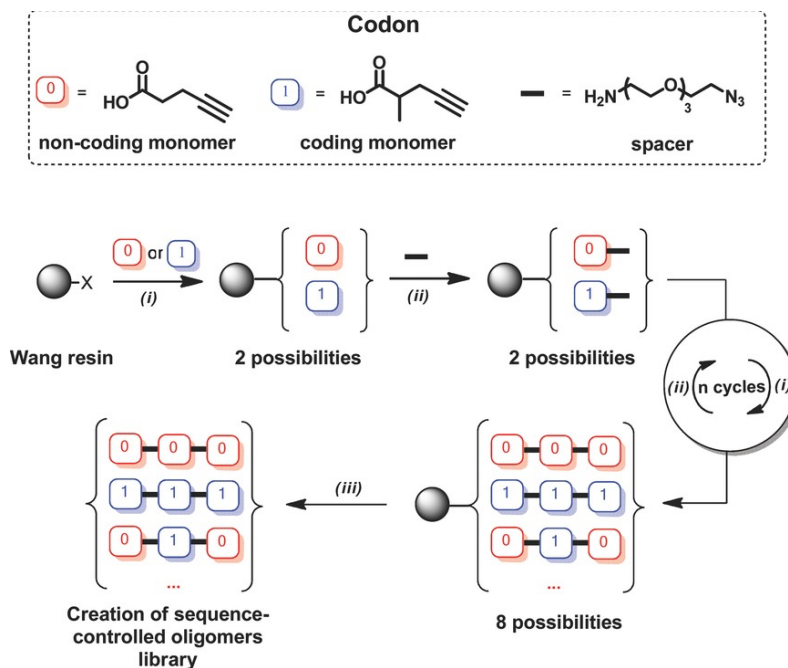


Figure 7. AB+CD Approach to sequence defined oligomers

In another example shown by the same group, they used modified amino acid, propargyl amine and azido hexanoic acid to synthesize amino acid-based SD oligomers. By this approach, they synthesized polypeptides with different spacers between amino acids. Although they generated a library of synthetic amino acid oligomers for every addition of monomer, three reactions were required as shown in Figure 5.⁴³

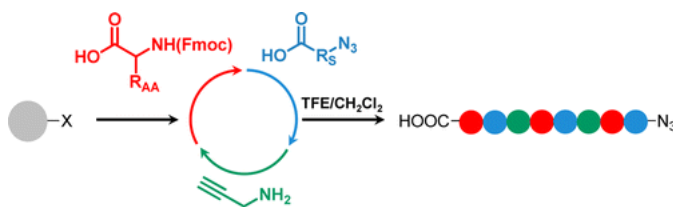
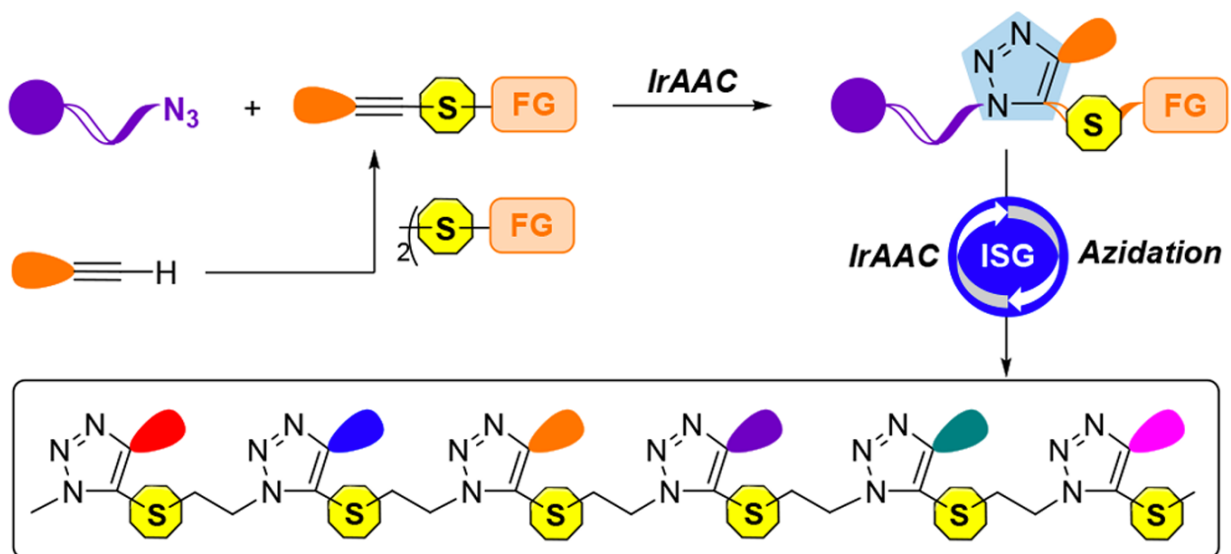


Figure 8. Synthetic amino acid-based sequence define oligomerization

Recently, Ding and coworkers have shown new strategies using Iridium based click chemistry between azides and thioalkynes (IrAAC).⁴⁴ In their first approach they encoded thioalkynes with different groups to build their SD oligomers.⁴⁵ The authors showed robustness of their method by synthesizing a hexamer using this technique as shown in Figure 9a. In another publication, Ding group encoded two functional groups in thioalkyne and used similar IrAAC strategy to build SD oligomers.⁴⁶ The advantage of this strategy is that it encodes two different molecules with one monomer addition, making it more economical as compared to the first one as shown in Figure 9b.



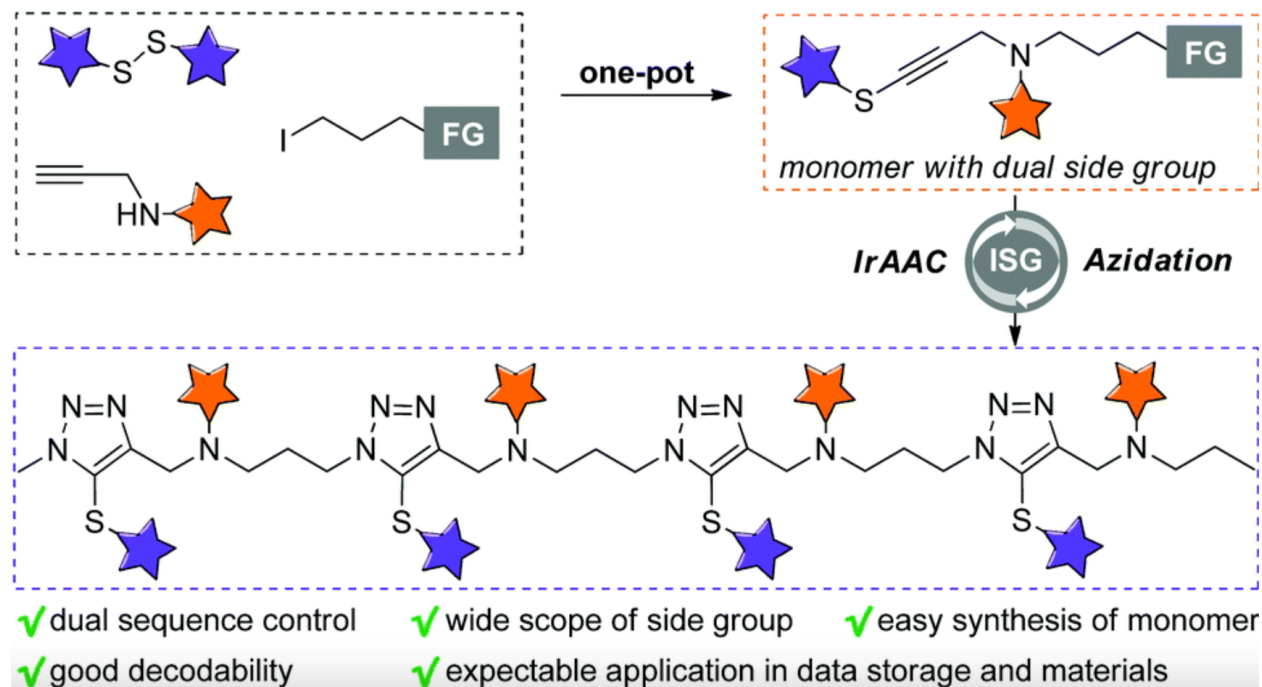


Figure 9. a) IrAAC based SD oligomer synthesis with one encoded molecule, b) IrAAC based

SD oligomer synthesis strategy with two encoded molecule

The reported methods used multiple equivalents of catalysts and/or coupling reagents to derive the reaction to completion. These methods have the general problem of build-up of unreacted reagents and by-products with each step of monomer addition hence need purification at every step. Solid phase supported synthesis has shown to simplify the purification, but it limits the amount of material generated. Also, it is difficult to monitor real time reaction kinetics and progress as some material must be cleaved from the solid support.

1.3 Introduction to Macrocyclization

Macrocycles are large cyclic structures consisting of twelve or larger member rings. They are found in nature with unique drug like activity, which led to development of new drugs for example erythromycin and rapamycin.⁴⁷ Another application of macrocycles was found in supramolecular

chemistry where due to preorganized cavities and multivalent binding sites, they were used in molecular recognition^{48, 49} and sensing.^{50, 51} Molecular device and machines^{52, 53}, stimuli-responsive materials and drug delivery systems are some of applications of functionalized macrocycles reported in literature.⁵⁴ However, design and synthesis of macrocycles remains a challenge. In most of the macrocyclic synthesis, yields are generally low as high dilution conditions were used to avoid the step growth polymerization.⁵⁵ Copper click azide alkyne cycloaddition (CuAAC) has shown great potential for synthesizing macrocycles.⁵⁶ Fast reaction rates and mild reaction conditions provide an efficient way of synthesizing macrocycles. Moreover, triazole ring has polar C-H and N-H bonds which enhances binding efficiency.⁵⁷ The use of copper click chemistry can be problematic as copper binds to the multiple electron donor and multivalent binding sites in macrocycle precursors.^{58, 59} Strain Promoted Azide Alkyne Cycloaddition (SPAAC) reaction can be better alternative for macrocyclization as compared to copper click chemistry as it does not require any catalyst. Multiple reports have shown that SPAAC reactions yield cyclic structures even with as high concentration as 0.5 M.⁶⁰ Ke Zhang and coworkers explored polymerization using DIBOD and bis-azides. When DIBOD/azide \sim 0.83, reaction produce low molecular weight cyclic products whereas with DIBOD/azide \sim 1.2 reaction produces high molecular weight polymers and cyclic structures as shown in figure 10.⁶¹ Same group explored similar reaction with either excess of bis-azide or DIBOD. With excess of azide, reaction produces low molecular weight polymer which can be cyclized using excess of DIBOD in highly dilute conditions as shown in figure 11.⁶⁰ Similar results are shown by Adronov and coworkers using bis-ADIBO and bis-azide, which produces \sim 40% cyclic structure.⁶² However, due to fast reaction rates it is difficult to form one major product or isolate them from multiple cyclic compounds as well as polymers.^{61, 62} In current methods, due to the need of activation step

of the bifunctional molecule, it polymerizes in concentrated solution and hence diluted conditions are needed. This effect both yield and cost of macrocycle. There is a need of high yielding and mild condition for synthesizing macrocycles.

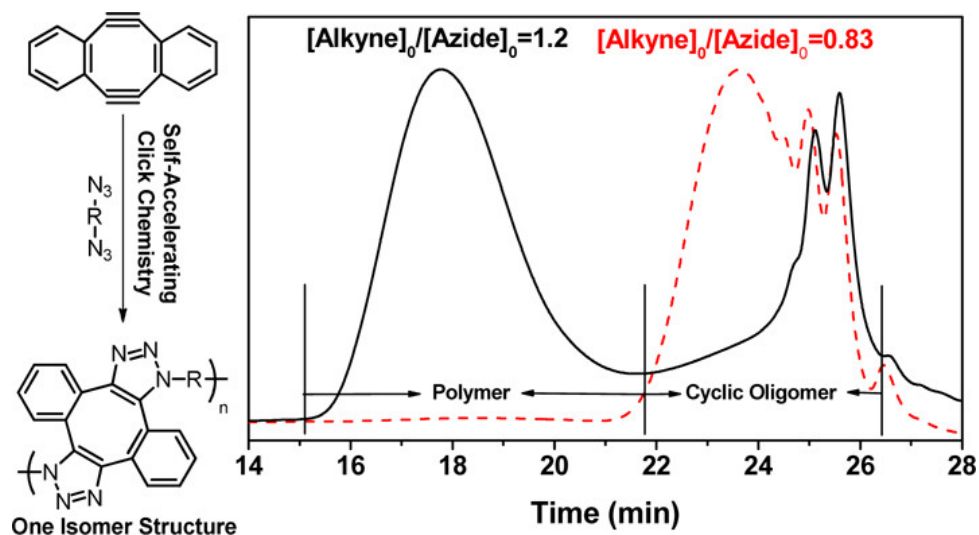


Figure 10. Synthesis of cyclic polymer using DIBOD/azide ~ 0.83 and DIBOD/azide ~ 1.2

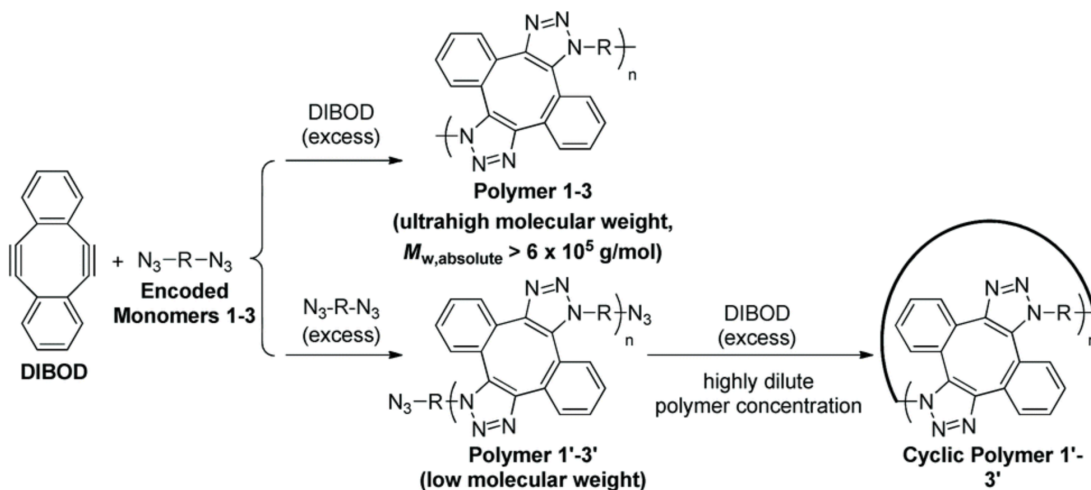


Figure 11. Synthesis of cyclic polymer using either excess DIBOD and excess azide

CHAPTER 2

Synthesis of Macrocycles via PhotoClick Chemistry

2.1 Results and Discussions

Herein we report a purification free method for synthesizing macrocycles using SPAAC. We first investigated one component system with Photo-DIBO and azide group as bifunctional monomer. We were able to cyclize the fifty-member ring as shown in Figure 12. photo-DIBO absorb UV irradiation at 350 nm and unmasked into DIBO.⁶³ Upon irradiation, bifunctional monomer quantitatively converted into 50 member monomer macrocycle at 30 mM and 60 mM concentration as shown in Figure 12. No dimer and higher oligomer macrocycle or open chain oligomers were observed.

To understand the kinetics of cyclization, we followed consumption of alkyne at 324 nm by using UV-Vis spectroscopy in methanol and dichloromethane. Rate constant was obtained as $9.7\text{e}^{-4}\text{ s}^{-1}$ in DCM and 0.138 s^{-1} in methanol by fitting the disappearance curve of the alkyne with first order decay kinetic equation as shown in Figure 12. These results agree with the general trend observed in SPAAC reactions.¹⁶

We want to explore this cyclization at higher concentration to find out the maximum concentration at which we can form macrocycles, but direct increment of concentration didn't work as the formation of alkyne is the rate limiting step. For 60 mM concentration, it took 8 min irradiation time for complete deprotection of the alkyne which suggested that the effective concentration of alkyne in our system is likely much below 60 mM. To increase the effective concentration of alkyne, we developed an emulsions-based system to increase the local concentration of our

monomer at a lower overall concentration of the compound in the emulsion. We used water dichloromethane system to achieve 120 mM concentration of alkyne which produced monomer

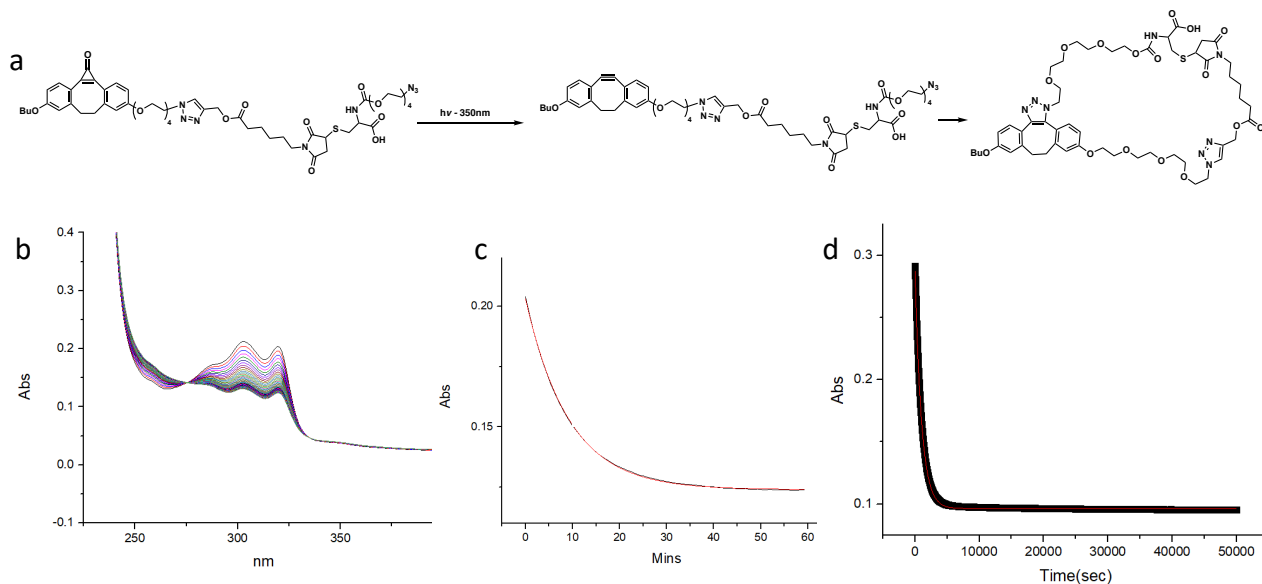


Figure 12. Photo-DIBO-Azide cyclization. a) Reaction scheme of cyclization, b) UV-Vis spectra of cyclization in methanol, c) Kinetics plot of cyclization at 10 uM in methanol, d) Kinetics plot of cyclization at 10 uM in dichloromethane

cyclization. We also irradiated neat monomer on glass slide incubated for 12 hours and then washed with 1 M sodium azide to quench unreacted alkynes and to our surprise, MALDI data shows only monomer cycle. This proves the robustness of our system to produce selectively macrocycles at much higher concentration than reported in literature.

We further explored small macrocycle formation with MC-DIBOT-TEG-N₃ cyclization (Figure 13a) and photo-DIBOD with Bis-TEG-Azide (Figure 13b) shows the similar results with efficient and quantitative conversion in macrocycles.

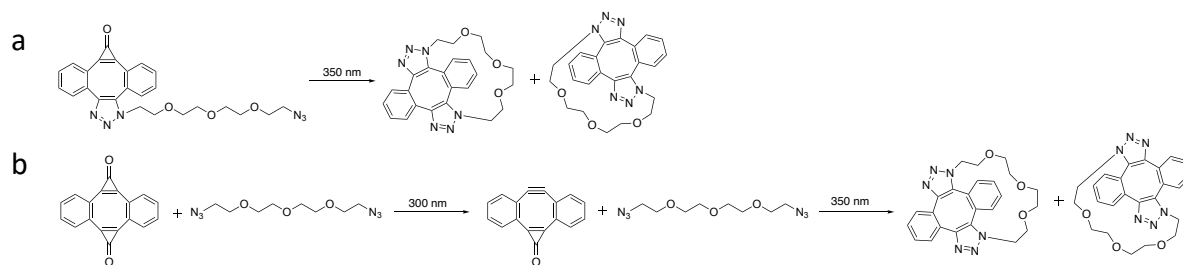
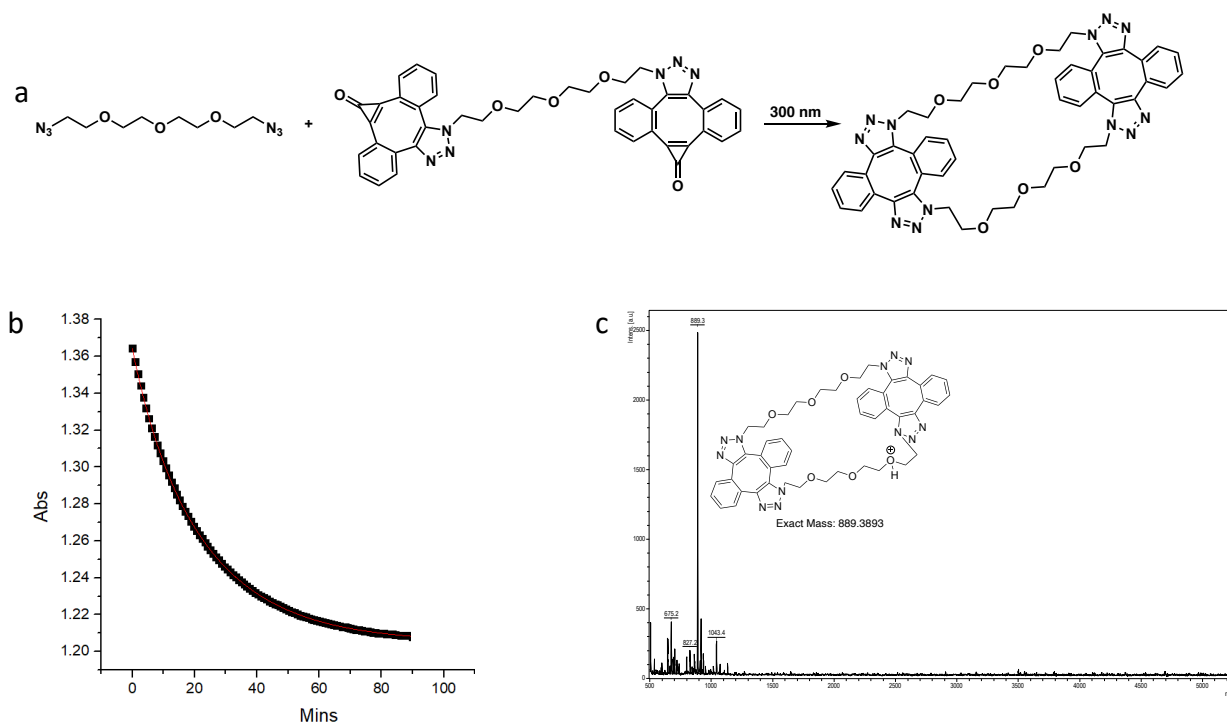


Figure 13. a) MC-DIBOT-TEG-N₃ cyclization at 350 nm. b) two step cyclization of photo-DIBOD with bis-TEG-Azide

Two component systems are usually difficult to cyclize due to added entropy in the system. We tried our method with two-component systems by synthesizing bis-photo-DIBOT and reacting it with bis-TEG-Azide and observed cyclization with only one cycle formation in quantitative conversion shown by in Figure 14. These results indicate that by using 1:1 mixture of azide and photo caged alkyne, cyclization reaction is preferred as compare to oligomerization.



d

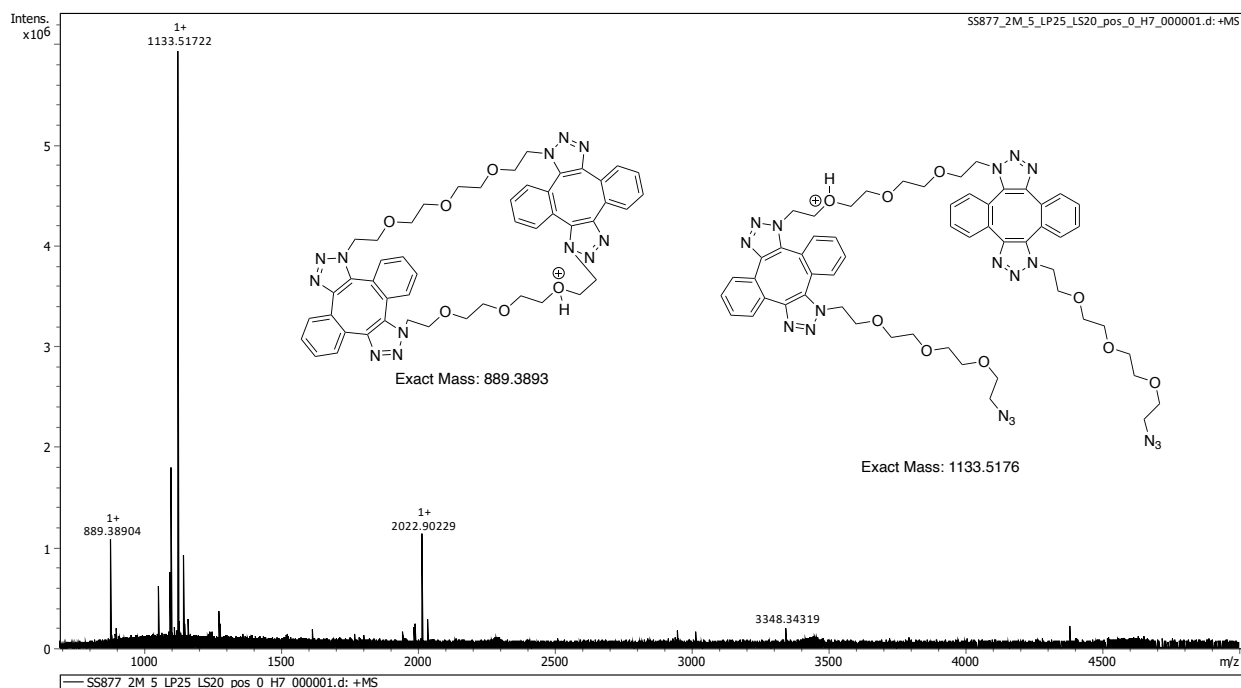
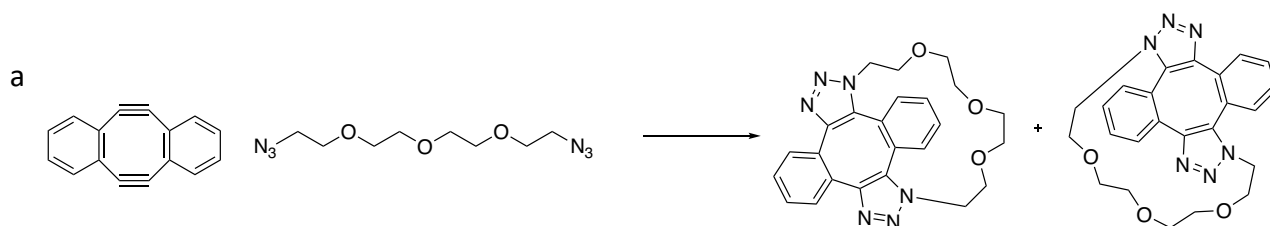


Figure 14. a) bis-photo-DIBOT and bis-TEG-Azide cyclization at 300 nm, b) Kinetics plot of cyclization at 10 μ M in DCM, c) MALDI spectra of macrocycle, d) HRMS of cyclization with 100 eq excess bis-TEG-Azide in bis-photo-DIBOT

Kinetics of cyclization of bis-photo-DIBOT observe two first order kinetics equation. The formation of first triazole ring is the rate limiting step as it is slower compared to the second triazole ring formation which formed the macrocycle. To further confirm our kinetics data, we irradiated bis-photo-DIBOT with 100 equivalent bis-TEG-azide. MALDI analysis of the reaction mixture shows attachment of two bis-TEG-azide units to bis-DIBOT as major peak and minor peak as macrocycle. The presence of macrocycle with 100 equivalent excess bis-TEG-azide confirms after first SPAAC reaction, the second SPAAC reaction rate increases as indicated by kinetics plot as shown in Figure 14b.

We further explored SPAAC macrocyclization by using DIBOD and bis-TEG-azide. We tried three different reaction conditions, a) DIBOD added slowly in bis-TEG-azide solution, b) bis-TEG-azide solution added slowly in DIBOD, c) DIBOD and bis-TEG-azide added simultaneously. In first two conditions, we got majority of monomer cycle and trace amount of dimer rings were formed. In condition c, we observed 80% of monomer cycle and 15% of dimer cycle and trace amount of trimer cycles as shown in figure 15. Purified monomer cycle NMR shows both the isomers with one major and minor. Unfortunately, we were not able to isolate these isomers or characterize which one is major. None of the conditions gave any open chain isomers as all reactions were quenched by sodium azide to react with any unreacted cyclooctynes, before taking any spectra. These results shows that SPAAC reaction is also a powerful tool to build macrocycles. In conclusion, we have shown that photo-SPAAC and SPAAC reactions are a robust method for macrocyclization that can be used for one and two component reactions. The reactions show quantitative conversion and doesn't need any purification. Also, method is concentration independent hence can be used for bulk synthesis of macrocycles.



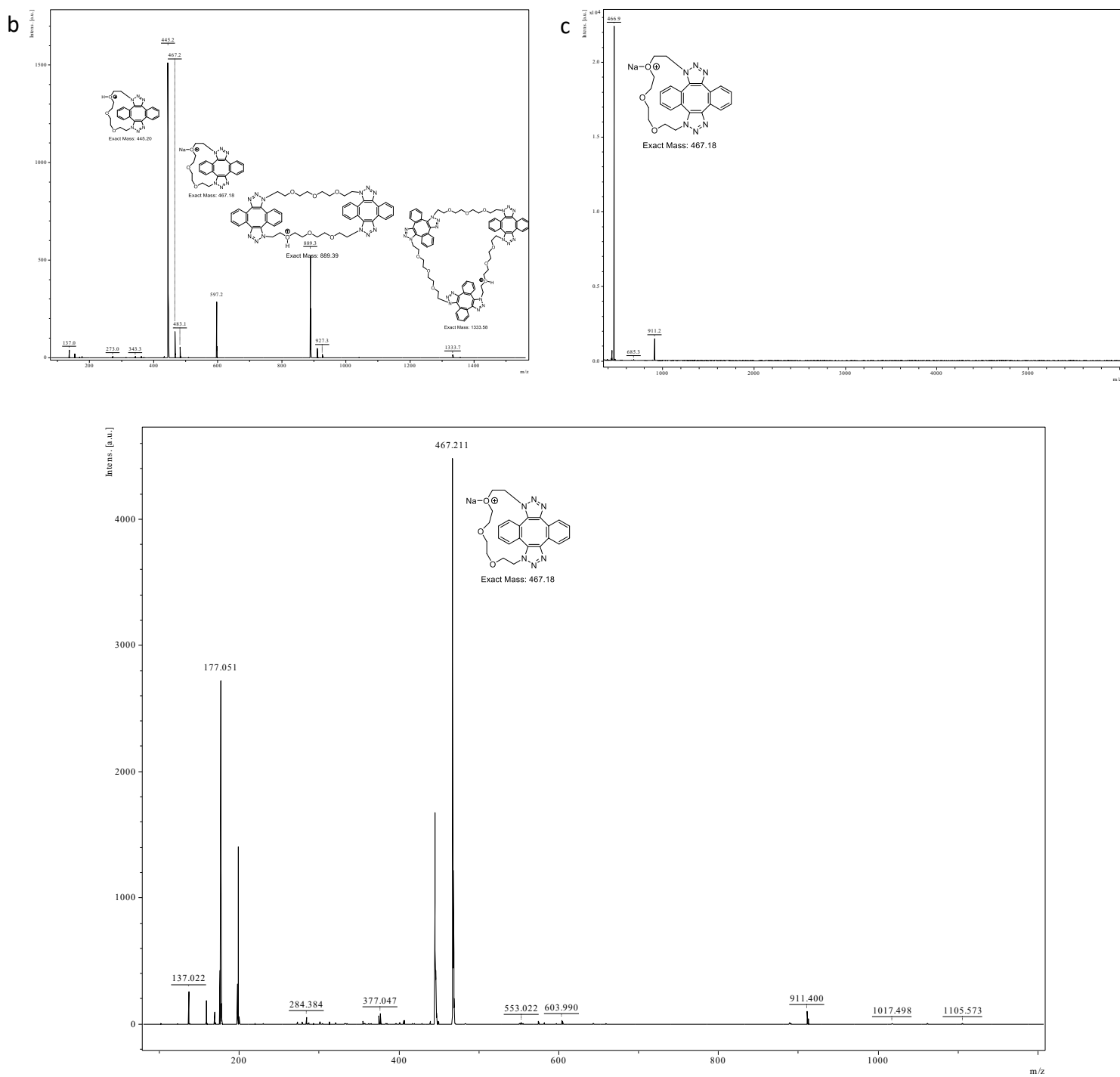


Figure 15. a) Reaction scheme of macrocyclization via DIBOD, b) MALDI of DIBOD and bis-TEG-azide mixed together, c) DIBOD slowly added into bis-TEG-azide, d) bis-TEG-azide slowly added into DIBOD

Chapter 3

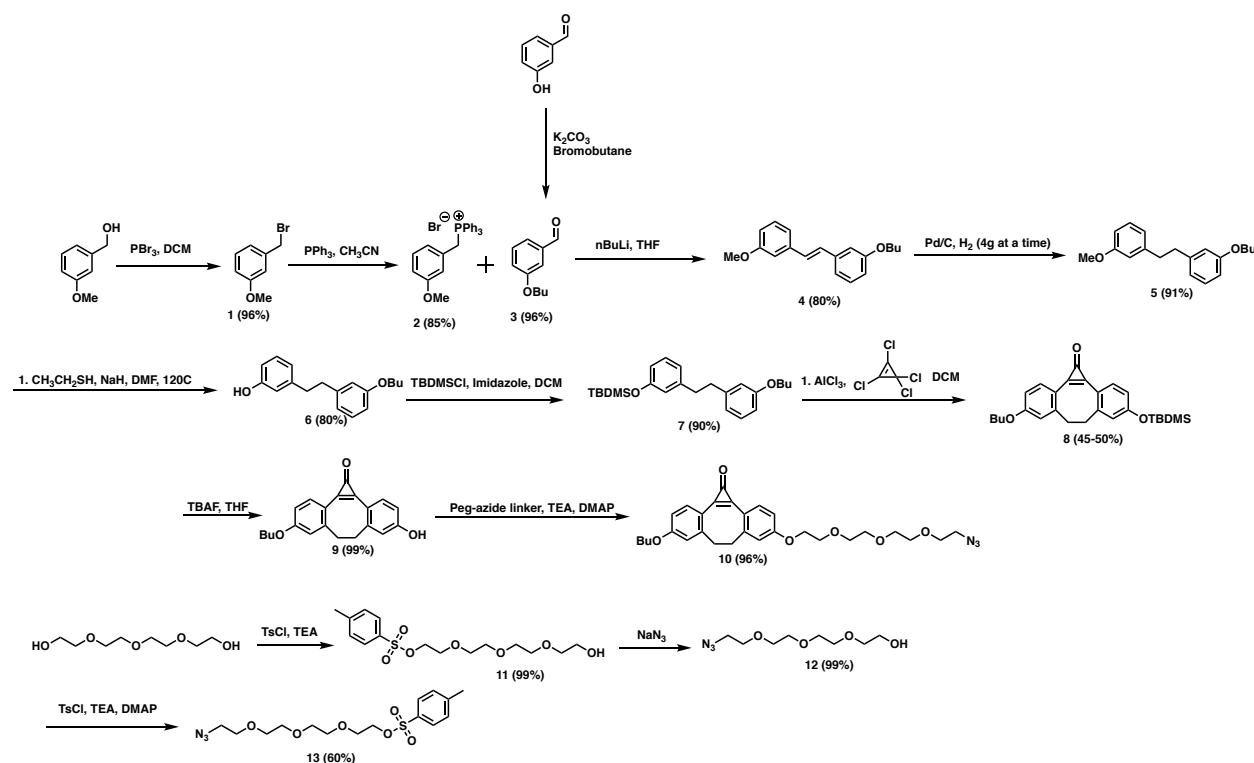
Synthesis of Sequence Defined Oligomers via Photo-Click Chemistry

3.1 Results and Discussions

The reported methods used multiple equivalents of catalysts and/or coupling reagents to derive the reaction to completion. Every addition of bifunctional monomer in step growth polymerization needs two reactions. First to addition of monomer in growing chain and then deprotection to allow further addition. These methods demonstrate the general problem of build-up of unreacted reagents and by-products with each step of monomer addition. Solid phase supported synthesis has shown to simplify the purification, but it limits the amount of material generated. Also, it is difficult to monitor real time reaction kinetics and progress as some material must be cleaved from the solid support.

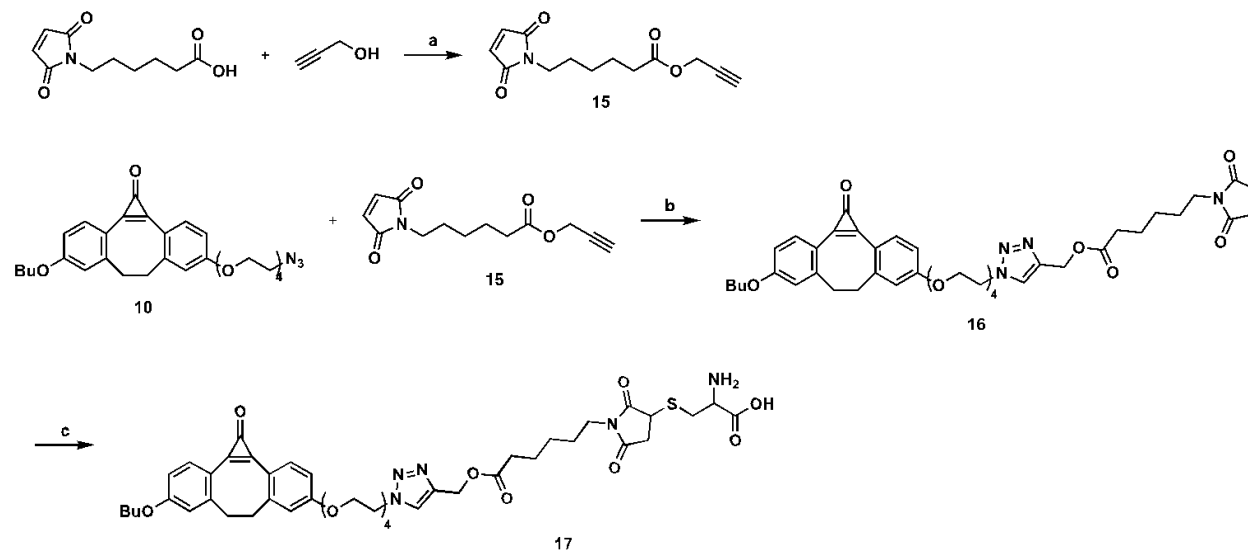
Herein, we report a novel ACB-type trifunctional monomer, suitable for photo-SPAAC ligation, where A is photo-caged cyclooctyne; B is azide; and C is carboxylic acid for derivatizing monomer with various functionalities compatible with SPAAC reactions. The use of solution phase SPAAC chemistry can be used to synthesize SD oligomers in a bulk quantity as compared to the solid phase approaches reported in the literature. Moreover, SPAAC chemistry is selective towards strained cyclooctyne and azide hence this SD oligomers can be synthesized in various environments including biological conditions. Photo-activation of the growing chain terminus allows for the attachment of the next monomer. The advantage of our method is the use of a light source to deprotect the alkyne moieties and generate carbon monoxide as side product. This allows us to synthesize oligomers without purification (carbon monoxide is the side product) at intermediate steps.

monotosylated by using tosyl chloride to form 2-(2-(2-(2-Hydroxyethoxy)ethoxy)ethoxy) ethyl ester (**11**). Tosyl group of compound (**11**) was converted into azide by refluxing it with sodium azide to produce 2-(2-(2-(2-Azidoethoxy)ethoxy)ethoxy)ethanol (**12**). The hydroxy group of compound (**12**) was activated by reacting it with tosyl chloride and then coupled with photo-DIBO-OH in the presence of triethylamine to get photo-DIBO-TEG-N₃ (**10**) in quantitative yield as shown in Scheme 2.



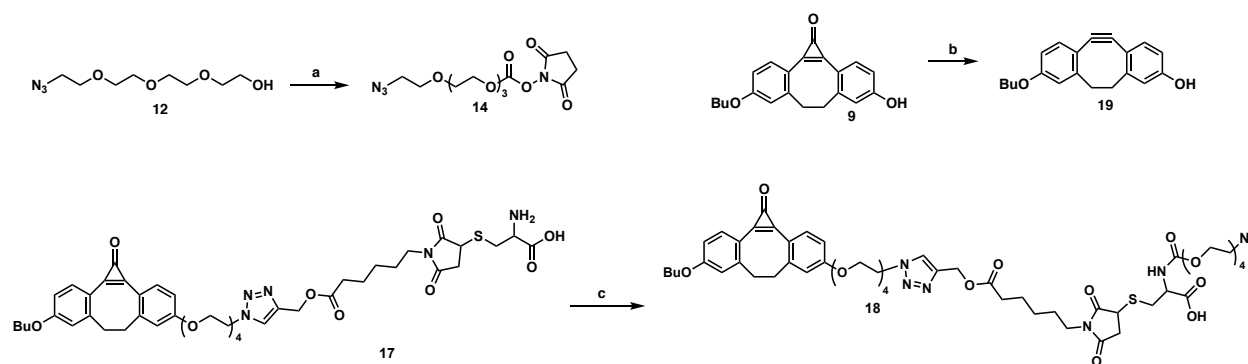
Scheme 2. (a) PBr₃ DCM (96%); (b) PPh₃ acetonitrile (85%); (c) butanol, DIAD, THF, PPh₃ (96%); (d) n-butyllithium, THF (80%); (e) H₂, Pd/C, ethylacetate (91%); (f) ethanethiol, NaH, DMF, 120°C (80%); (g) TBDMSCl, imidazole, DCM (96%); (h) aluminum chloride, tetrachlorocyclopropene, DCM (50%); (i) TBAF, THF (99%); (j) **13**, TEA, DMAP, DMF (96%); (k) TsCl, TEA, DCM (82%); (l) NaN₃, Acetone (99%); (m) TsCl, TEA, DMAP, DCM (60%).

Maleimide hexanoic acid was esterified using propargyl alcohol and a catalytic amount of sulfuric acid. The resulting ester (**15**) was reacted with photo-DIBO-TEG-N3 (**10**) using copper click chemistry to get maleimide photo-DIBO (**16**), which then reacted with the thiol group of cysteine to yield photo-DIBO modified cysteine (**17**) as shown in Scheme 3.



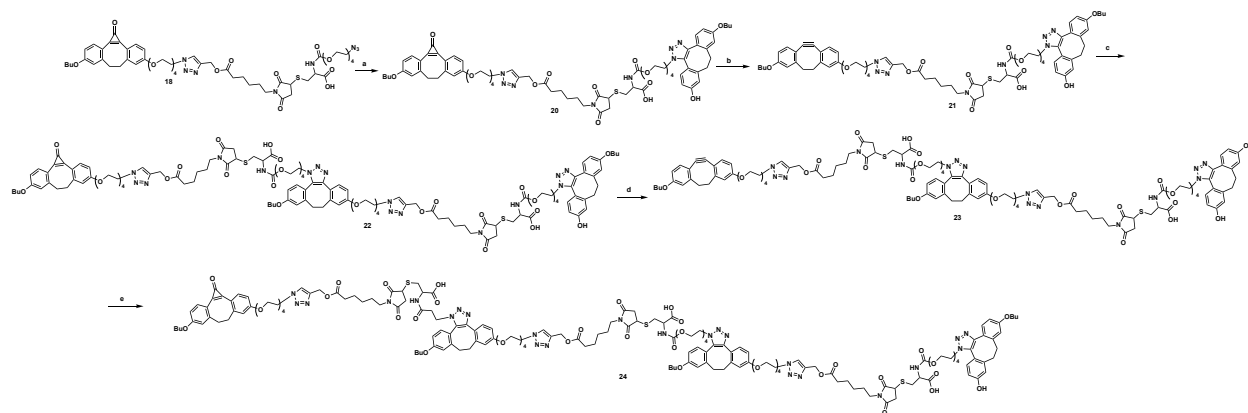
Scheme 3. (a) H^+ , toluene (68%); (b) CuI , ascorbic acetate, THF, H_2O (80%); (c) cysteine, TEA, DMF (75%)

To modify the amino group of cysteine with azide, a tetra ethylene glycol-based linker was synthesized by reacting compound (**12**) with di(*N*-succinimidyl) carbonate (DSC) to form linker (**14**). Amino group of compound (**12**) was then reacted with compound (**17**) in presence of DIPEA to give the monomer, (**18**) as shown in Scheme 4. This monomer was used to build step by step SD oligomers with a carboxylic acid, which can be potentially used for attaching functional motifs for potential applications.



Scheme 4. (a) DSC, TEA, DCM (76%); (b) 350 nm, methanol (94%); (c) **14**, TEA, DCM (56%)

To start building up oligomer sequence, the first monomer was capped with DIBO-OH which was obtained by irradiating photo-DIBO-OH with a 350 nm light to form compound (**19**). Latter was irradiated with a 350 nm light to deprotect the alkyne which was confirmed by disappearance of 350 nm band and appearance of 303 nm band in UV-Vis spectra. To cyclooctyne (**21**), one equivalent of monomer (**18**) was added and stirred overnight to form the dimer (**22**) which was purified by size exclusion chromatography and characterized by high-resolution mass spectrometry. Similarly, a trimer (**24**) was synthesized by deprotecting the dimer (**22**) using 350nm photoirradiation and then letting it to react with one eq of the monomer (**18**). The resulting trimer was purified by size exclusion column and characterized by the high-resolution mass spectra as shown in Scheme 5.



Scheme 5. (a) **19**, DCM (80%); (b) 350nm, DCM (91%); (c) **18**, DCM (77%); (d) 350nm, DCM (93%); (e) **18**, DCM (78%)

To better understand the reaction, rate of dimerization was estimated using a second order rate. Active concentration of product was measured by UV-Vis spectra taken every 30 min of the dimerization reactions at 50 uM and 100 uM concentration. Active concentration was correlated to absorption by using beer lambert equation as shown below



$$[A] = [A]_0 / ([A]_0 * k_1 * t + 1) \quad 2 \quad \text{Second order rate law}$$

$$\text{Abs} - \epsilon * c * l \quad 3 \quad \text{Beer Lambert law}$$

Total absorption and concentration of product at time(t) can be written as equation 4 and 5

$$\text{Abs}(t) = [A] * \epsilon_A + [P] * \epsilon_P \quad 4$$

$$[P] = ([A]_0 - [A]) / 2 \quad 5$$

$$\text{Abs}(t) = [A](\epsilon_A - \epsilon_P / 2) + [A]_0 * \epsilon_P / 2 \quad 6$$

ϵ_A and ϵ_P can be calculated by putting $t = 0$ and ∞ in equation 6

$$\epsilon_A = \text{Abs}(0) / [A]_0, \quad \epsilon_P = 2 * \text{Abs}(\infty) / [A]_0 \quad 7$$

Final rate law was obtained by substituting the value of ϵ_A , ϵ_P and $[A]$ from equation 7 and 2 in equation 6

$$\text{Abs}(t) = d\text{Abs}/(2*k_1*t + 1) + \text{offset}$$

We also observed a linear loss of material from the solution which we attributed to aggregation and/or adsorption of material on the walls of cuvette. Hence rate law was modified with another rate constant k_2 as shown in the equation below

$$\text{Abs}(t) = d\text{Abs}/(2*k_1*t + 1) + k_2*t + \text{offset} \quad \mathbf{8}$$

(Abs - Absorption at time t, dAbs - change in absorption, k_1 and k_2 - rate constants, t - time, ϵ_A and ϵ_P - extinction coefficient, c - concentration, l - path length of light (1cm) A - monomer, P - Dimer

Rate constant was obtained as $0.75\text{M}^{-1}\text{s}^{-1}$ by fitting the UV-Vis spectra data in equation 8 as shown in Figure 2

The complete disappearance of the monomer and dimer from the mass spectra of the reaction mixture prove that the reaction has a very high conversion rate and can be used to build complex sequences without any purification required at the intermediate steps. This will be the major advantage in the synthesis of the SD oligomers in contrast to the reported literature methods that required multiple equivalents of ligation reagents, coupling partners, and purification steps. In our method, we are using just one equivalent of coupling partner and no ligation reagent.

To show that our method can be used to synthesize SD oligomers with precise sequences, we synthesized a rhodamine coupled monomer (**26**). The carboxylic acid of rhodamine was modified using 1,3 diaminopropane (**25**) and then the free amino group of compound (**25**) was conjugated to the carboxylic acid of the monomer (**18**) to form the rhodamine modified monomer (**26**) as shown in Scheme 6.

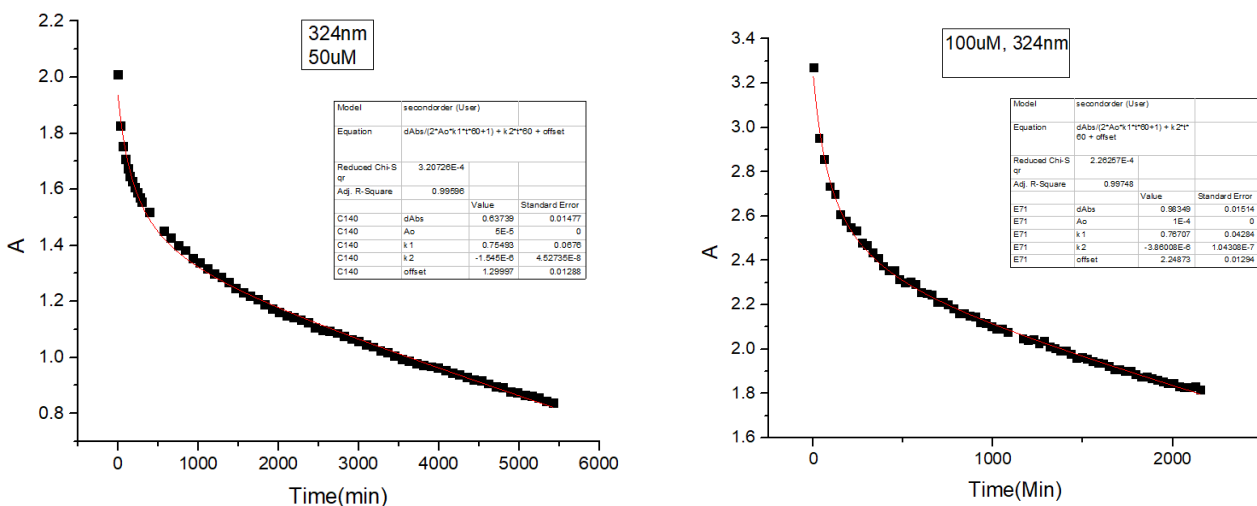
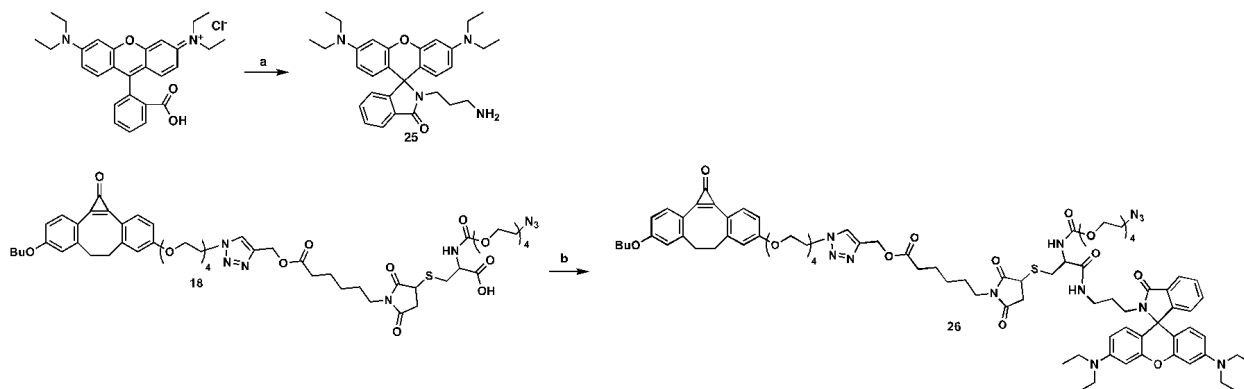


Figure 2. UV-Vis trace at 324nm at 50 and 100uM respectively

With these two monomers, we attempted the synthesis of two different sequences AAABA and AAABB, where A is the monomer with carboxylic acid (**18**) and B is the rhodamine modified



monomer (**26**). We also hypothesized that the reaction rate for the formation of the trimer, tetramer and pentamer will not vary much from the rate of formation of the dimer. To test this theory, all the click reactions in the pentamer synthesis were conducted with a 1:1 ratio of the reactants at 30mM concentration and stirred for 2 hours, which was estimated time of 99% conversion according to the rate constant for the formation of the dimer. No purification steps were done until

the formation of the pentamer sequence. The formation of oligomers and the consumption of reactants were monitored by mass spectrometry. MS spectra results show a high conversion at each step with no or a trace amount of unreacted reactants left after each click reaction which proves that oligomerization till pentamer have similar reaction rates.

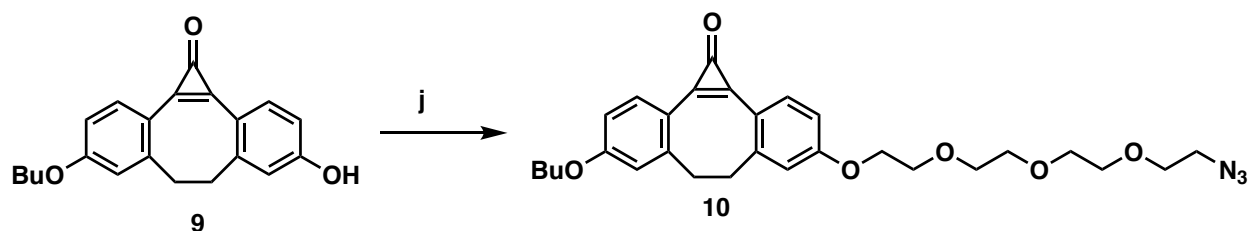
In conclusion, we have successfully developed a novel monomer for synthesizing sequence defined oligomers using photo-SPAAC reaction. This monomer has shown to quench itself that avoids its further participation hence no purification needed. In our method, we are using just 1.05 eq of coupling partner and no ligation reagent. We have achieved one pot synthesis of two pentamer sequences without any purification to show the viability of this method for automated synthesis. Due to liquid-phase synthesis, these monomers can be scaled up and potentially be used for catalysis, drug delivery, data storage and many more applications.

CHAPTER 4

Experimental Data

4.1 Synthesis

Photo-DIBO was synthesized using previously published methods.⁶³ photo reactions were done by using Rayonet photo reactors with 16 lamps. UV-Vis spectra were taken using Cary 5000. All other chemicals were purchased from Alfa Aesar, Sigma Aldrich, or TCI, and were used as received. Flash chromatography was performed using 40-63 μ m silica gel. All NMR spectra were recorded in CDCl_3 (unless otherwise noted) using 400 MHz instrument.



4-(2-(2-(2-(2-azidoethoxy)ethoxy)ethoxy)ethoxy)-9-butoxy-6,7-dihydro-1H-

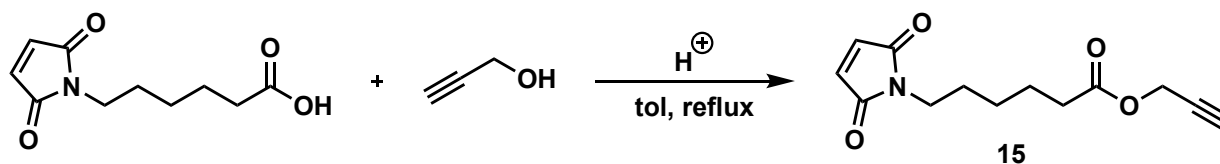
dibenzo[a,e]cyclopropa[c][8]annulen-1-one(10)

2-(2-(2-(2-azidoethoxy)ethoxy)ethoxy)ethyl 4-methylbenzenesulfonate (1.6 g, 1.7 Eq, 4.3 mmol), 4-butoxy-9-hydroxy-6,7-dihydro-1H-dibenzo[a,e]cyclopropa[c][8]annulen-1-one(9) (812 mg, 1 Eq, 2.53 mmol) and potassium carbonate (350 mg, 1 Eq, 2.53 mmol) were dissolved in DMF (25 mL) and heated for 4 hours at 70°C. After that reaction mixture was diluted with 200ml ethyl acetate and washed with brine, dried over magnesium sulphate and concentrated. Crude product was subjected to silica gel column chromatography (20-60% ethyl acetate in hexane) to get yellow wax type solid. Yield - 1.28 g (96%).

^1H NMR (400 MHz, CDCl_3) δ 7.93 (d, J = 8.6 Hz, 2H), 6.97 – 6.84 (m, 4H), 4.21 (dd, J = 5.6, 3.9 Hz, 2H), 4.04 (t, J = 6.5 Hz, 2H), 3.94 – 3.85 (m, 2H), 3.76 – 3.65 (m, 10H), 3.38 (t, J = 5.1 Hz, 2H), 3.33 (d, J = 10.6 Hz, 2H), 2.70 – 2.54 (m, 2H), 1.79 (m, 2H), 1.58 – 1.44 (m, 2H), 0.99 (t, J = 7.4 Hz, 3H).

^{13}C NMR (101 MHz, CDCl_3) δ 162.55, 162.09, 161.59, 153.79, 147.80, 142.41, 141.98, 135.82, 135.71, 116.61, 116.35, 116.23, 116.16, 112.37, 112.28, 77.38, 77.06, 76.74, 70.89, 70.73, 70.71, 70.68, 70.05, 69.52, 68.01, 67.67, 50.68, 37.19, 37.16, 31.15, 19.20, 13.83.

Compound 9 - *Chem. Commun.*, **2014**,50, 5307-5309

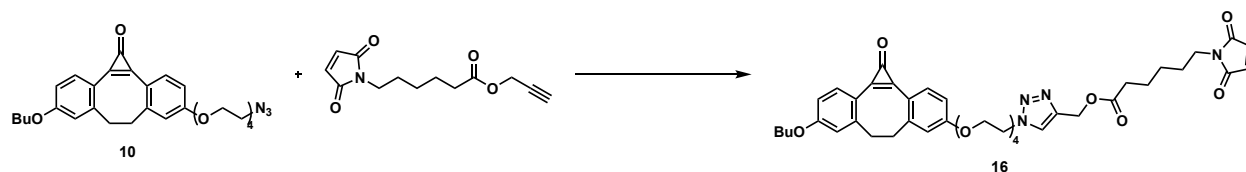


Prop-2-yn-1-yl 6-(2,5-dioxo-2,5-dihydro-1H-pyrrol-1-yl)hexanoate (15) - propargyl alcohol (265 mg, 0.28 mL, 2 Eq, 4.73 mmol), 6-(2,5-dioxo-2,5-dihydro-1H-pyrrol-1-yl)hexanoic acid (400 mg, 67.8 %) were dissolved in Toluene (4 mL). 3 drops of concentrated sulfuric acid was added and reaction was refluxed for overnight. Reaction mixture was diluted with ethyl acetate (100 ml) and washed with brine (2 * 50 ml) and dried over magnesium sulfate. Crude product was purified with silica gel column chromatography to get yellow color oil. Yield – 400 mg (68%).

^1H NMR (400 MHz, $\text{Chloroform-}d$) δ 6.65 (s, 2H), 4.61 (s, 2H), 3.48-3.43 (m, 2H), 2.45 (s, 1H), 2.32 - 2.27 (m, 2H), 1.64 - 1.51 (m, 4H), 1.30 - 1.25 (m, 2H).

^{13}C NMR (101 MHz, $\text{Chloroform-}d$) δ 172.53, 170.81, 134.06, 77.72, 74.86, 51.80, 37.54, 33.68, 28.15, 24.21.

Reference - **Known Compound** - *J. Polym. Sci. Part B: Polym. Phys.*, 56: 355-361

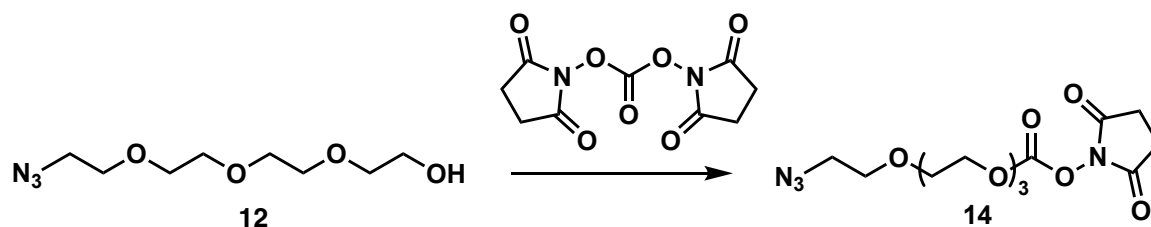


(1-(2-(2-(2-(2-((9-butoxy-1-oxo-6,7-dihydro-1H-dibenzo[a,e]cyclopropa[c][8]annulen-4-yl)oxy)ethoxy)ethoxy)ethoxy)ethyl)-1H-1,2,3-triazol-4-yl)methyl 6-(2,5-dioxo-2,5-dihydro-1H-pyrrol-1-yl)hexanoate (16). 4-(2-(2-(2-(2-azidoethoxy)ethoxy)ethoxy)ethoxy)-9-butoxy-6,7-dihydro-1H-dibenzo[a,e]cyclopropa[c][8]annulen-1-one (261 mg, 1 Eq, 0.50 mmol) , prop-2-yn-1-yl 6-(2,5-dioxo-2,5-dihydro-1H-pyrrol-1-yl)hexanoate (137 mg, 1.1 Eq, 0.55 μ mol) , copper(I) iodide (28.6 mg, 0.3 Eq, 0.15 mmol) , Sodium ascorbate (52.9 mg, 0.6 Eq, 0.3 mmol) were dissolved in THF (4 mL) and Water (1 mL). Reaction mixture was stirred for 24 hours at room temperature. After TLC analysis indicated completion of reaction, reaction mixture was diluted with DCM (50 ml) and washed with brine (2 * 25 ml) and concentrated. Crude product was purified by silica gel column chromatography (10-30% acetone in ethyl acetate). Yield – 310 mg (80 %).

^1H NMR (400 MHz, Chloroform-*d*) δ 7.91 - 7.89 (m, 2H), 7.80 (s, 1H), 6.90 - 6.87 (m, 4H), 6.67 (s, 2H), 5.20 (s, 2H), 4.53 (t, J = 5 Hz, 2H), 4.19 (t, J = 4 Hz, 2H), 4.03 (t, J = 6 Hz, 2H), 3.87 (t, J = 5 Hz, 4H), 3.73 - 3.70 (m, 2H), 3.65 - 3.61 (m, 6H), 3.47 (t, J = 7 Hz, 2H), 3.33 - 3.31 (m, 2H), 2.62 - 2.59 (m, 2H), 2.30 (t, J = 7 Hz, 2H), 1.82 - 1.75 (m, 2H), 1.66 - 1.45 (m, 6H), 1.30 - 1.21 (m, 2H), 0.98 (t, J = 7.4 Hz, 3H).

^{13}C NMR (101 MHz, Chloroform-*d*) δ 173.16, 161.50, 142.39, 141.88, 135.60, 134.04, 124.91, 116.54, 116.28, 116.16, 116.06, 112.32, 70.80, 70.56, 70.50, 69.48, 69.32, 67.96, 67.62, 57.48, 50.24, 37.52, 37.13, 37.09, 33.82, 31.10, 28.15, 26.13, 24.25, 19.16, 13.82.

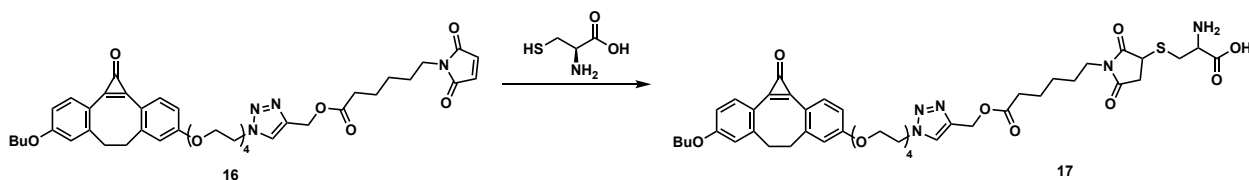
Mass – $[M+H]^+$ $C_{42}H_{51}N_4O_{10}^+ - 771.3600$, found - 771.3606.



2-(2-(2-(2-azidoethoxy)ethoxy)ethoxy)ethyl (2,5-dioxopyrrolidin-1-yl) carbonate (14) - 2-(2-(2-(2-azidoethoxy)ethoxy)ethoxy)ethan-1-ol (1 g, 1 Eq, 4.5 mmol), bis(2,5-dioxopyrrolidin-1-yl) carbonate (3 g, 2.5 Eq, 11.4 mmol) and potassium carbonate (630 mg, 1 Eq, 4.6 mmol) were dissolved in Acetonitrile (20 mL) and stirred for overnight. After that acetonitrile was evaporated and the reaction mixture was diluted with ethyl acetate (60 ml) and washed with brine (2 * 30 ml). Aqueous layer was extracted by DCM (50 ml). Both the organic layer was combined and dried. Yield – 1.4g (85%). No further purification was done to this compound.

1H NMR (400 MHz, Chloroform- d) δ 4.50 - 4.41 (m, 2H), 3.82 - 3.74 (m, 2H), 3.69 - 3.67 (m, 10H), 3.39 (t, J = 5 Hz, 2H), 2.84 (s, 4H)

^{13}C NMR (101 MHz, $CDCl_3$) δ 168.62, 168.57, 151.65, 70.90, 70.73, 70.68, 70.66, 70.27, 70.03, 68.33, 50.69, 25.47.

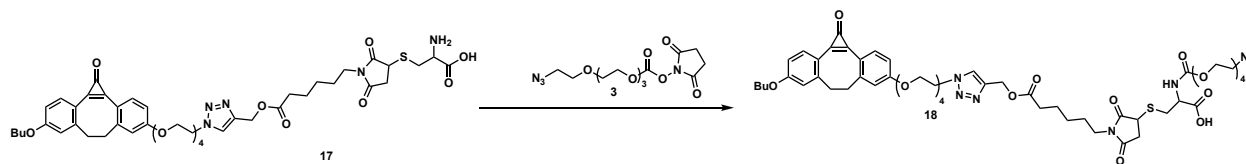


S-(1-(6-(((1-(2-(2-(2-(2-((9-butoxy-1-oxo-6,7-dihydro-1H-dibenzo[a,e]cyclopropa[c][8] annulen-4-yl)oxy)ethoxy)ethoxy)ethoxy)ethyl)-1H-1,2,3-triazol-4-yl)methoxy)-6-oxohexyl)-2,5-dioxopyrrolidin-3-yl)cysteine(17) - Compound 16(200 mg, 1 Eq, 259 μ mol), cysteine (63 mg, 2 Eq, 0.52 mmol) were dissolved in DMF (5 mL) and triethylamine (39 mg, 1.5 Eq, 0.39 mmol) was added dropwise. The reaction was stirred for 4 hours and then diluted with DCM (50 ml) and washed with brine (2 * 30 ml). The organic layer was concentrated and purified by silica gel column chromatography (5-20% Methanol in DCM). Yield – 170 mg (75%).

^1H NMR (400 MHz, DMSO) δ 8.13 (s, 1H), 7.78 (d, J = 8.4 Hz, 2H), 7.18 – 6.98 (m, 4H), 5.10 (s, 2H), 4.52 (t, J = 5.2 Hz, 2H), 4.27 – 4.05 (m, 5H), 3.79 (m, 4H), 3.64 – 3.27 (m, 18H), 3.17 (d, J = 2.5 Hz, 3H), 2.46 (d, J = 10.8 Hz, 2H), 2.28 (t, J = 7.4 Hz, 2H), 1.77 – 1.65 (m, 2H), 1.46 (m, 6H), 1.19 (t, J = 7.2 Hz, 3H), 0.94 (t, J = 7.4 Hz, 3H).

^{13}C NMR (101 MHz, DMSO) δ 177.62, 177.35, 175.59, 175.53, 172.98, 162.78, 162.03, 161.75, 152.50, 148.46, 142.49, 142.27, 142.18, 135.41, 135.36, 125.57, 116.65, 116.44, 116.23, 113.28, 70.36, 70.22, 70.10, 69.98, 69.19, 69.09, 68.09, 68.02, 57.49, 49.84, 45.66, 40.58, 40.37, 40.16, 39.95, 39.74, 39.54, 39.33, 36.74, 36.26, 33.56, 31.06, 27.12, 25.94, 24.33, 19.15, 14.14.

Mass - $[\text{M}-\text{H}^+]$ $\text{C}_{45}\text{H}_{56}\text{N}_5\text{O}_{12}\text{S}^-$ - 890.3652, found - 890.3632



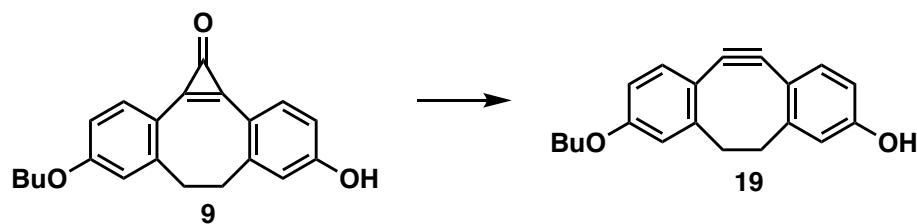
N-(13-azido-2,5,8,11-tetraoxatridecanoyl)-S-(1-(6-(((1-(2-(2-(2-(2-((9-butoxy-1-oxo-6,7-dihydro-1H-dibenzo[a,e]cyclopropa[c][8]annulen-4-yl)oxy)ethoxy)ethoxy)ethoxy)ethyl)-1H-1,2,3-triazol-4-yl)methoxy)-6-oxohexyl)-2,5-dioxopyrrolidin-3-yl)cysteine (18) - Compound 17 (80 mg, 1 Eq, 90

μmol) and triethylamine (11 mg, 15 μL , 1.2 Eq, 0.11 mmol) were stirred in DCM (3 mL) for 10 minutes and then 2-(2-(2-(2-azidoethoxy)ethoxy)ethoxy)ethyl (2,5-dioxopyrrolidin-1-yl) carbonate (65 mg, 2 Eq, 0.18 mmol) was added in 1 mL DCM. Reaction mixture was stirred for overnight. After TLC indicated completion of reaction, DCM was evaporated, and crude product was purified by silica gel column chromatography (2-10% methanol in DCM). Yield – 58 mg (57%).

^1H NMR (600 MHz, CDCl_3) δ 7.91 (d, $J = 6.0$ Hz, 2H), 7.80 (s, 1H), 6.94 – 6.81 (m, 4H), 5.17 (s, 2H), 4.52 (t, $J = 5.1$ Hz, 2H), 4.18 (dt, $J = 6.9, 3.4$ Hz, 3H), 4.02 (td, $J = 6.6, 2.2$ Hz, 3H), 3.85 (dd, $J = 6.8, 3.3$ Hz, 4H), 3.71 – 3.57 (m, 15H), 3.47 – 3.28 (m, 5H), 3.08 (d, $J = 7.4$ Hz, 2H), 2.59 (d, $J = 11.1$ Hz, 2H), 2.27 (q, $J = 5.5$ Hz, 2H), 1.82 – 1.71 (m, 2H), 1.58 – 1.39 (m, 12H), 0.97 (td, $J = 7.3, 1.4$ Hz, 4H).

^{13}C NMR (151 MHz, CDCl_3) δ 174.75, 173.27, 173.21, 162.30, 161.74, 154.03, 148.02, 142.62, 142.01, 141.59, 135.92, 135.88, 125.03, 116.42, 116.39, 116.28, 115.87, 112.45, 112.43, 112.40, 77.30, 77.08, 76.87, 70.84, 70.63, 70.59, 70.54, 70.52, 70.01, 69.52, 69.46, 69.33, 68.05, 67.68, 57.42, 53.68, 53.47, 50.67, 50.33, 41.97, 37.16, 37.12, 33.79, 33.77, 31.13, 29.69, 29.65, 24.23, 19.19, 13.83, 11.98.

Mass - $[\text{M}-\text{H}^+]$ $\text{C}_{54}\text{H}_{71}\text{N}_8\text{O}_{17}\text{S}^-$ - 1135.4663, found - 1135.4677

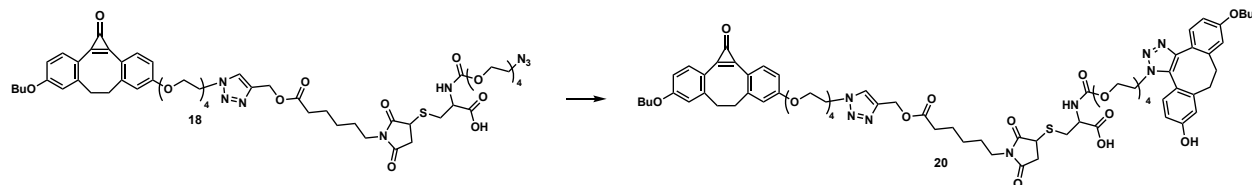


DIBO(19) - 4-butoxy-9-hydroxy-6,7-dihydro-1H-dibenzo[a,e]cyclopropa[c][8]annulen-1-one(9) (17 mg, 1 Eq, 53 μmol) was dissolved in methanol (17 mL). Compound was irradiated in rayonet photoreactor with

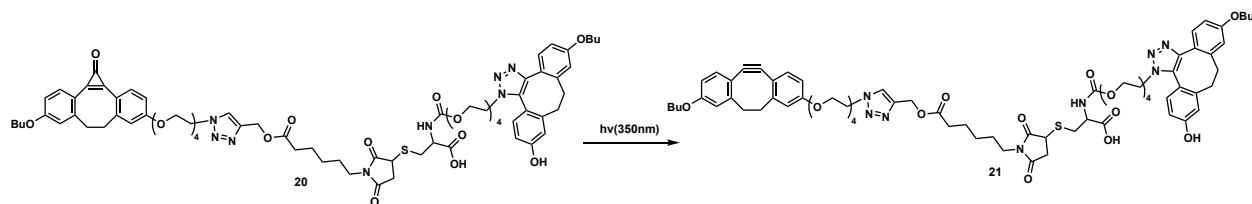
16 lamps of 350 nm for 10 minutes. UV spectra were recorded after 2, 6 and 10 minutes with 3 μ M concentration. Yield - 15 mg (97%)

^1H NMR (400 MHz, CDCl_3) δ 7.16 – 7.06 (m, 2H), 6.80 (d, J = 2.6 Hz, 1H), 6.74 (d, J = 2.5 Hz, 1H), 6.69 (dd, J = 8.4, 2.6 Hz, 1H), 6.63 (dd, J = 8.3, 2.5 Hz, 1H), 3.90 (t, J = 6.5 Hz, 2H), 3.15 – 3.04 (m, 2H), 2.41 – 2.29 (m, 2H), 1.70 (dq, J = 8.0, 6.5 Hz, 2H), 1.47 – 1.38 (m, 2H), 0.91 (t, J = 7.4 Hz, 3H).

Compound **19** - *Chem. Commun.*, **2014**,50, 5307-5309

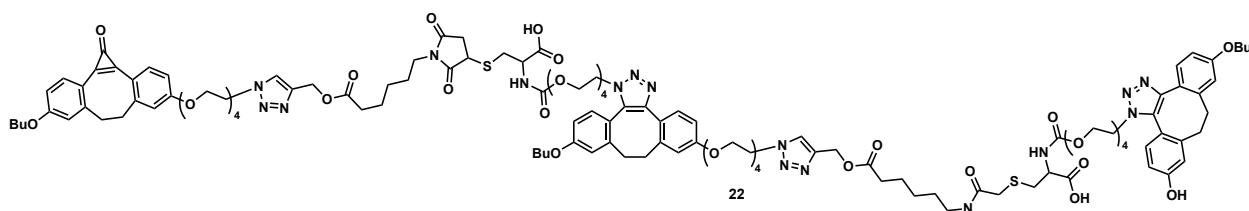


S-(1-(6-((1-(2-(2-(2-(2-((9-butoxy-1-oxo-6,7-dihydro-1H-dibenzo[a,e]cyclopropa[c][1,8] annulen-4-yl)oxy)ethoxy)ethoxy)ethoxy)ethyl)-1H-1,2,3-triazol-4-yl)methoxy)-6-oxohexyl)-2,5-dioxopyrrolidin-3-yl)-N-(13-(6-butoxy-11-hydroxy-8,9-dihydro-1H-dibenzo[3,4:7,8] cycloocta[1,2-d][1,2,3]triazol-1-yl)-2,5,8,11-tetraoxatridecanoyl)cysteine(20) - Compound 18 (10.000 mg, 1 Eq, 8.79 μ mol) and DIBO (3.0000 mg, 1.16 Eq, 10.25 μ mol) were dissolved in Methanol (1 mL). Reaction mixture was stirred overnight, concentrated and purified by silica gel column chromatography (10% methanol in DCM). Yield – 10 mg (80%).



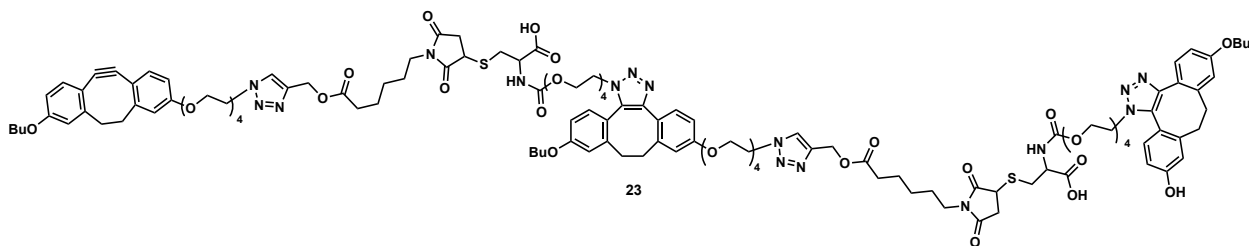
Compound (21) - Compound 20 (14.0 mg, 1 Eq, 9.78 μmol) was dissolved in methanol (3.20 mL) to get 3.06 mM concentration. Solution was irradiated with 16 lamps of 350 nm for 4 minutes in 8 mL glass vial, to complete disappearance of 350 nm peak. It was tracked using UV-Vis spectrometry at 3.06 μM concentration. No further purification was done. Yield - 12.5 mg (91%).

Mass - $[\text{M}+\text{H}^+]$ - 1401.6323, found - 1401.6317



Compound (22) - Compound 21 (10 mg, 1 Eq, 7.1 μmol) and compound 18 (8.1 mg, 1 Eq, 7.1 μmol) were dissolved in Methanol (330 μL) and DCM (110 μL). Reaction mixture was stirred overnight and concentrated. Product was purified using LH-20 column (20% DCM in methanol). Yield – 14 mg (77%).

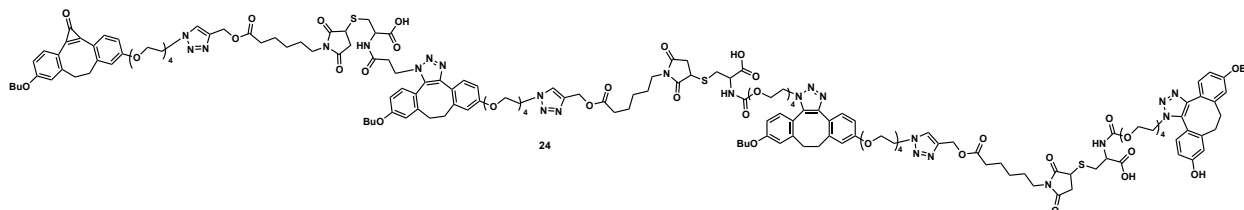
Mass - $[\text{M}+2\text{H}^+]^{2+}$ - 1270.0583, found - 1270.0578



Compound (23) - Compound 22 (13 mg, 1 Eq, 5.1 μmol) was dissolved in DCM (2.0 mL) to get 2.6 mM concentration. The solution was irradiated with 16 lamps of 350nm for 2.5 minutes in an 8mL glass vial, to

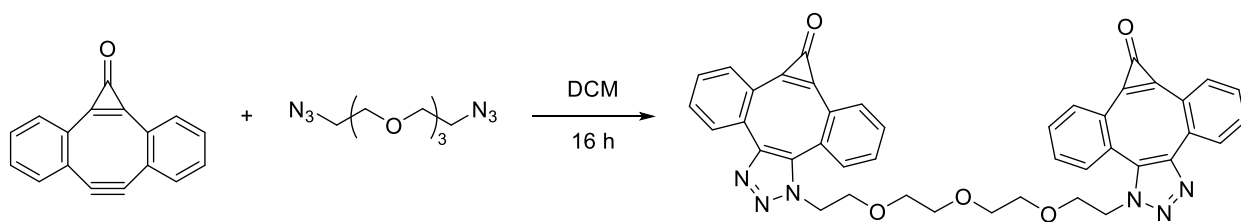
complete disappearance of the 350 nm peak. It was tracked using UV-Vis spectrometry with 2.6 μM concentration. No further purification was done. Yield – 12 mg (93%).

Mass $[\text{M}+2\text{Na}^+]^{2+}$ - 1278.0428, found - 1278.0421



Compound (24) - Compound 23 (12.0 mg, 1 Eq, 4.78 μmol) and compound 18 (5.4 mg, 1 Eq, 4.78 μmol) were dissolved in DCM (165 μL). The reaction mixture was stirred overnight and concentrated. Product was purified using LH-20 column (50% DCM in methanol). Yield - 13.2mg (78%).

Mass $[\text{M}+3\text{H}^+]^{3+}$ - 1216.5342, found - 1216.5303

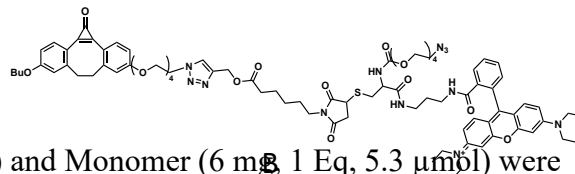
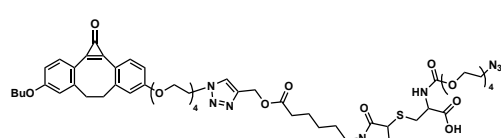
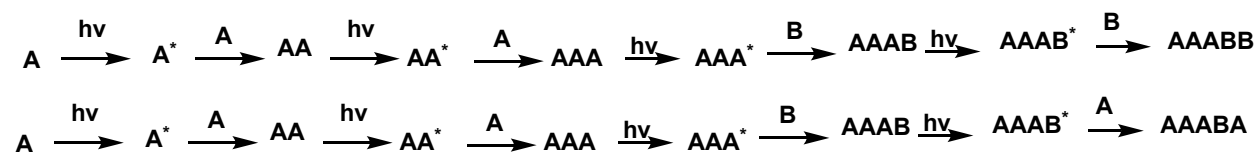


MC-DIBOD (100 mg, 0.44 mmol) and the bis-azido-TEG (45 mg, 0.20 mmol) were mixed together in DCM (2 mL) and stirred for 16 hours. The resulting product was concentrated under vacuum and purified by chromatography (50% acetone/hexanes) to give 100 mg (71%) of the product as a waxy yellow solid.

^1H NMR: (400 MHz, Chloroform-*d*) δ 7.87 (m, 2H), 7.69 – 7.65 (m, 2H), 7.63 – 7.49 (m, 10H), 7.45 (m, 2H), 4.45 – 4.37 (m, 2H), 4.31 – 4.22 (m, 2H), 3.99 – 3.92 (m, 2H), 3.86 – 3.79 (m, 2H), 3.52 – 3.43 (m, 8H).

^{13}C NMR: (101 MHz, CDCl_3) δ 157.49, 154.67, 152.04, 142.83, 133.93, 133.87, 133.18, 132.53, 132.38, 132.28, 131.58, 131.41, 130.58, 129.47, 128.71, 127.11, 124.59, 70.74, 70.58, 69.60, 48.96.

Pentamer Synthesis (Conditions) - Click Reactions are performed at 30 mM concentration, Photo deprotection was done using a lower concentration (< 10 mM) using Rayonet Photoreactor. Deprotection was followed by observing disappearance of 350nm band from UV-Vis Spectroscopy.



Dimer (AA) - Alkyne linker (8 mg, 1.0 Eq, 5.7 μmol) and Monomer (6 mg, 1 Eq, 5.3 μmol) were dissolved in DCM (200 μL) to achieve reaction concentration of 30 mM. The reaction mixture was stirred for 2.5 hours, and ESI-MS was done which indicated the formation of product and complete disappearance of alkyne linker. Without any purification, dimer was subjected to the next step.

Dimer Alkyne (AA*) - Dimer (13.4 mg, 1 Eq, 5.3 μmol) was dissolved in DCM (2 mL) to get 2.64 mM concentration and irradiated with 350 nm light from 16 lamps in rayonet photoreactor for 4 mins. ESI-MS indicated the complete deprotection of dimer.

Trimer (AAA) - Dimer alkyne (13.30 mg, 1 Eq, 5.3 μmol) and monomer (6.00 mg, 1 Eq, 5.3 μmol) were dissolved in DCM (180 μL) to achieve reaction concentration of 29 mM. The reaction mixture was stirred for 2.5 hours, and ESI-MS was done which indicated the formation of the product. Without any purification, Trimer was subjected to the next step.

Trimer Alkyne (AAA^{*}) - Trimer (19.32 mg, 1 Eq, 5.3 μmol) was dissolved in DCM (2mL) to get 2.65 mM concentration and irradiated with 350 nm light from 16 lamps in Rayonet photoreactor for 3 mins. ESI-MS indicated the complete deprotection of Trimer.

Tetramer (AAAB) - Trimer alkyne (19 mg, 1 Eq, 5.3 μmol) and monomer (8.5 mg, 1 Eq, 5.3 μmol) were dissolved in DCM (180 μL) to achieve reaction concentration of 29 mM. The reaction mixture was stirred for 2.5 hours, and ESI-MS was done which indicated the formation of the product. Without any purification, tetramer was subjected to the next step.

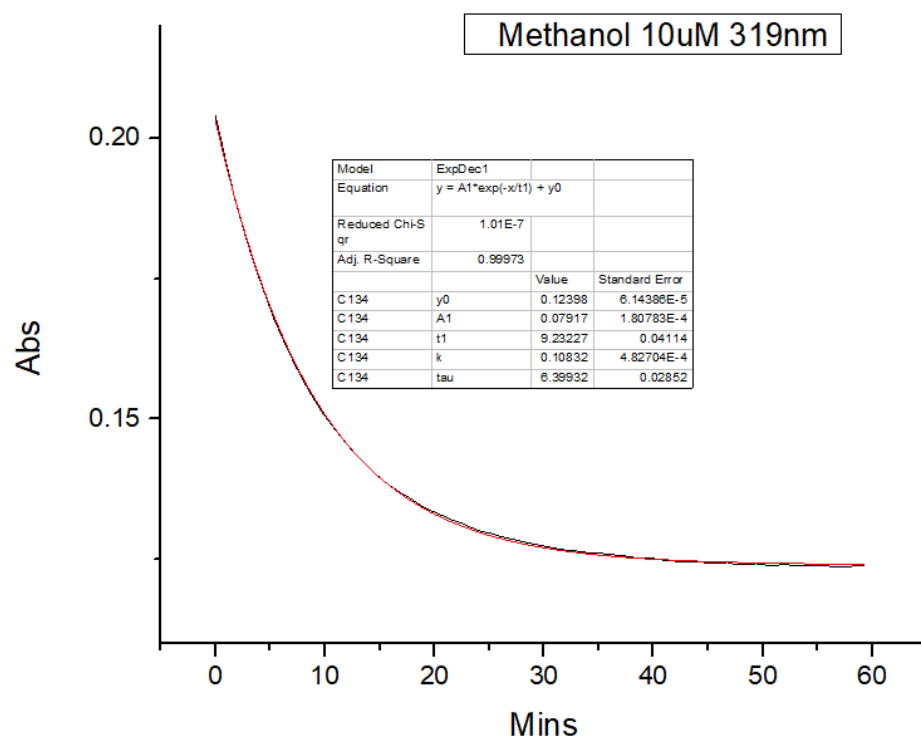
Tetramer Alkyne (AAAB^{*}) - Tetramer (28 mg, 1 Eq, 5.3 μmol) was dissolved in DCM (750 μL) to get reaction concentration as 7 mM and irradiated with 350 nm light from 16 lamps in Rayonet photoreactor for 5 mins. ESI-MS indicated the complete deprotection of Tetramer.

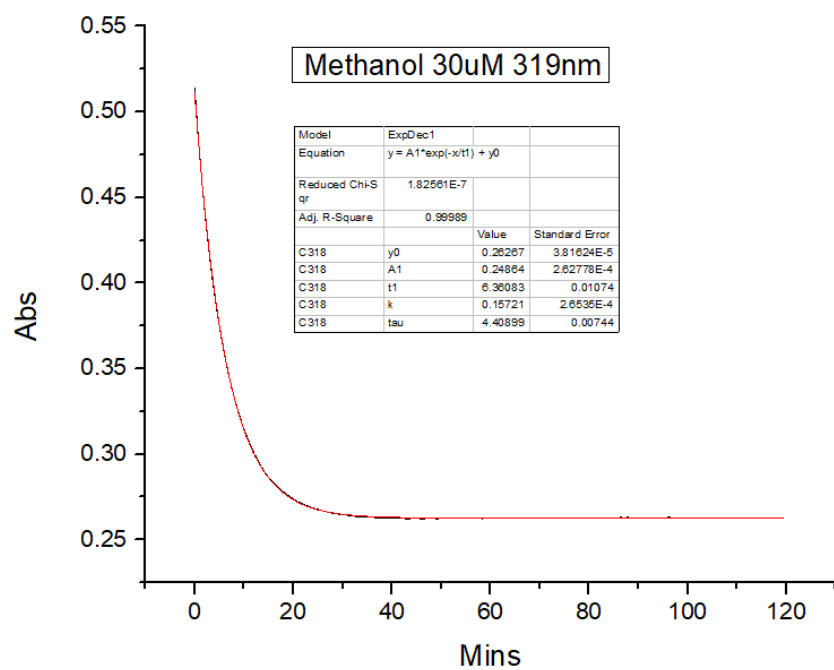
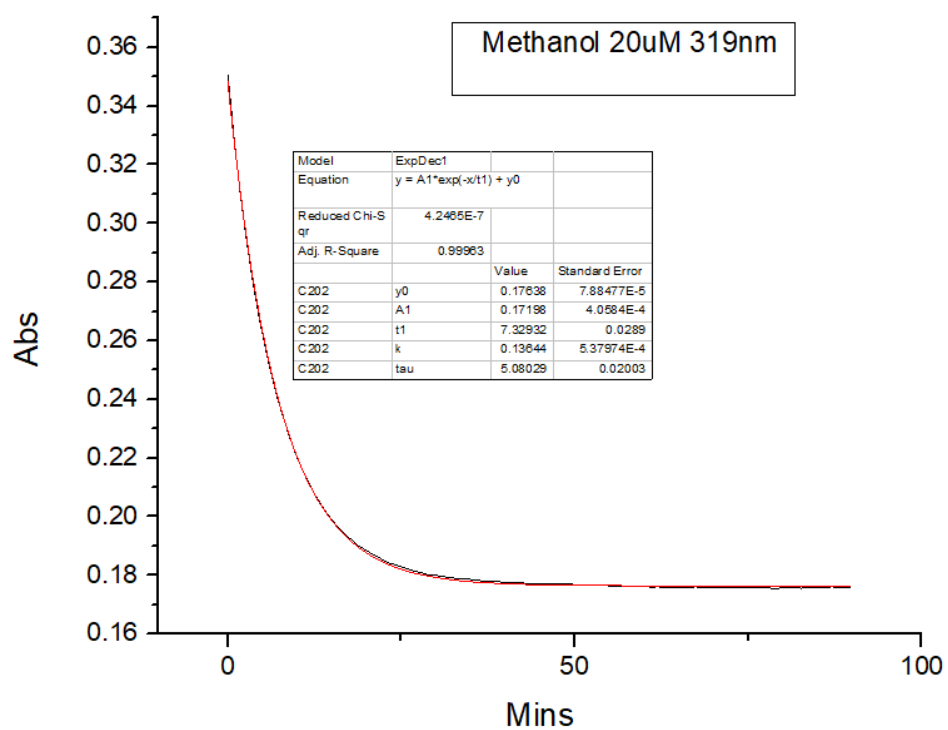
Pentamer Synthesis (AAABA, AAABA) – 28 mg of tetramer alkyne was divided into two parts and 1 eq of A (3 mg) and 1 eq of B (4.3 mg) were added in separate vials. The reaction was stirred for 2.5 hours and then subjected to ESI and MALDI.

4.2 Kinetics Data

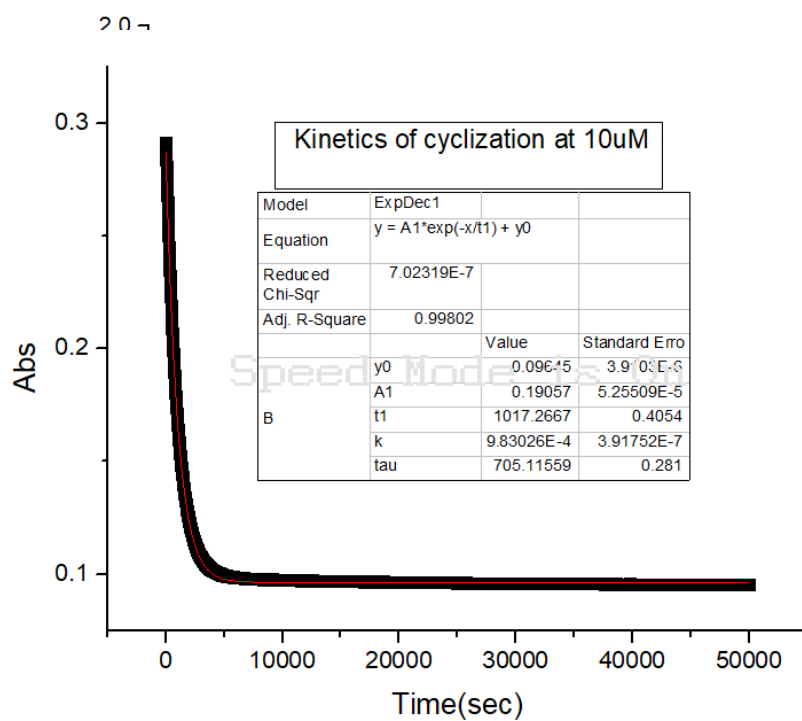
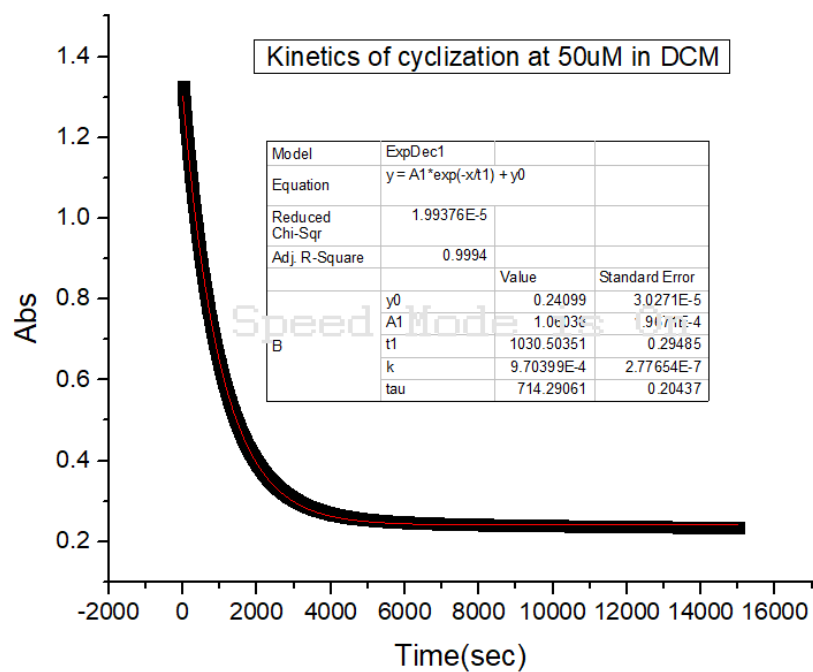
Kinetics plot were plotted using Carry 5000 by using first order decay kinetics equation

Kinetics in methanol for compound 18, $k = 0.15 \text{ s}^{-1}$

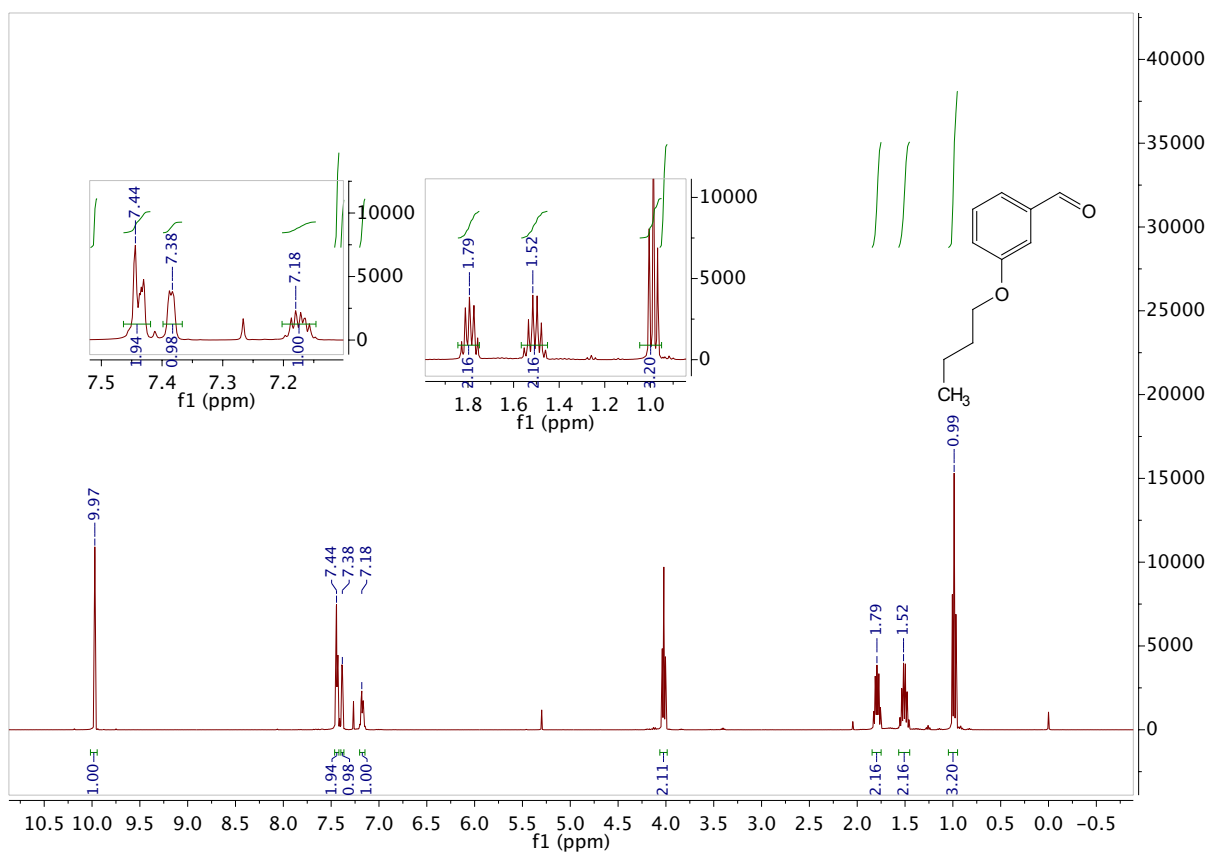
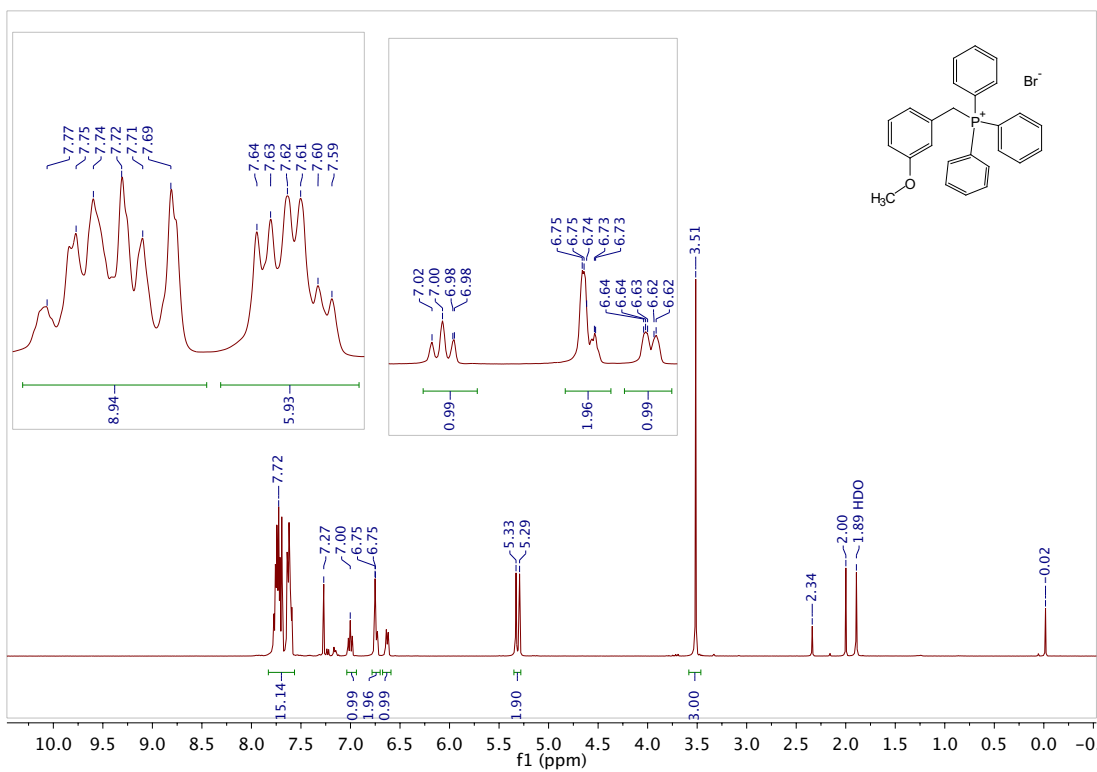


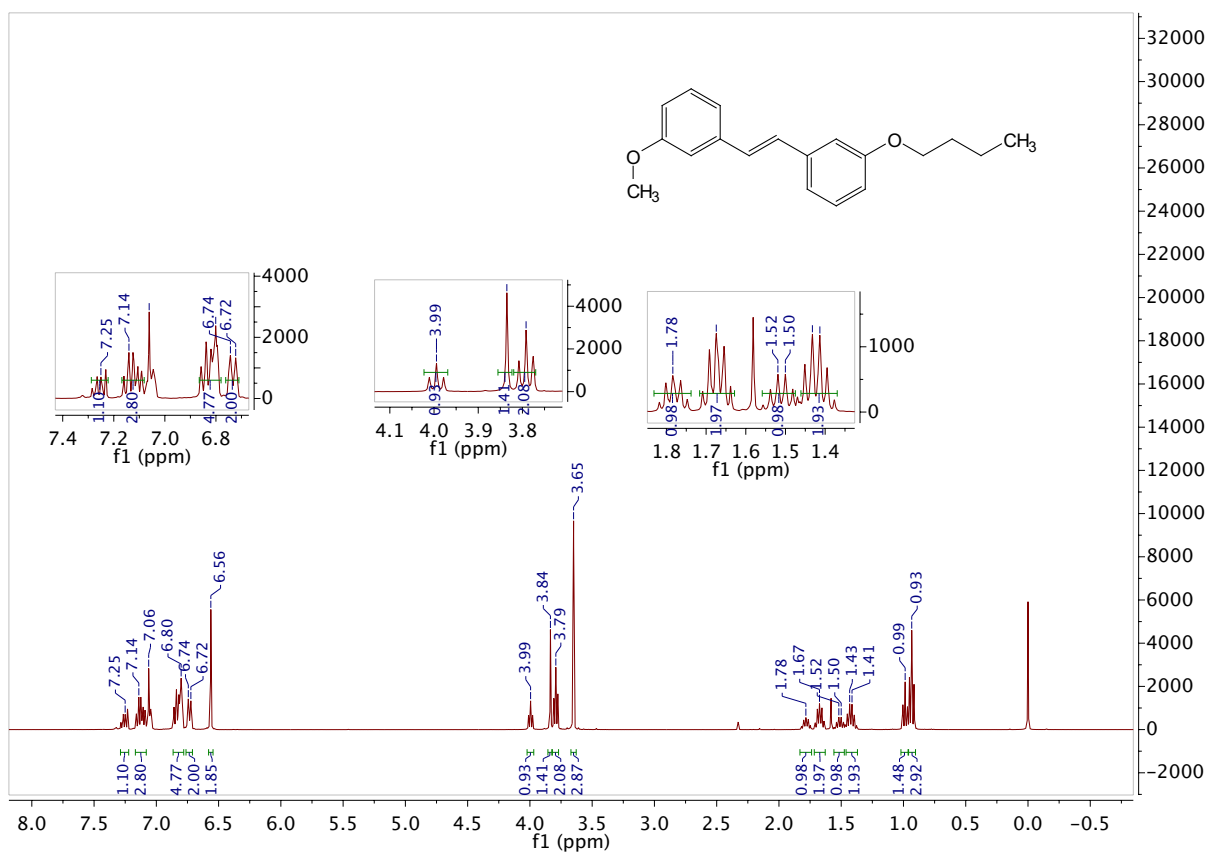


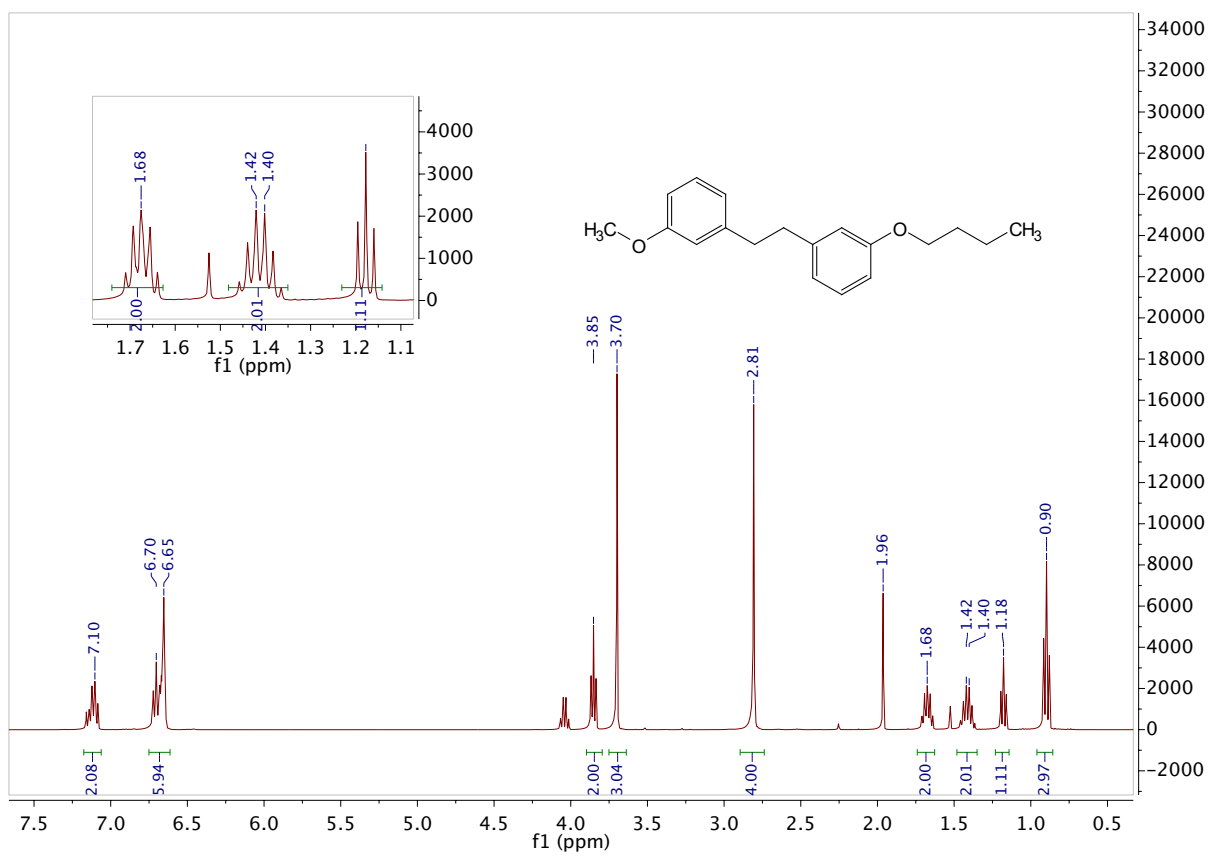
Kinetics in dichloromethane of compound 18, $k = 9.7\text{E-}4 \text{ s}^{-1}$

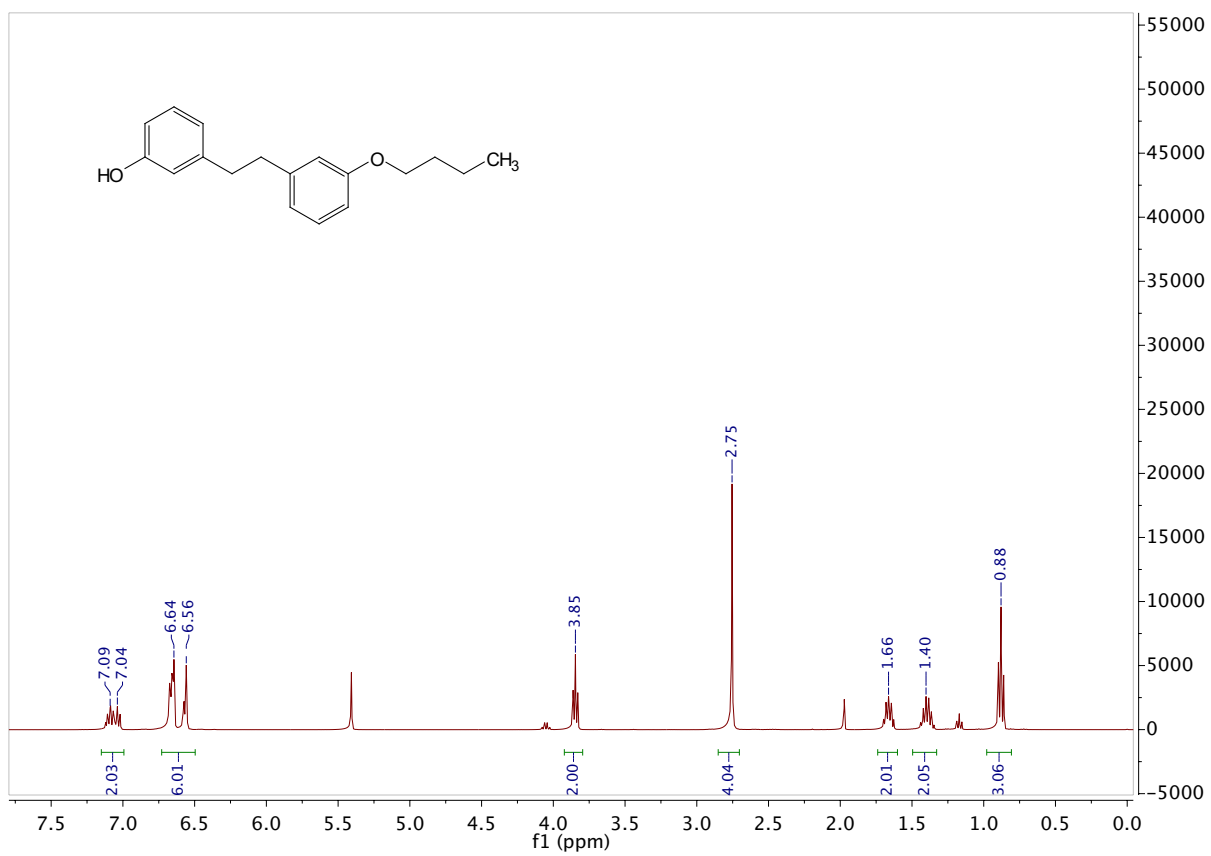


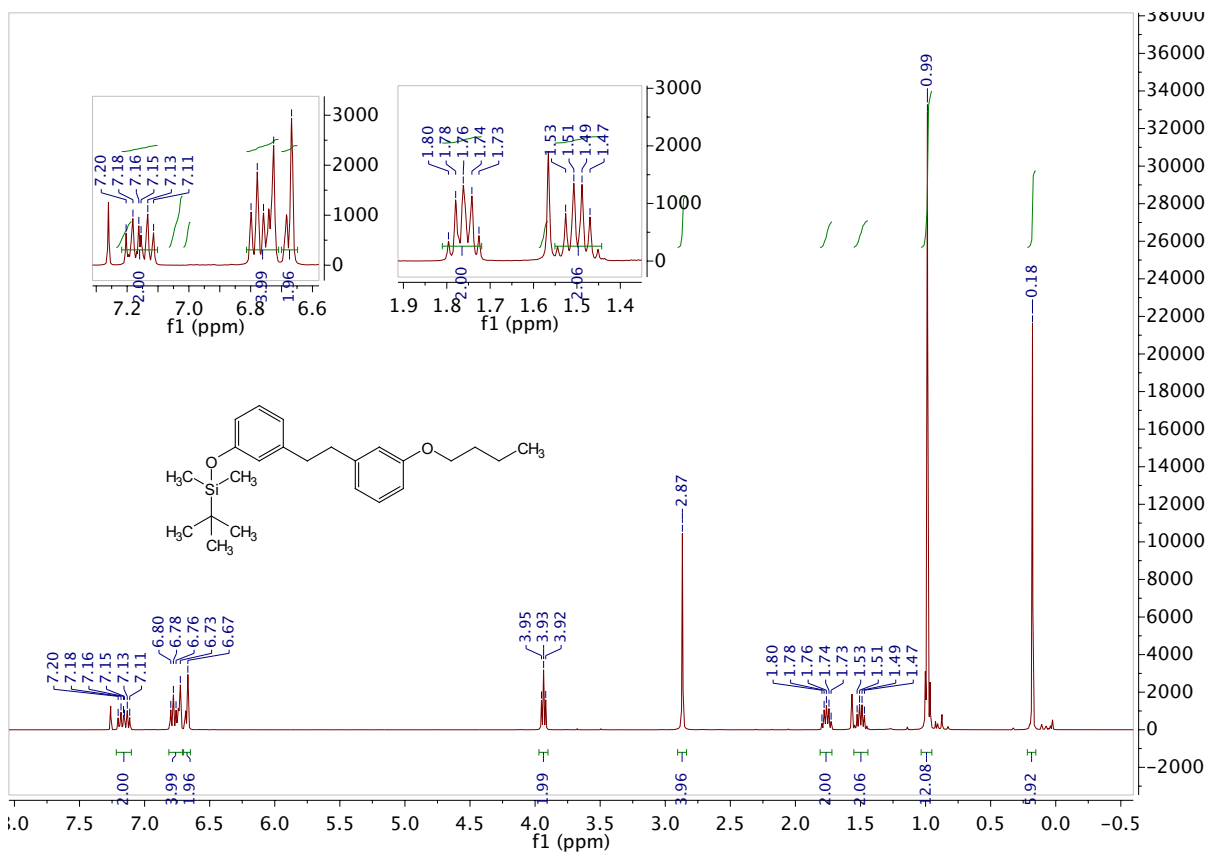
4.3 NMR Data

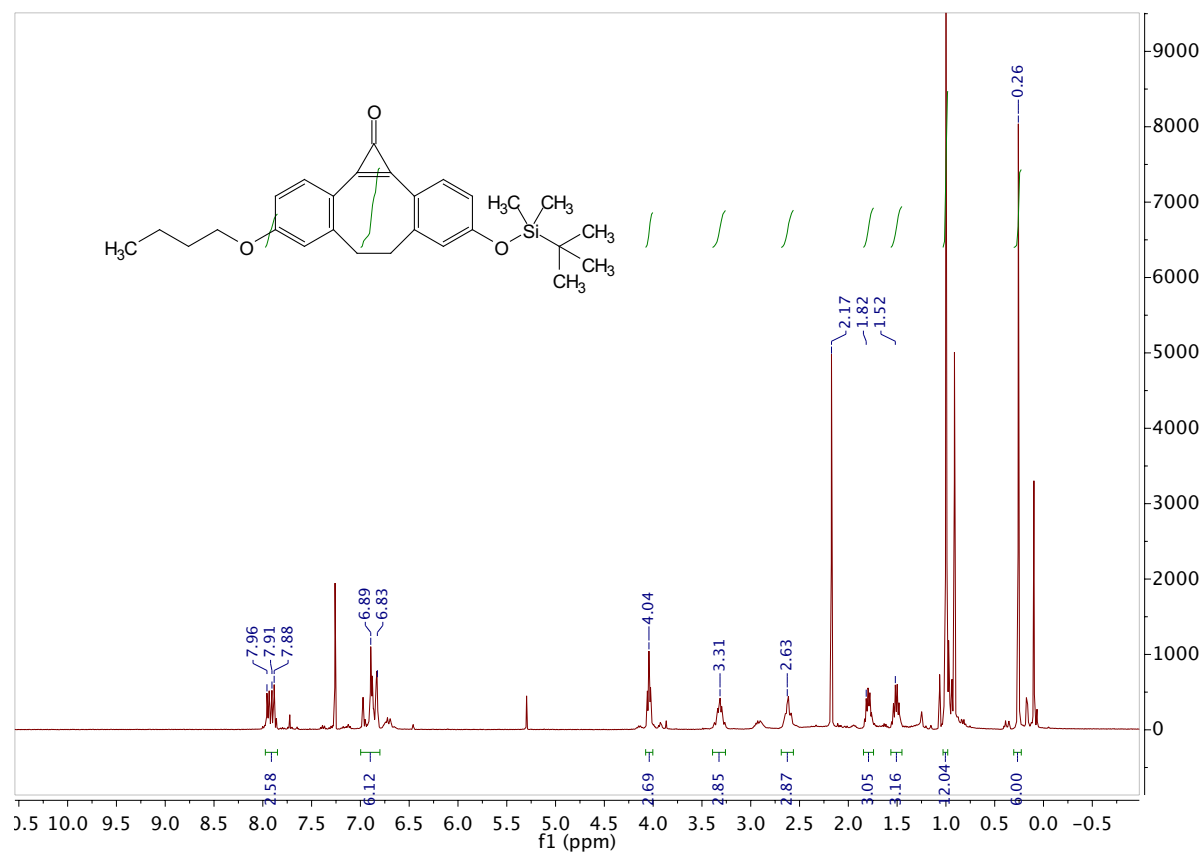




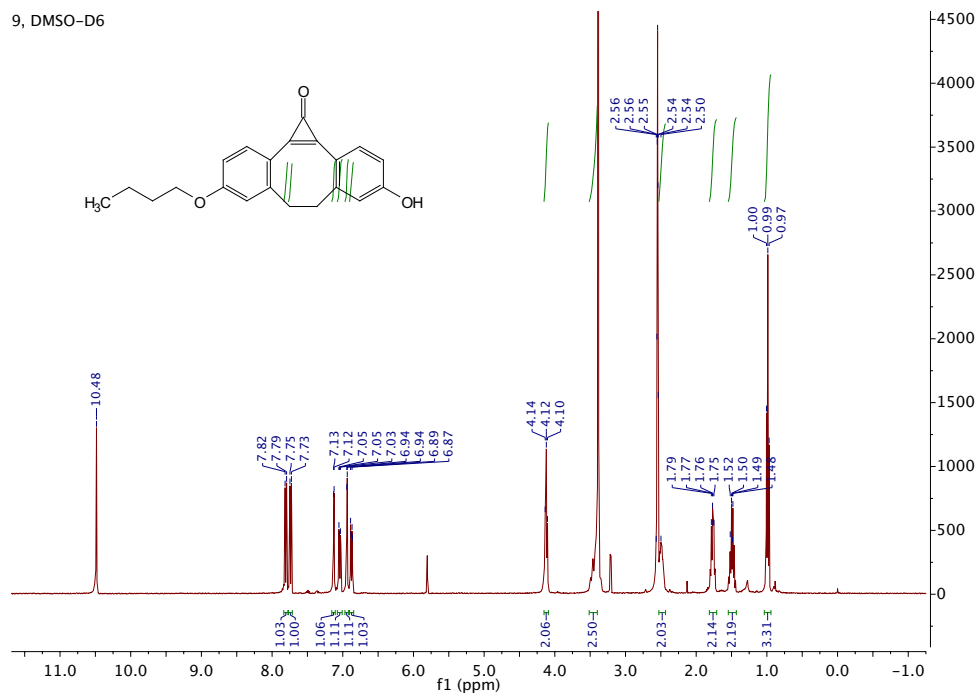








9, DMSO-D6



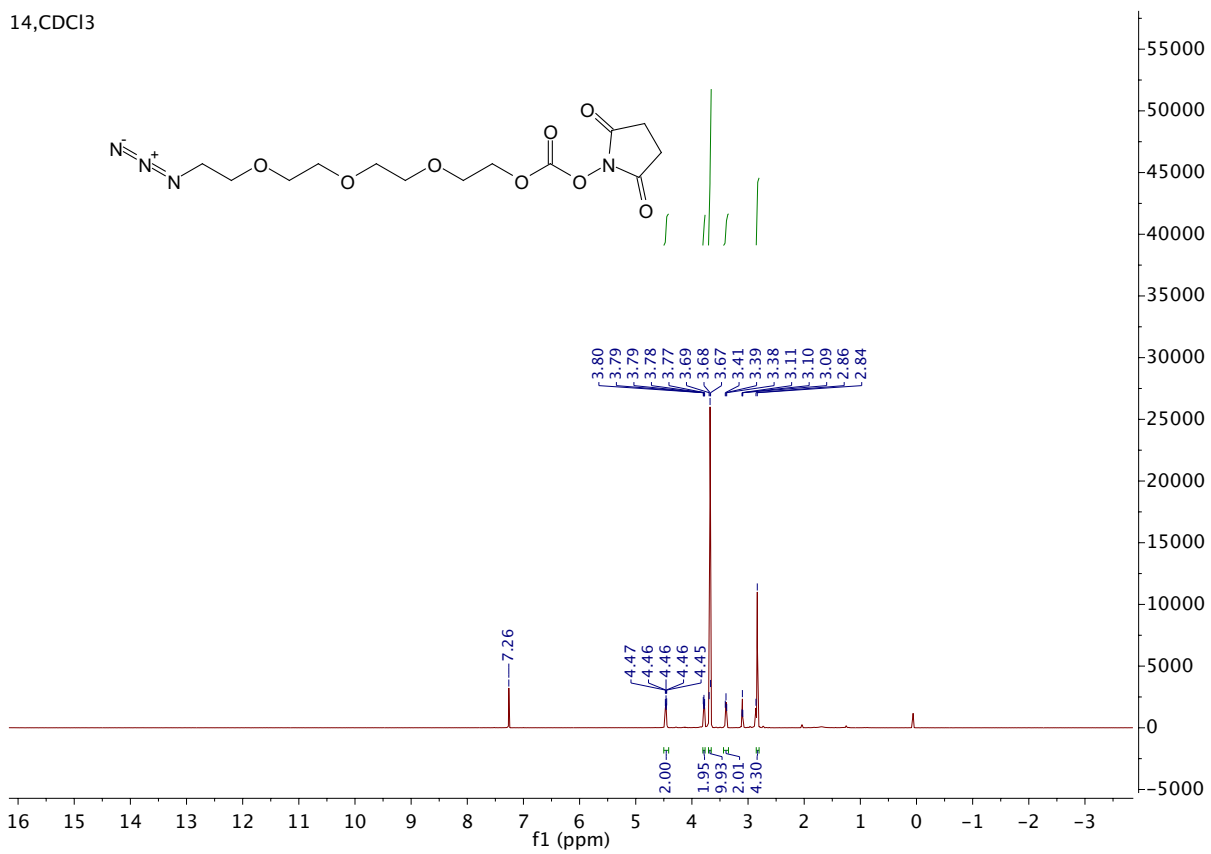


Chemical structure of compound 10 is shown above the spectrum. The spectrum displays peaks corresponding to the ^{13}C NMR data. The x-axis is labeled f1 (ppm) and the y-axis represents intensity.

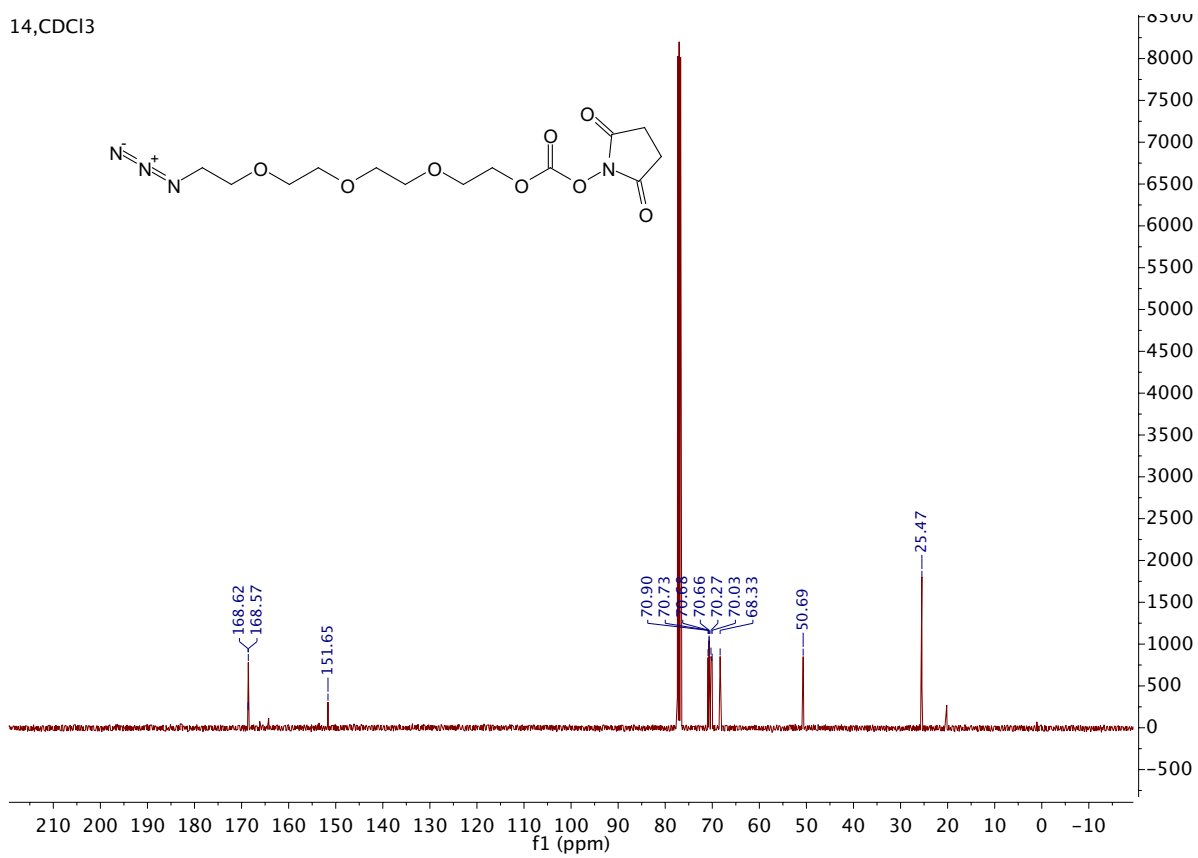
Key peaks (ppm) are labeled:

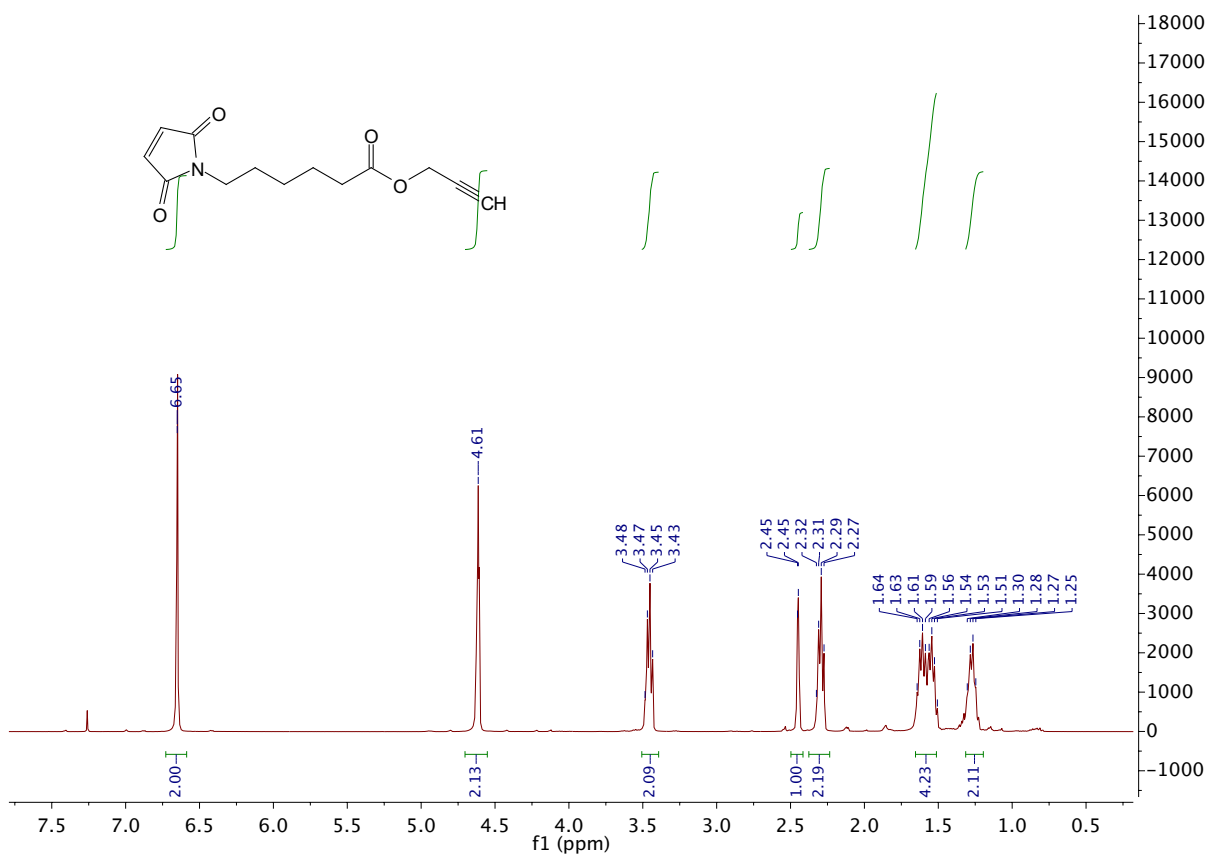
- 162.55, 162.09, 161.59
- 153.79, 147.80, 142.41, 141.98, 135.82, 135.71
- 116.61, 116.35, 116.23, 116.16, 112.37, 112.28
- 70.89, 70.73, 70.71, 70.68, 70.05, 69.52, 68.01, 67.67
- 50.68
- 37.19, 37.16, 31.15
- 19.20, 13.83

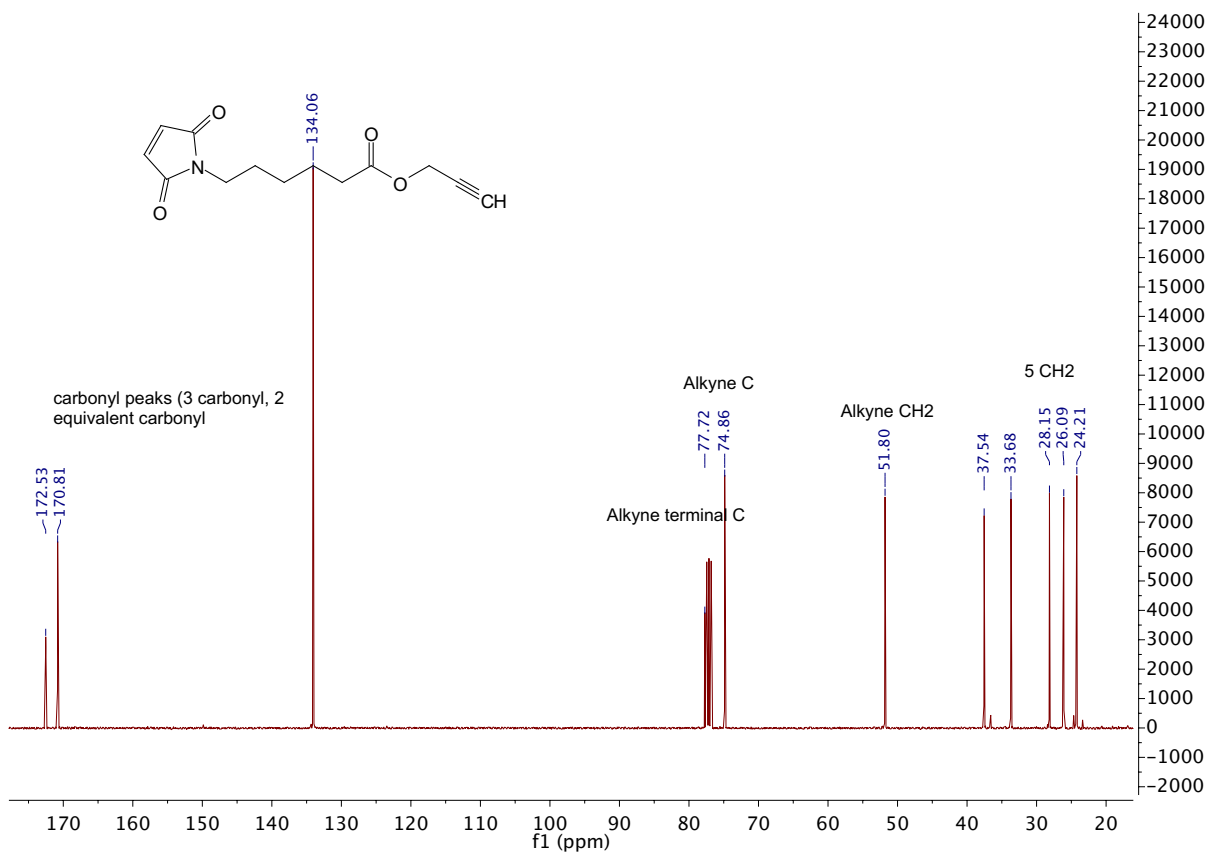
14, CDCl₃

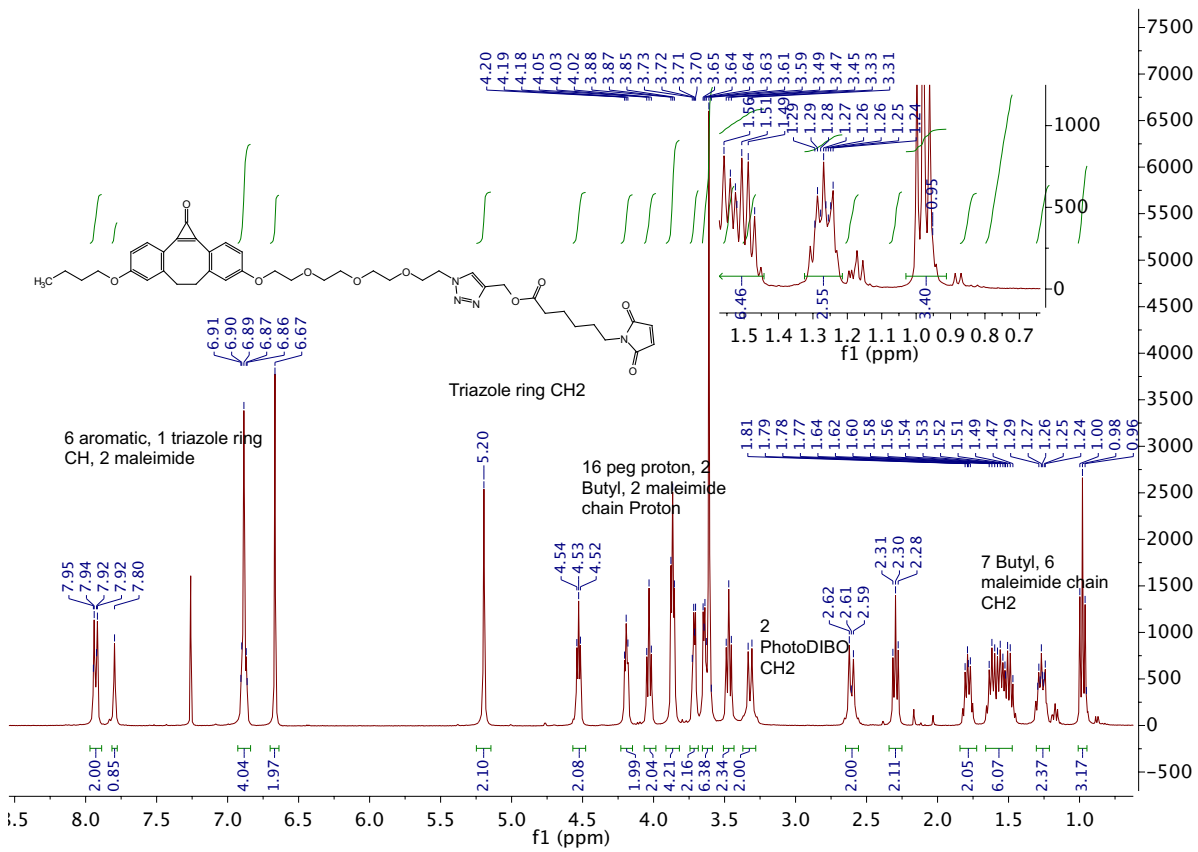


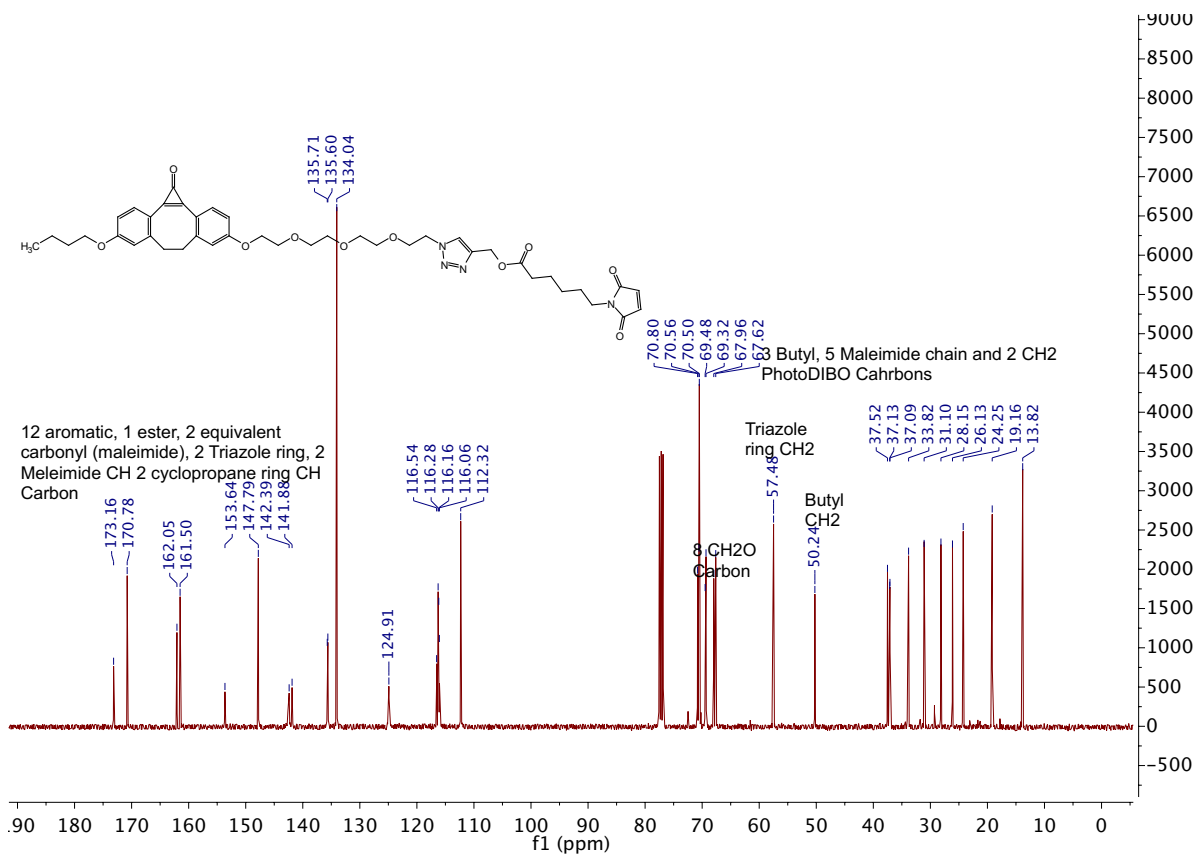
14, CDCl₃

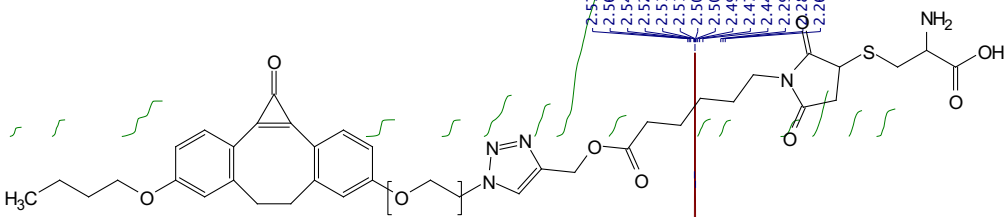


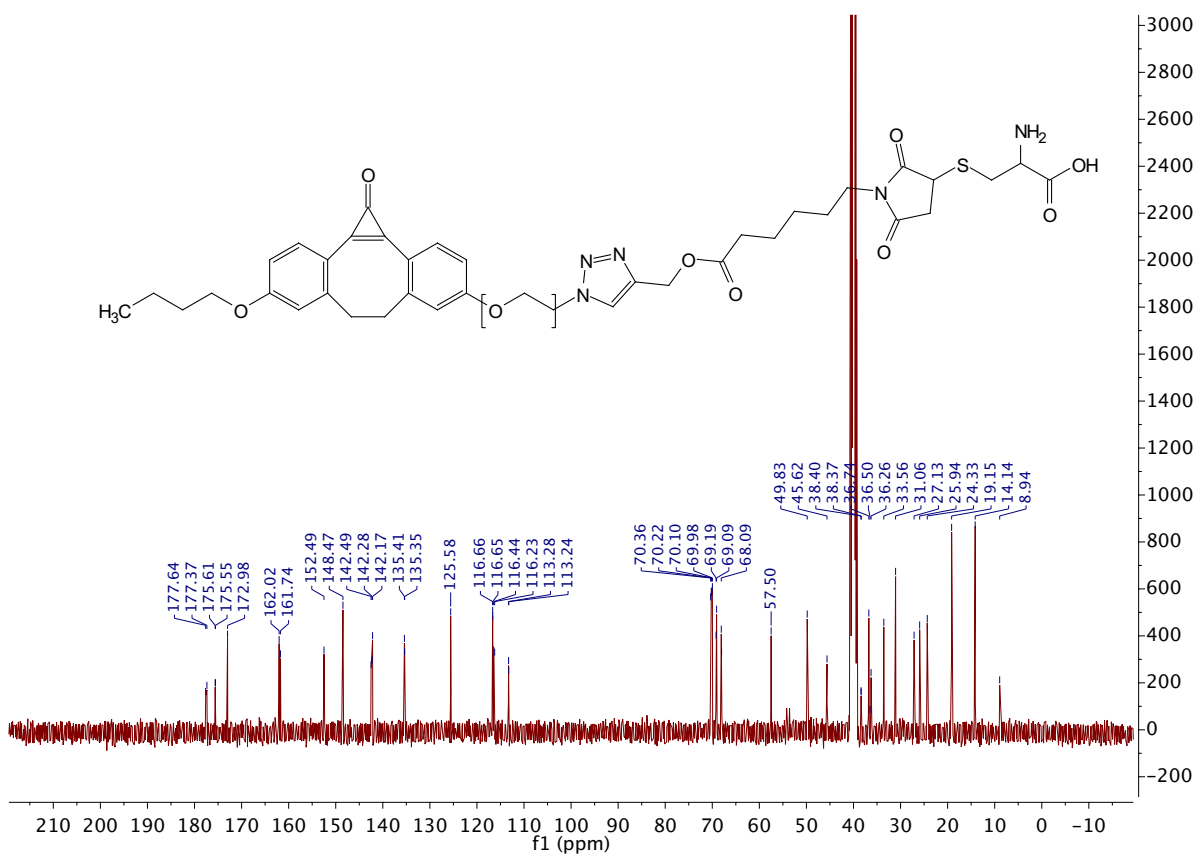


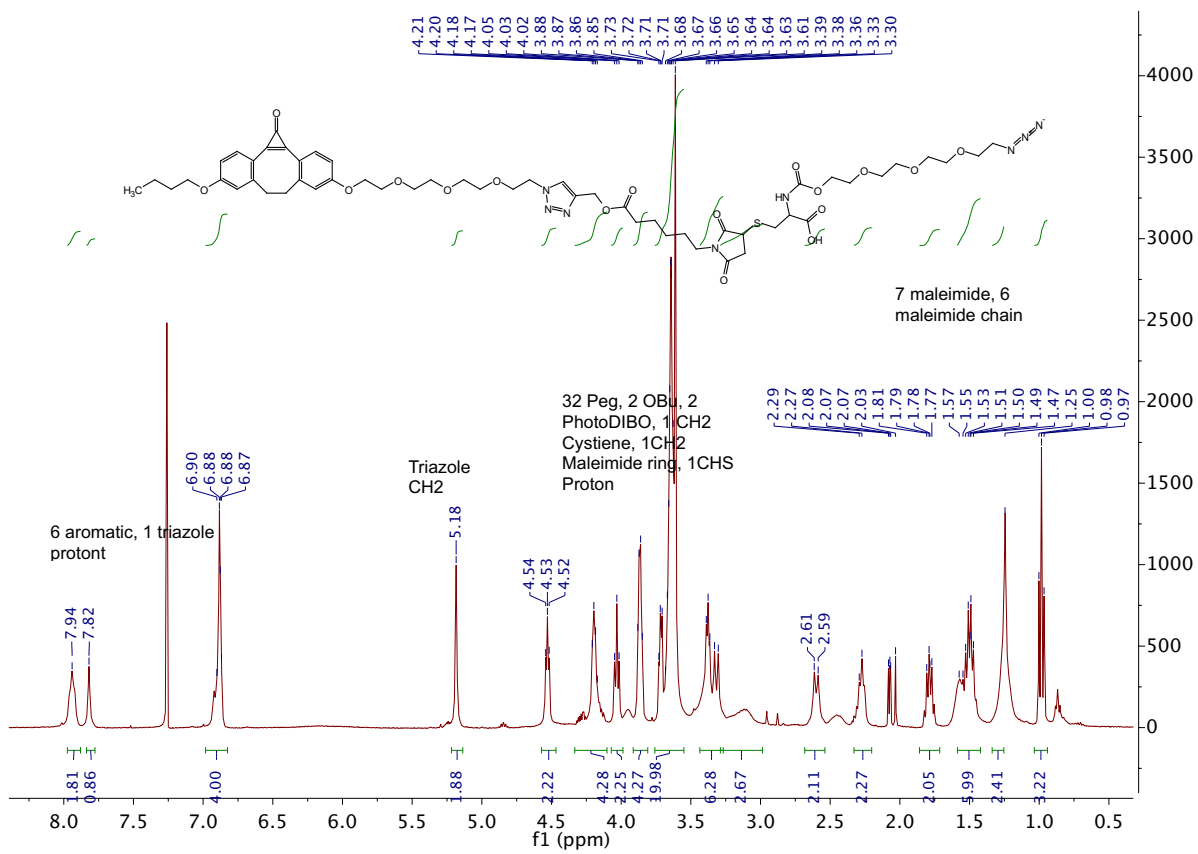


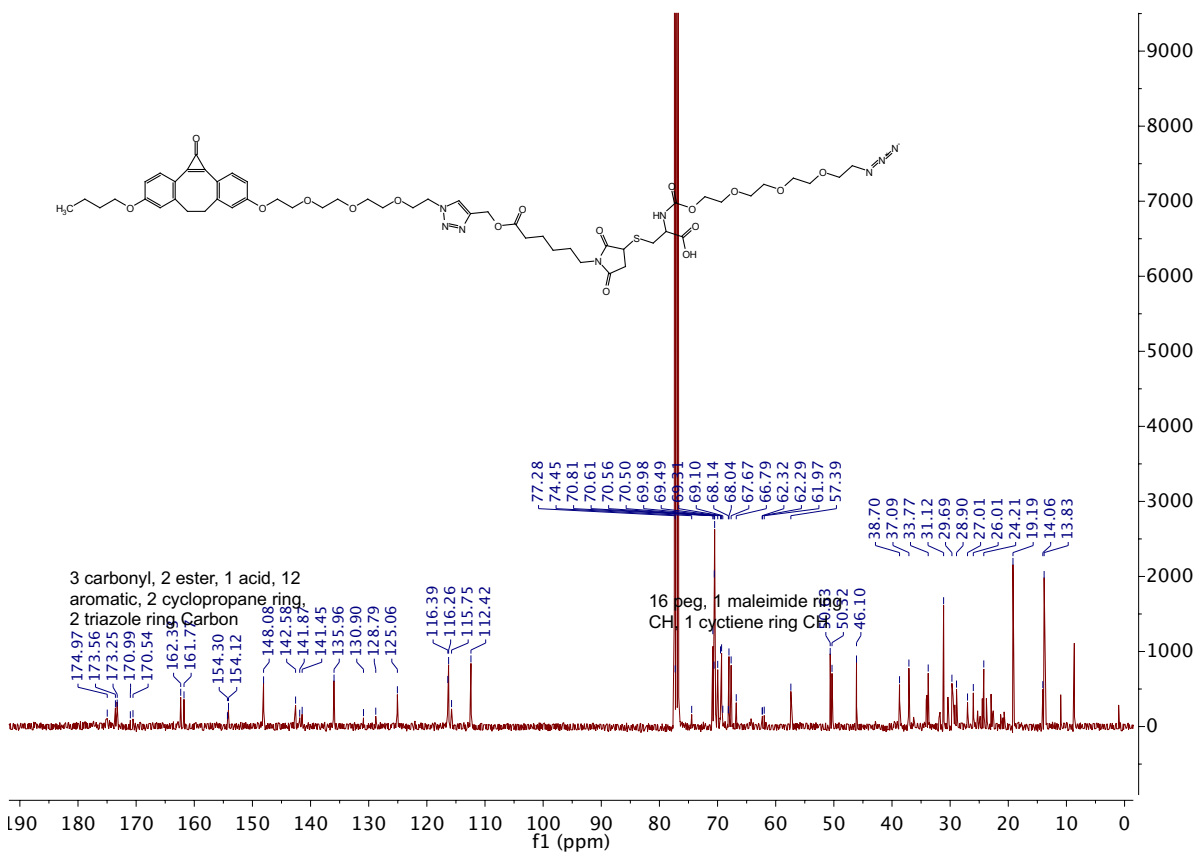


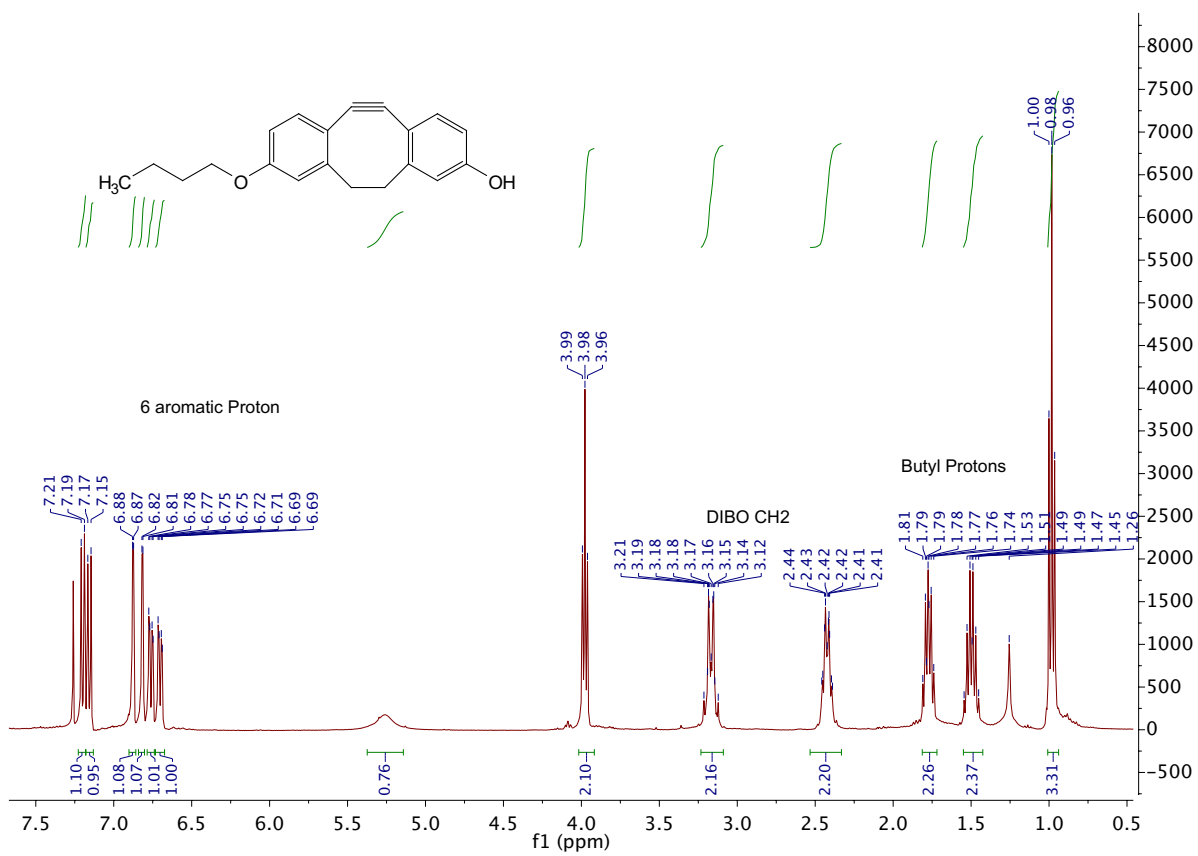


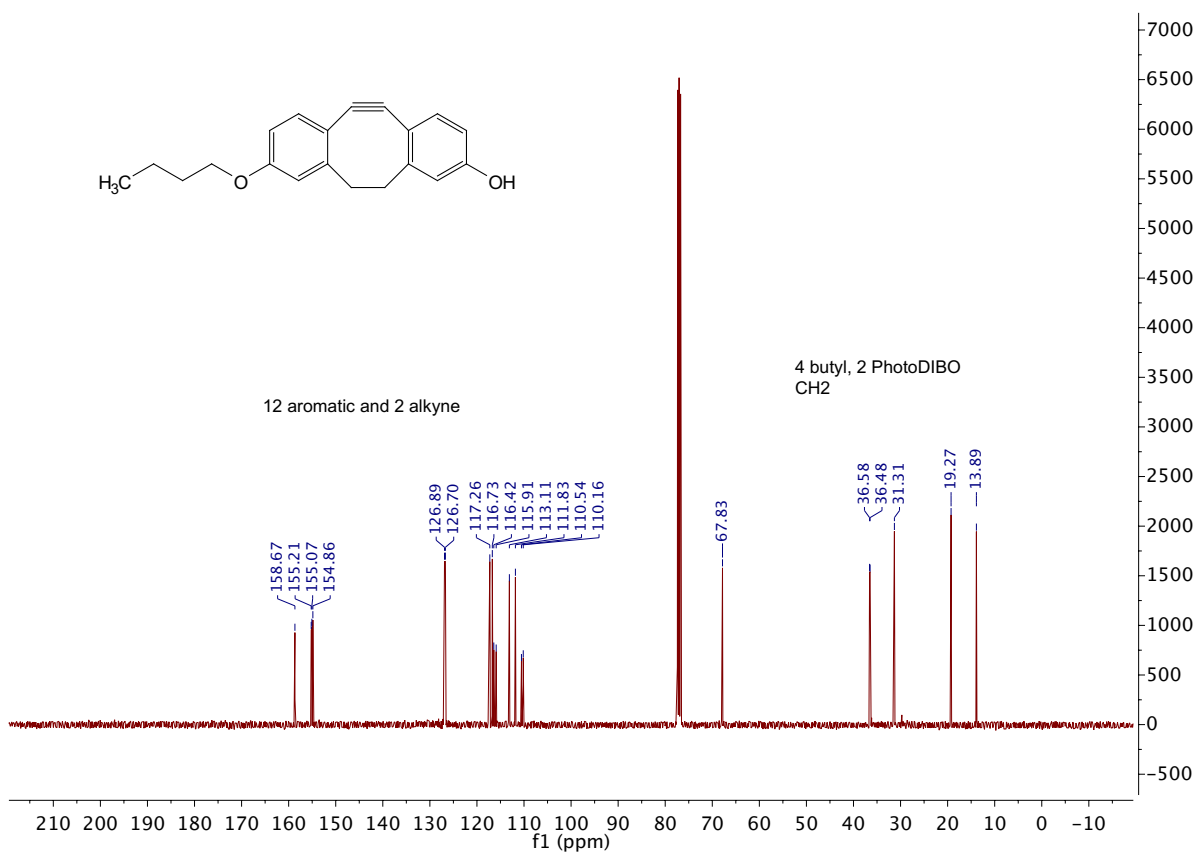








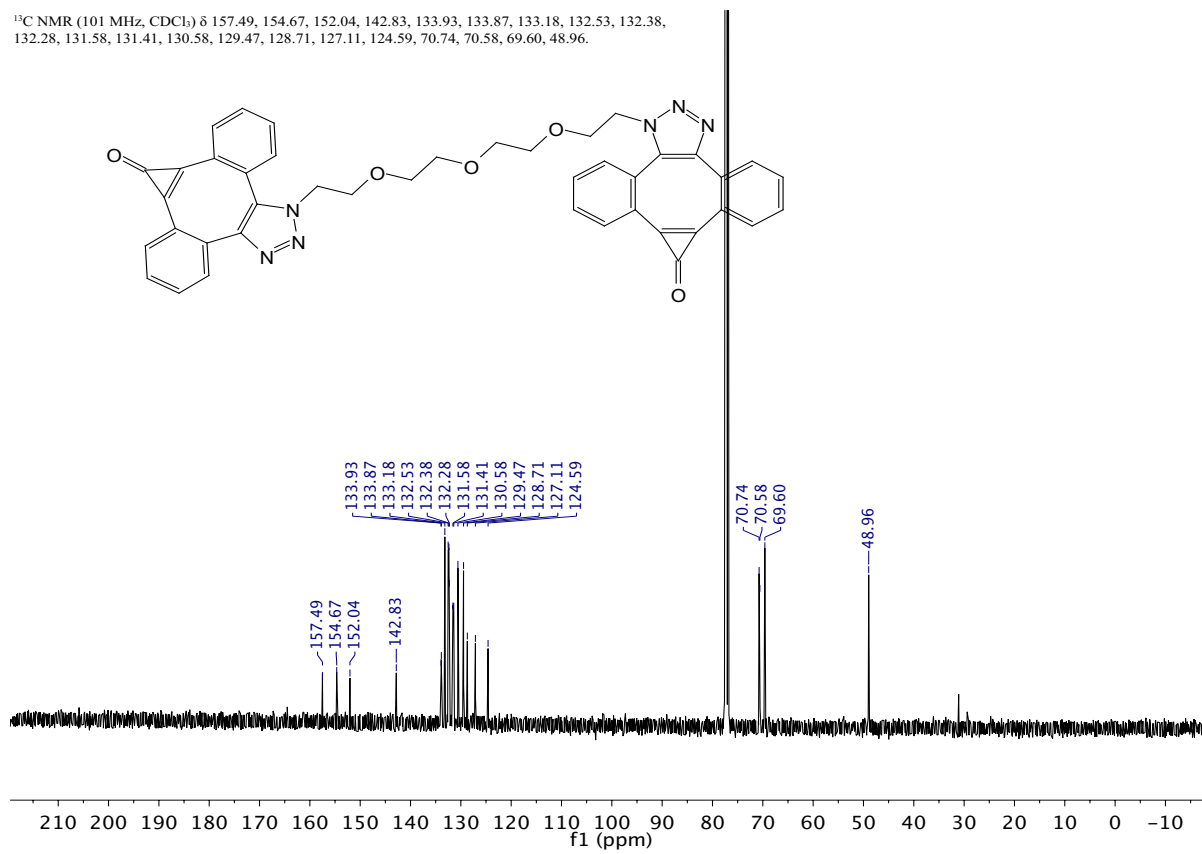


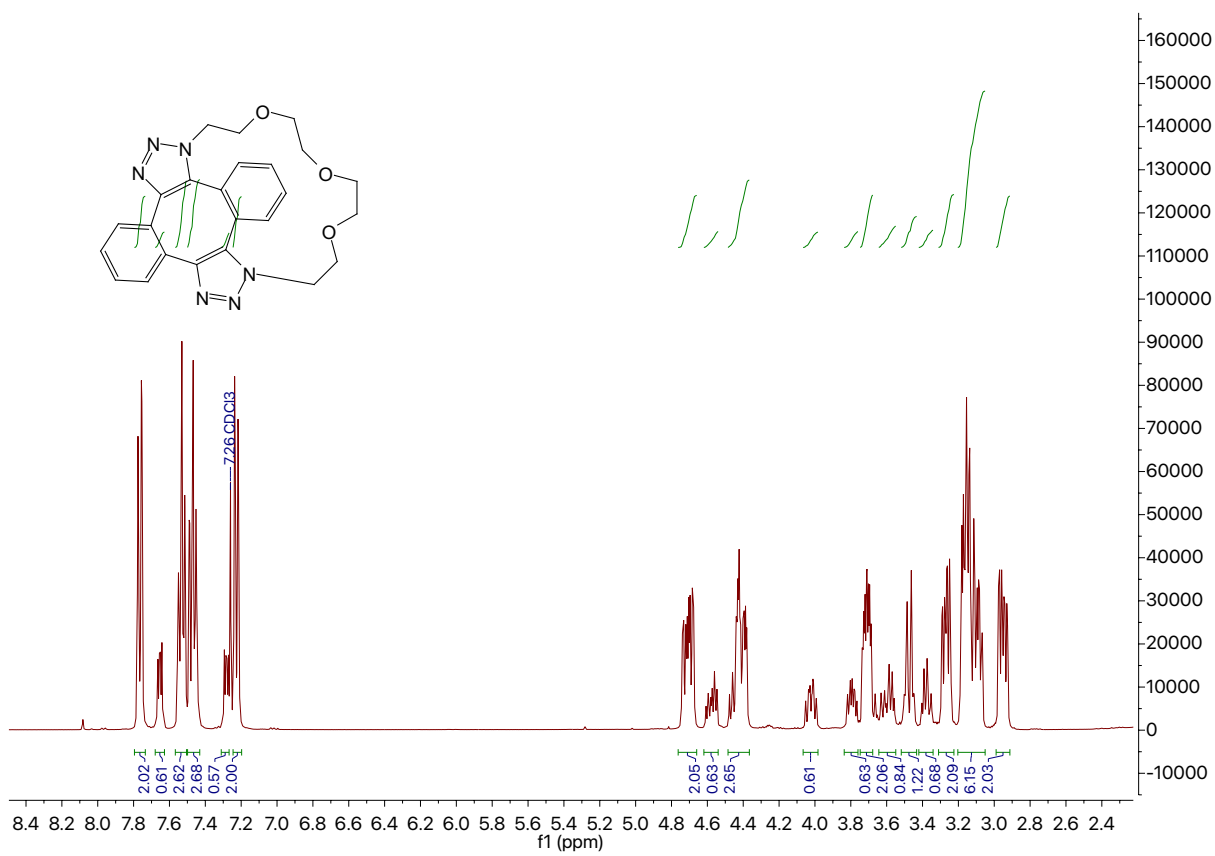


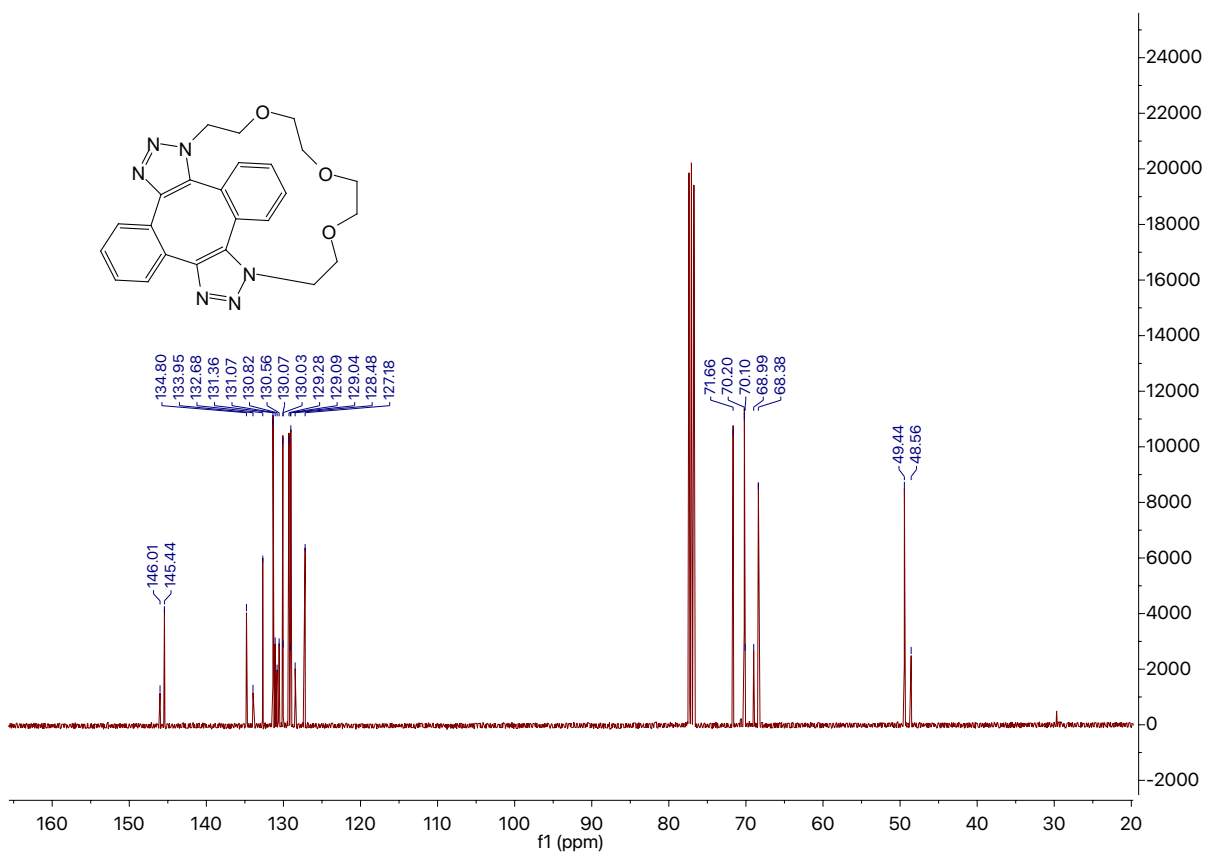
Chemical structure of compound 10 is shown above the spectrum. The spectrum displays peaks from 0.5 to 8.5 ppm. Aromatic protons appear as a complex multiplet between 7.2 and 7.7 ppm. A large solvent peak for CDCl₃ is at 7.26 ppm. Protons on the triazole ring and the linker are visible between 3.4 and 4.5 ppm. A sharp singlet at 2.17 ppm corresponds to the methyl group. Integration values are provided below the baseline for several peak groups.

Chemical Shift (ppm)	Integration
7.26	2.00
7.20 - 7.30	2.00
7.30 - 7.40	10.25
7.40 - 7.50	2.08
4.40 - 4.50	2.01
4.20 - 4.30	2.02
3.90 - 4.00	2.01
3.70 - 3.80	2.02
3.40 - 3.50	3.00
2.17	-

^{13}C NMR (101 MHz, CDCl_3) δ 157.49, 154.67, 152.04, 142.83, 133.93, 133.87, 133.18, 132.53, 132.38, 132.28, 131.58, 131.41, 130.58, 129.47, 128.71, 127.11, 124.59, 70.74, 70.58, 69.60, 48.96.



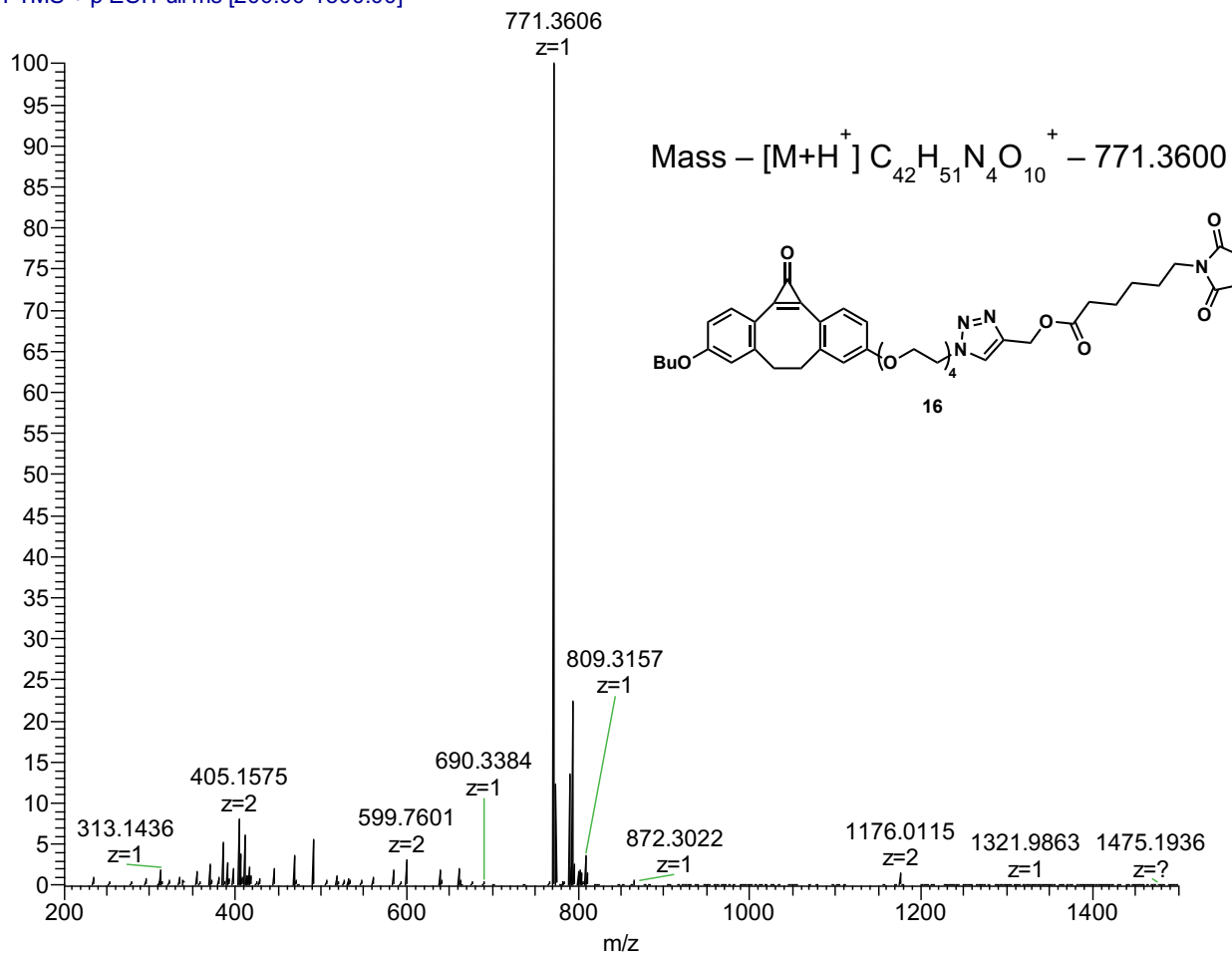




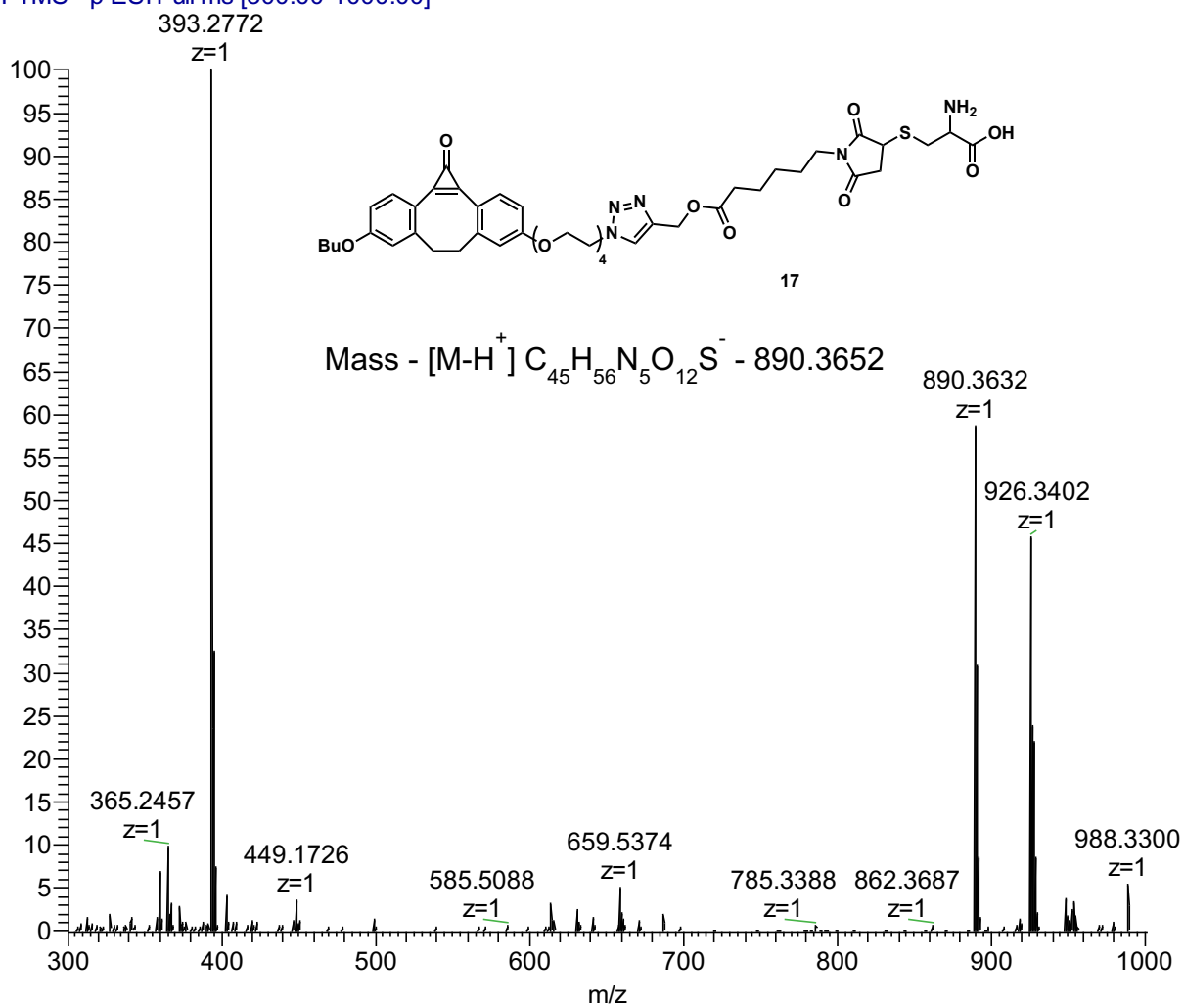
4.4 Mass DATA

SS_2019-0228_01 #33-41 RT: 0.68-0.84 AV: 9 SB: 68 08 NL: 1.90E5

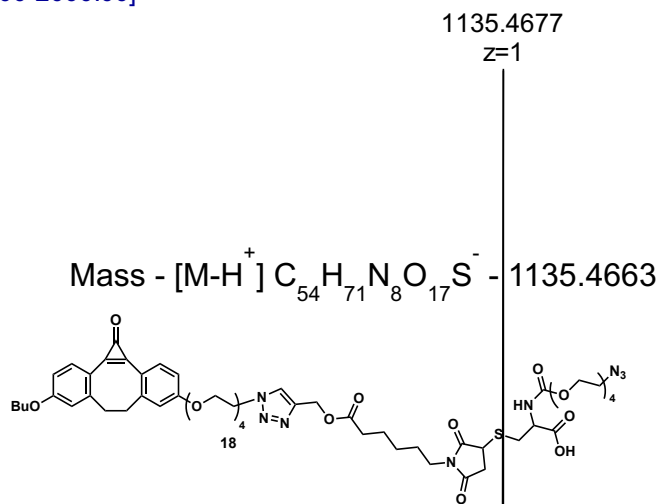
T: FTMS + p ESI Full ms [200.00-1500.00]



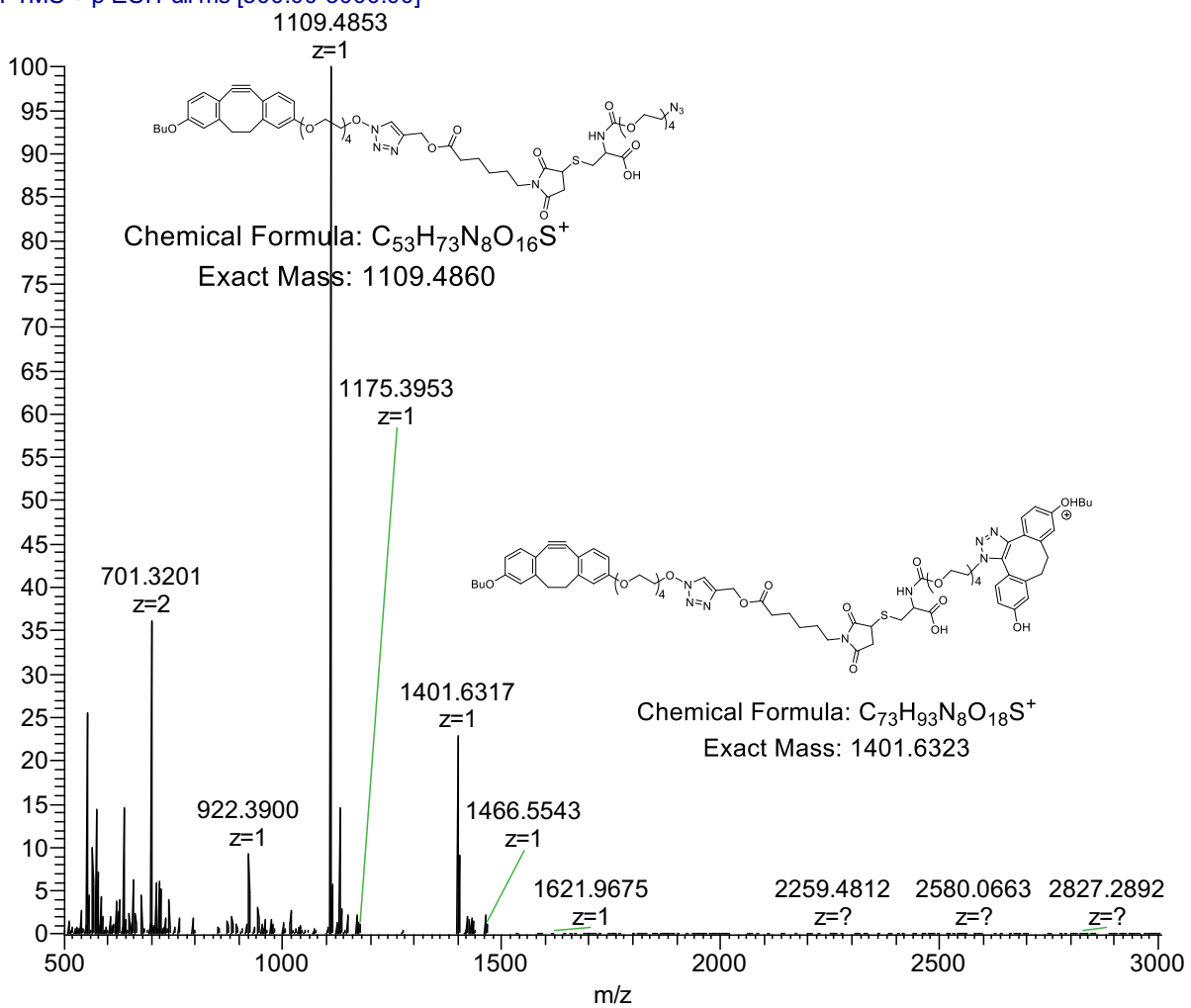
S_2019-0321N_49 #151-196 RT: 1.63-2.08 AV: 46 N :5
T: FTMS - p ESI Full ms [300.00-1000.00]



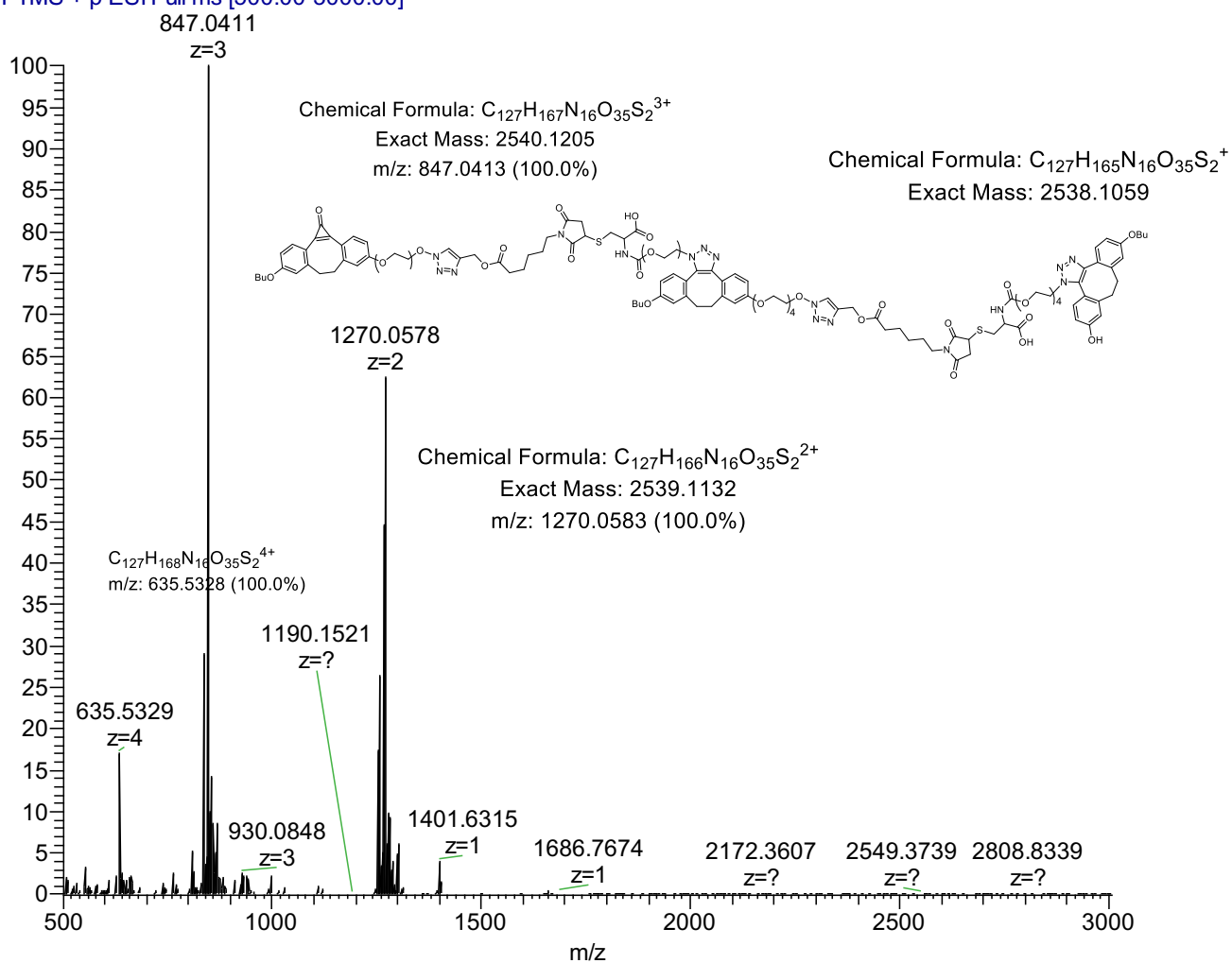
T: $\bar{F}TMS - p\ ESI\ Full\ ms\ [150.00-2000.00]$



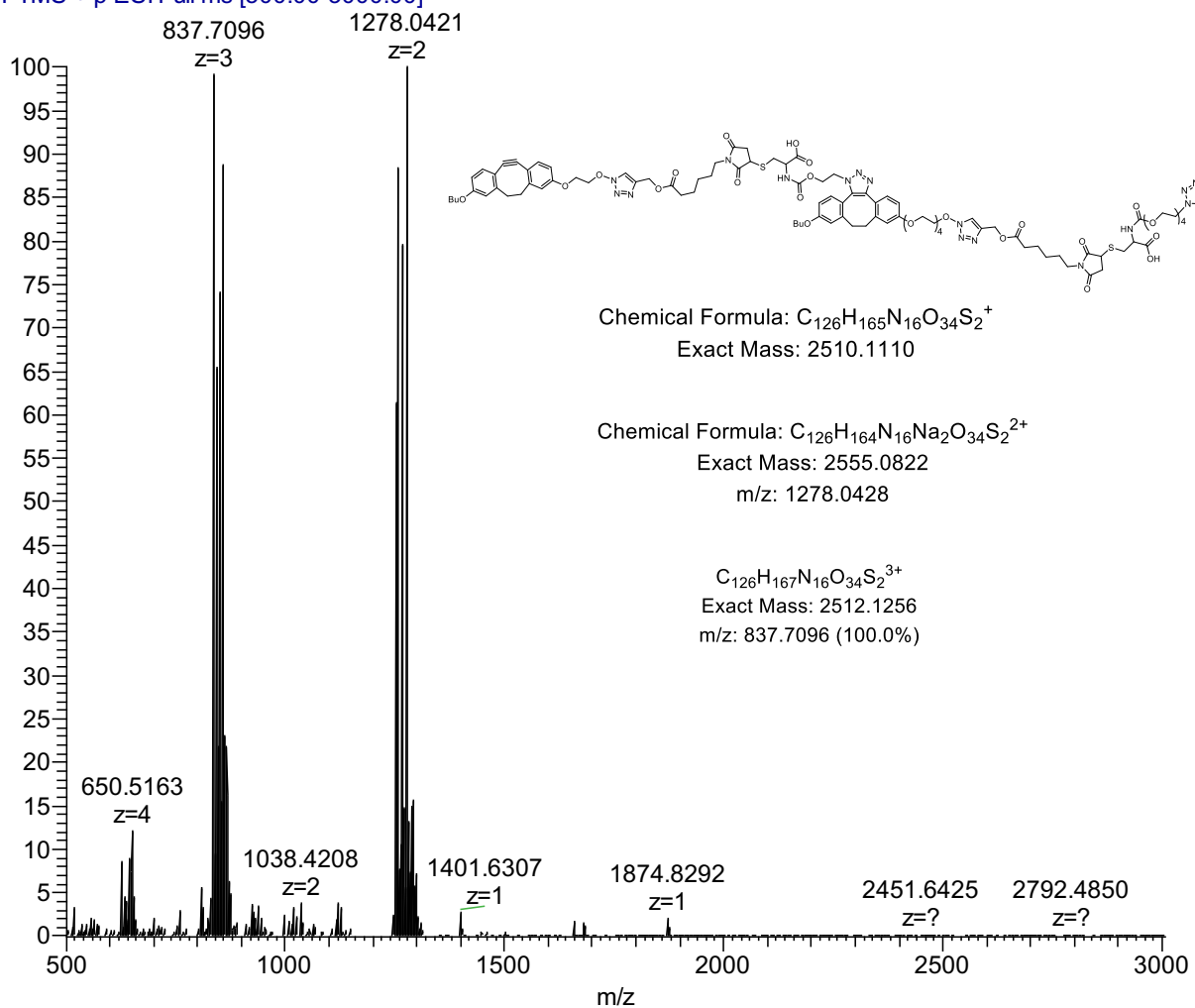
T: FTMS + p ESI Full ms [500.00-3000.00]



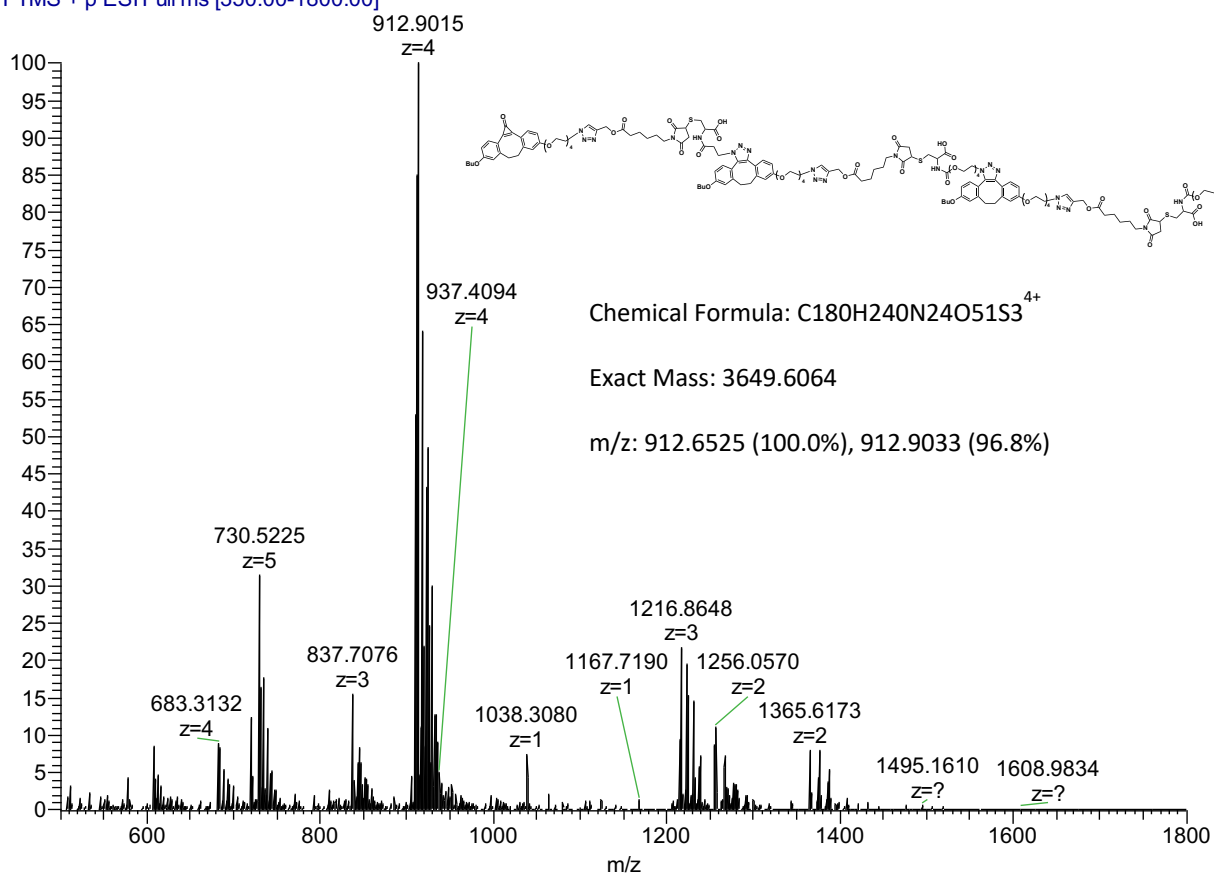
SS_2019-0613_56HP #260-301 RT: 2.26-2.54 AV: 33 : 0.05-0.39 NL: 4.69E5
T: FTMS + p ESI Full ms [500.00-3000.00]



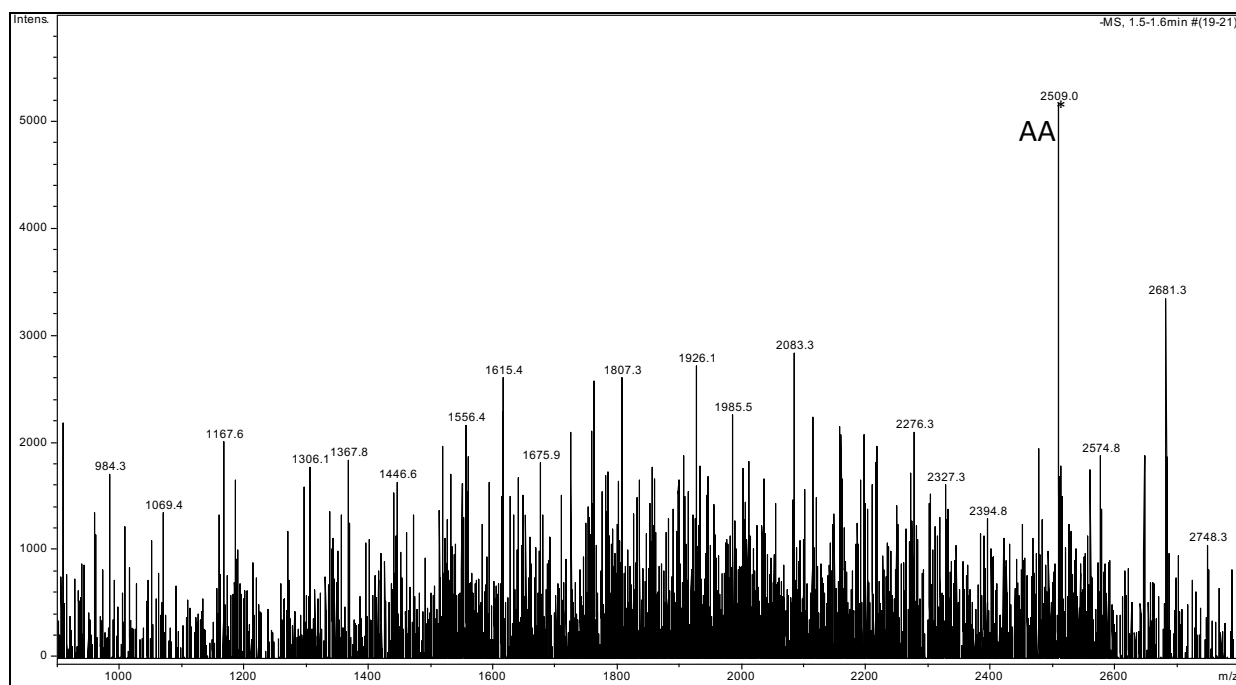
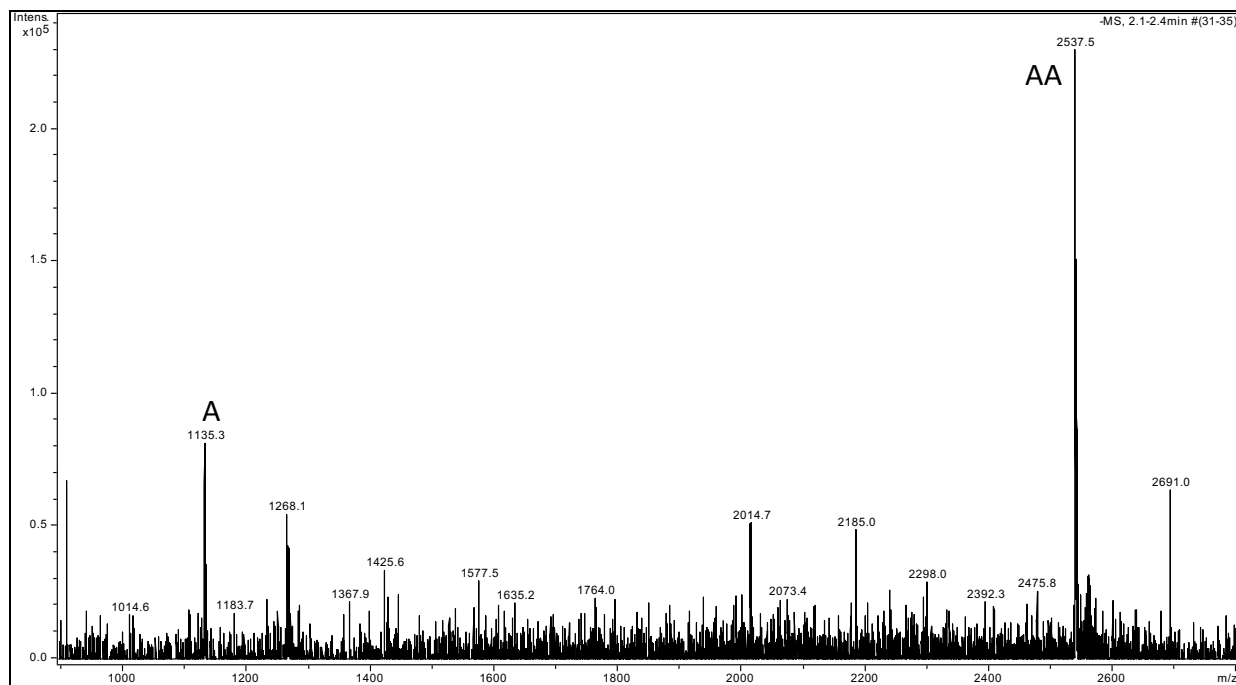
SS_2019-0613_57HP #286-305 RT: 2.34-2.48 AV: 20 : 1.76-2.11 NL: 5.55E5
T: FTMS + p ESI Full ms [500.00-3000.00]

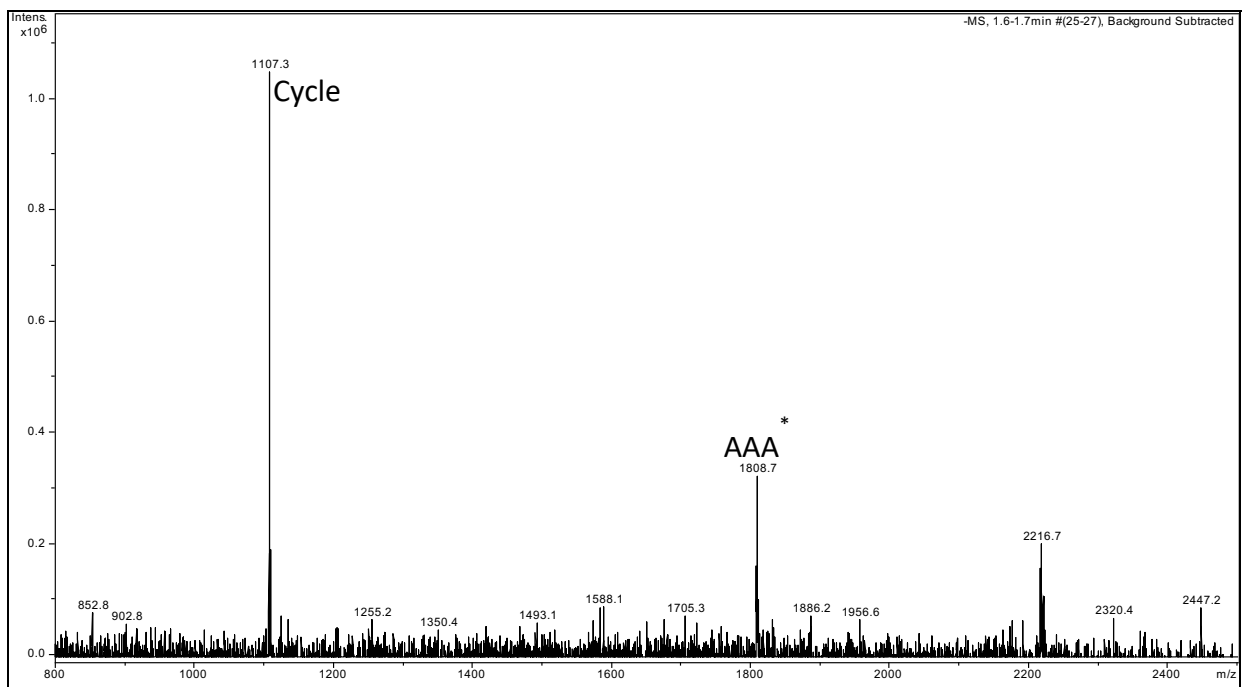
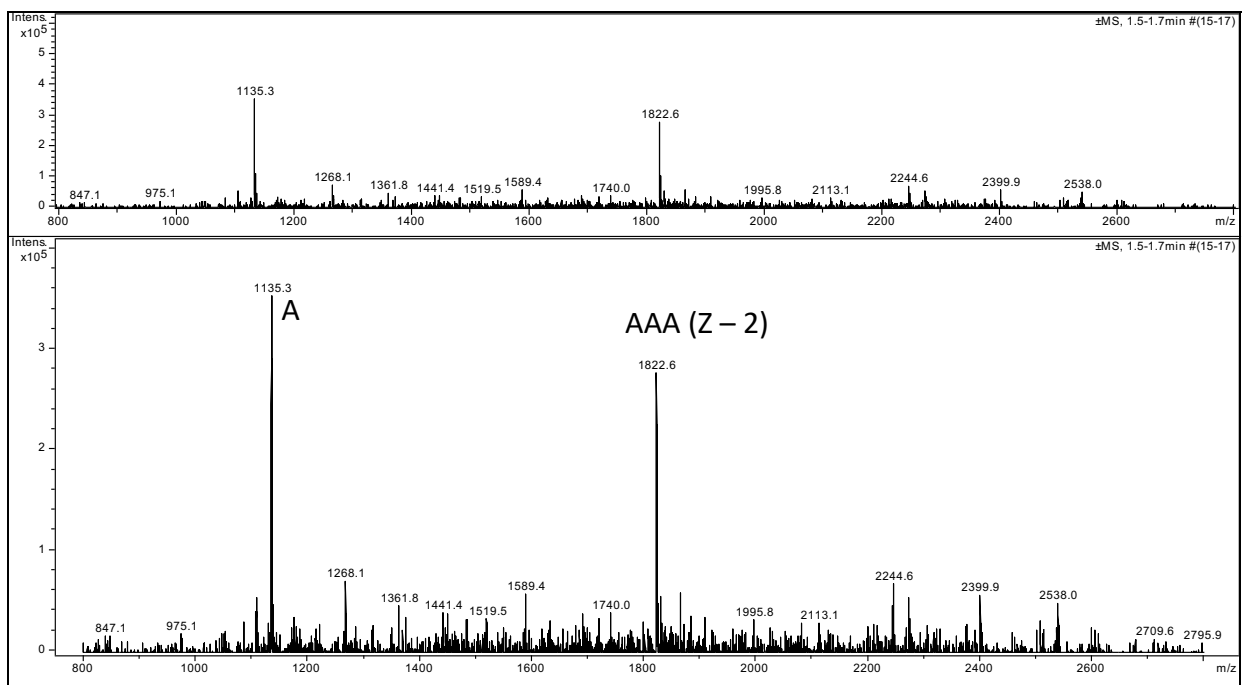


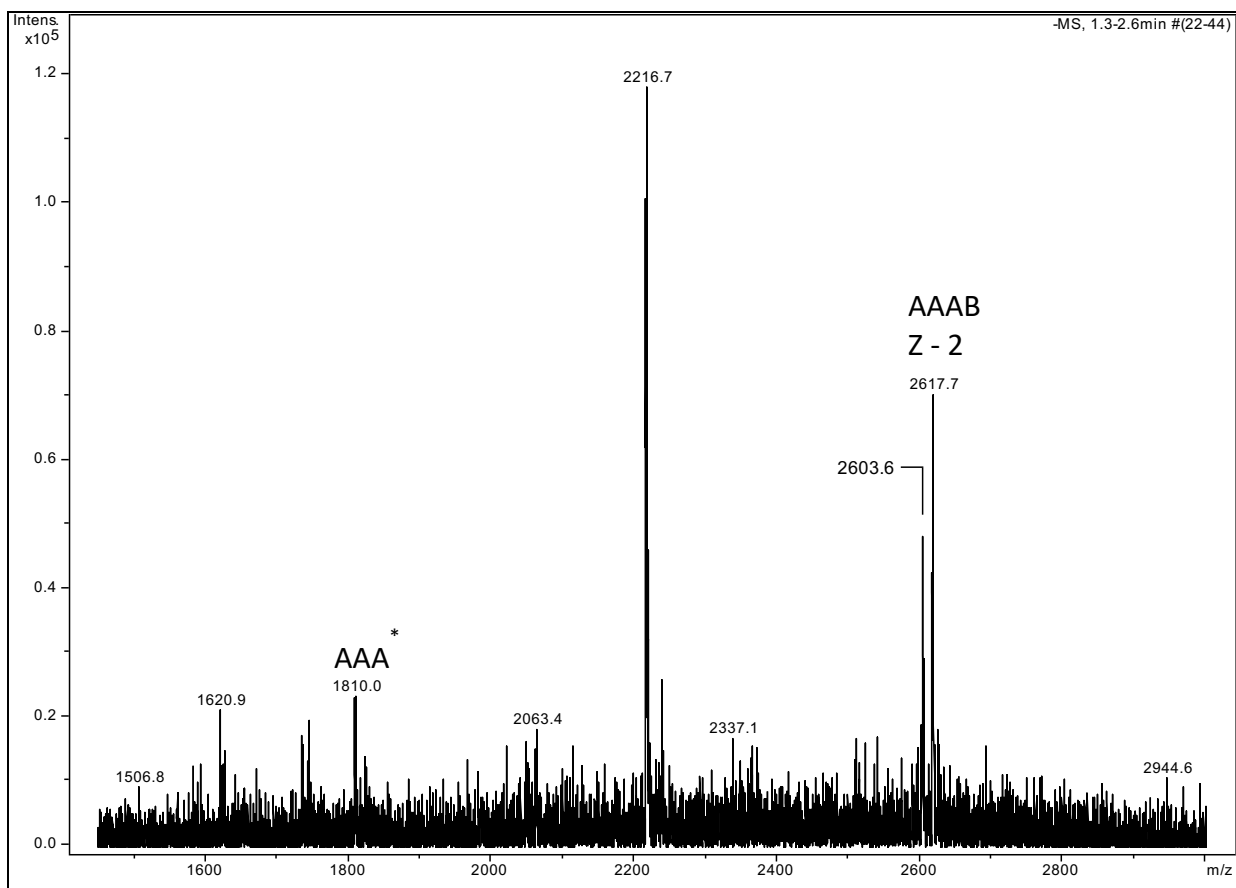
SSI 2019-0808_2 #428-430 RT: 3.38-3.40 AV: 3 NL:
T: FTMS + p ESI Full ms [350.00-1800.00]

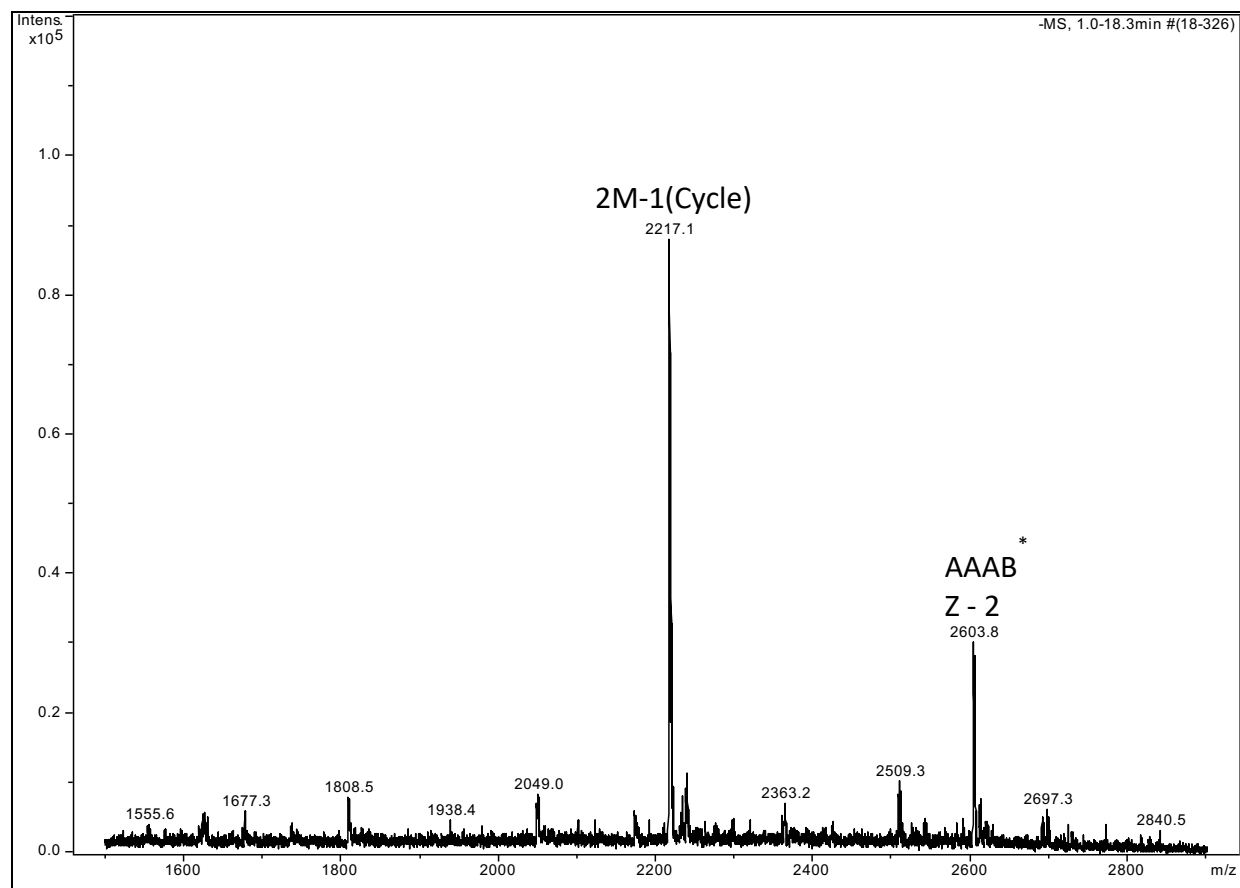


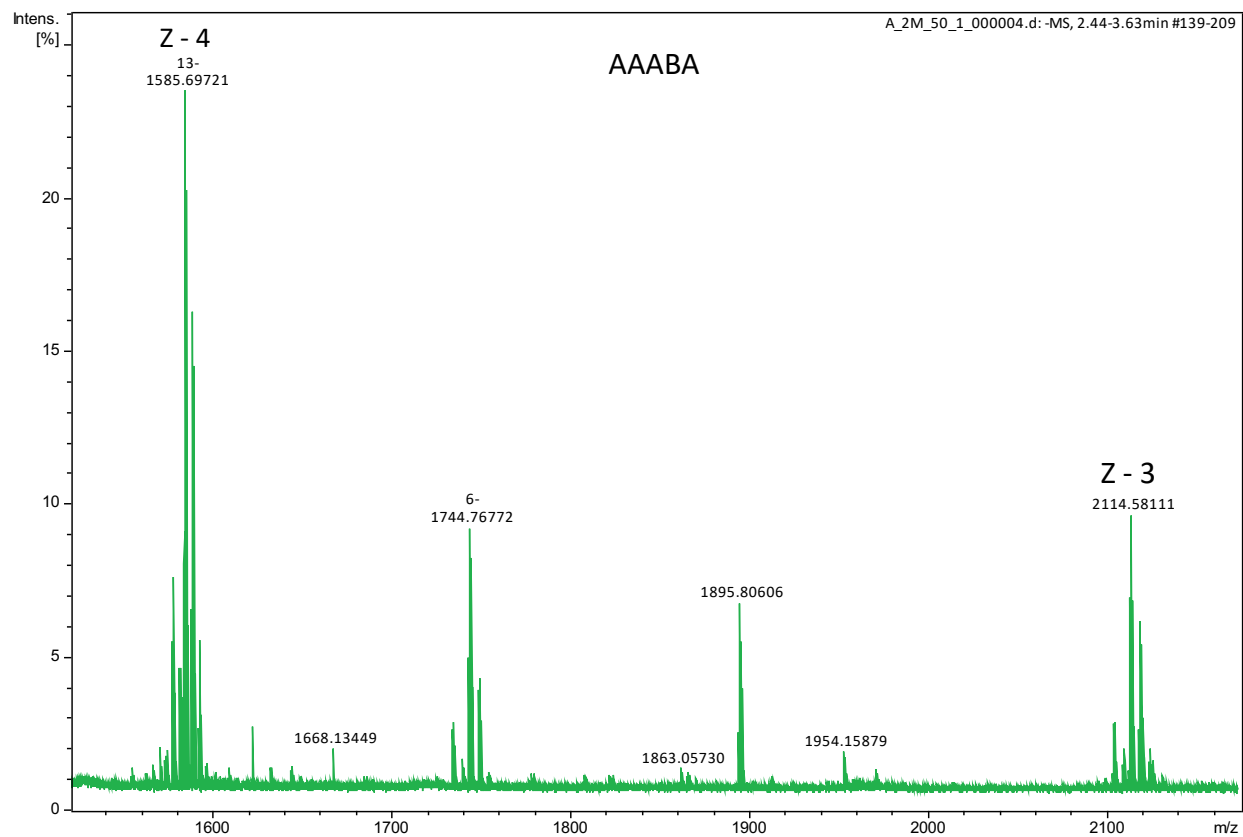
Pentamer Mass Data

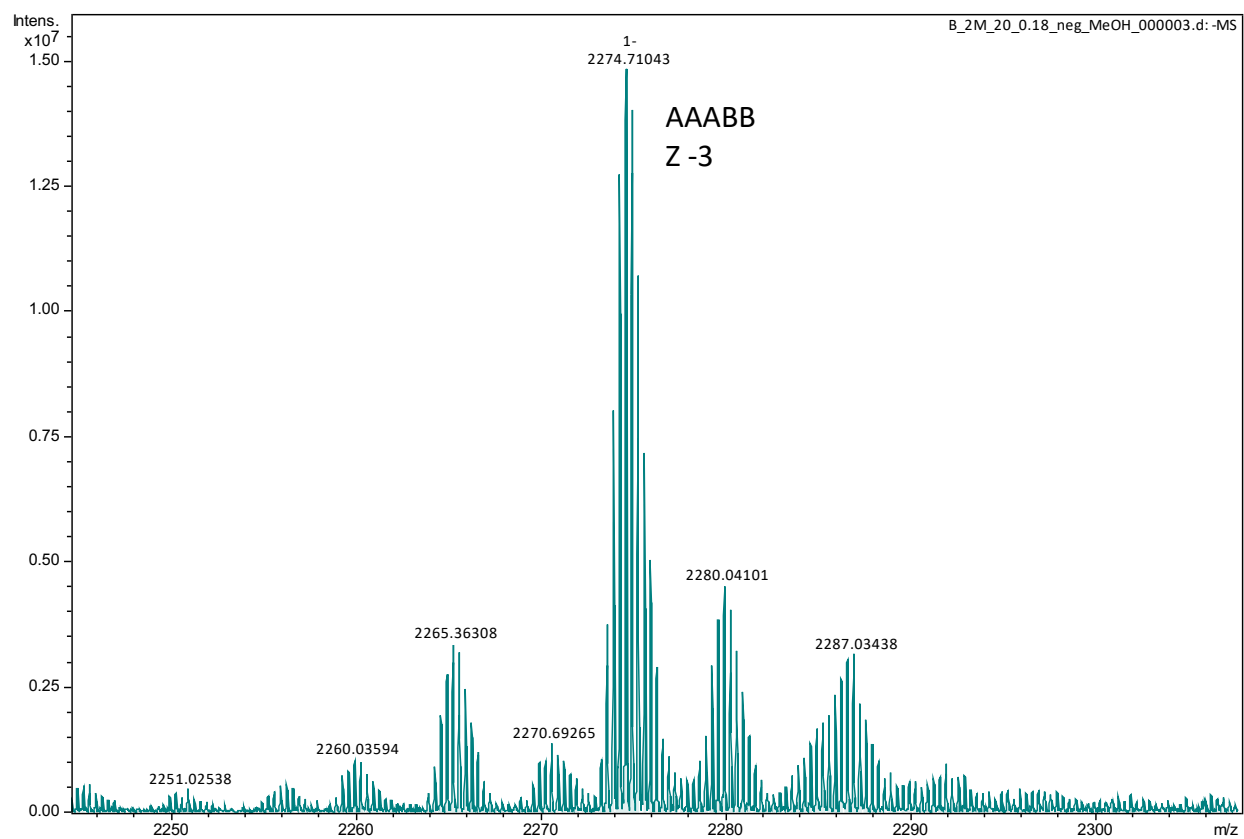












References

1. Rostovtsev, V. V.; Green, L. G.; Fokin, V. V.; Sharpless, K. B., A stepwise Huisgen cycloaddition process: copper (I)-catalyzed regioselective “ligation” of azides and terminal alkynes. *Angewandte Chemie* **2002**, *114* (14), 2708-2711.
2. Tornøe, C. W.; Christensen, C.; Meldal, M., Peptidotriazoles on solid phase: [1, 2, 3]-triazoles by regiospecific copper (I)-catalyzed 1, 3-dipolar cycloadditions of terminal alkynes to azides. *The Journal of organic chemistry* **2002**, *67* (9), 3057-3064.
3. Hong, V.; Udit, A. K.; Evans, R. A.; Finn, M., Electrochemically Protected Copper (I)-Catalyzed Azide-Alkyne Cycloaddition. *ChemBioChem* **2008**, *9* (9), 1481-1486.
4. Devaraj, N. K.; Dinolfo, P. H.; Chidsey, C. E.; Collman, J. P., Selective functionalization of independently addressed microelectrodes by electrochemical activation and deactivation of a coupling catalyst. *Journal of the American Chemical Society* **2006**, *128* (6), 1794-1795.
5. Ritter, S. C.; König, B., Signal amplification and transduction by photo-activated catalysis. *Chemical communications* **2006**, (45), 4694-4696.
6. Tasdelen, M. A.; Yagci, Y., Light-induced copper (I)-catalyzed click chemistry. *Tetrahedron Letters* **2010**, *51* (52), 6945-6947.
7. Guan, X.; Zhang, J.; Wang, Y., An efficient photocatalyst for the azide-alkyne click reaction based on direct photolysis of a copper (II)/carboxylate complex. *Chemistry Letters* **2014**, *43* (7), 1073-1074.
8. Harmand, L.; Cadet, S.; Kauffmann, B.; Scarpantonio, L.; Batat, P.; Jonusauskas, G.; McClenaghan, N. D.; Lastécouères, D.; Vincent, J. M., Copper catalyst activation driven by photoinduced electron transfer: a prototype photolabile click catalyst. *Angewandte Chemie International Edition* **2012**, *51* (29), 7137-7141.
9. Harmand, L.; Lambert, R.; Scarpantonio, L.; McClenaghan, N. D.; Lastécouères, D.; Vincent, J. M., A Photoreducible Copper (II)-Tren Complex of Practical Value: Generation of a Highly Reactive Click Catalyst. *Chemistry—A European Journal* **2013**, *19* (48), 16231-16239.
10. Beniazza, R.; Lambert, R.; Harmand, L.; Molton, F.; Duboc, C.; Denisov, S.; Jonusauskas, G.; McClenaghan, N. D.; Lastécouères, D.; Vincent, J. M., Sunlight-Driven Copper-Catalyst Activation Applied to Photolabile Click Chemistry. *Chemistry—A European Journal* **2014**, *20* (41), 13181-13187.
11. Beniazza, R.; Bayo, N.; Molton, F.; Duboc, C.; Massip, S.; McClenaghan, N.; Lastécouères, D.; Vincent, J.-M., Effective ascorbate-free and photolabile click reactions in water using a photoreducible copper (II)-ethylenediamine precatalyst. *Beilstein journal of organic chemistry* **2015**, *11* (1), 1950-1959.
12. Dadashi-Silab, S.; Yagci, Y., Copper (II) thioxanthone carboxylate as a photoswitchable photocatalyst for photoinduced click chemistry. *Tetrahedron letters* **2015**, *56* (46), 6440-6443.
13. Kumar, G. S.; Lin, Q., Light-triggered click chemistry. *Chemical Reviews* **2020**, *121* (12), 6991-7031.
14. Agard, N. J.; Prescher, J. A.; Bertozzi, C. R., A strain-promoted [3+ 2] azide-alkyne cycloaddition for covalent modification of biomolecules in living systems. *Journal of the American Chemical Society* **2004**, *126* (46), 15046-15047.

15. Jewett, J. C.; Bertozzi, C. R., Cu-free click cycloaddition reactions in chemical biology. *Chemical Society Reviews* **2010**, 39 (4), 1272-1279.
16. Dommerholt, J.; Rutjes, F. P.; Delft, F. L. v., Strain-promoted 1, 3-dipolar cycloaddition of cycloalkynes and organic azides. *Cycloadditions in Bioorthogonal Chemistry* **2016**, 57-76.
17. Pigge, F. C., Strain-Promoted Cycloadditions for Development of Copper-Free Click Reactions. *Current Organic Chemistry* **2016**, 20 (18), 1902-1922.
18. Poloukhine, A. A.; Mbua, N. E.; Wolfert, M. A.; Boons, G.-J.; Popik, V. V., Selective labeling of living cells by a photo-triggered click reaction. *Journal of the American Chemical Society* **2009**, 131 (43), 15769-15776.
19. McNitt, C. D.; Popik, V. V., Photochemical generation of oxa-dibenzocyclooctyne (ODIBO) for metal-free click ligations. *Organic & biomolecular chemistry* **2012**, 10 (41), 8200-8202.
20. Kuzmin, A.; Poloukhine, A.; Wolfert, M. A.; Popik, V. V., Surface functionalization using catalyst-free azide–alkyne cycloaddition. *Bioconjugate chemistry* **2010**, 21 (11), 2076-2085.
21. Orski, S. V.; Poloukhine, A. A.; Arumugam, S.; Mao, L.; Popik, V. V.; Locklin, J., High density orthogonal surface immobilization via photoactivated copper-free click chemistry. *Journal of the American Chemical Society* **2010**, 132 (32), 11024-11026.
22. Kim, Y.; Laradji, A. M.; Sharma, S.; Zhang, W.; Yadavalli, N. S.; Xie, J.; Popik, V.; Minko, S., Refining of Particulates at Stimuli-Responsive Interfaces: Label-Free Sorting and Isolation. *Angewandte Chemie* **2022**, 134 (7), e202110990.
23. Laradji, A. M.; McNitt, C. D.; Yadavalli, N. S.; Popik, V. V.; Minko, S., Robust, solvent-free, catalyst-free click chemistry for the generation of highly stable densely grafted poly (ethylene glycol) polymer brushes by the grafting to method and their properties. *Macromolecules* **2016**, 49 (20), 7625-7631.
24. Bjerknes, M.; Cheng, H.; McNitt, C. D.; Popik, V. V., Facile quenching and spatial patterning of cyclooctynes via strain-promoted alkyne–azide cycloaddition of inorganic azides. *Bioconjugate chemistry* **2017**, 28 (5), 1560-1565.
25. Luo, W.; Gobbo, P.; McNitt, C. D.; Sutton, D. A.; Popik, V. V.; Workentin, M. S., “Shine & Click” Photo-Induced Interfacial Unmasking of Strained Alkynes on Small Water-Soluble Gold Nanoparticles. *Chemistry—A European Journal* **2017**, 23 (5), 1052-1059.
26. Sun, L.; Gai, Y.; McNitt, C. D.; Sun, J.; Zhang, X.; Xing, W.; Li, Z.; Popik, V. V.; Zeng, D., Photo-Click-Facilitated Screening Platform for the Development of Hetero-Bivalent Agents with High Potency. *The Journal of organic chemistry* **2020**, 85 (9), 5771-5777.
27. Kii, I.; Shiraishi, A.; Hiramatsu, T.; Matsushita, T.; Uekusa, H.; Yoshida, S.; Yamamoto, M.; Kudo, A.; Hagiwara, M.; Hosoya, T., Strain-promoted double-click reaction for chemical modification of azido-biomolecules. *Organic & Biomolecular Chemistry* **2010**, 8 (18), 4051-4055.
28. Sutton, D. A.; Yu, S.-H.; Steet, R.; Popik, V. V., Cyclopropanone-caged Sondheimer diyne (dibenzo [a, e] cyclooctadiyne): a photoactivatable linchpin for efficient SPAAC crosslinking. *Chemical communications* **2016**, 52 (3), 553-556.
29. Sutton, D. A.; Popik, V. V., Sequential Photochemistry of Dibenzo [a, e] dicyclopropa [c, g][8] annulene-1, 6-dione: Selective Formation of Didehydrodibenzo [a, e][8] annulenes with Ultrafast SPAAC Reactivity. *The Journal of organic chemistry* **2016**, 81 (19), 8850-8857.
30. Lutz, J.-F.; Ouchi, M.; Liu, D. R.; Sawamoto, M., Sequence-controlled polymers. *Science* **2013**, 341 (6146), 1238149.

31. Merrifield, R. B., Solid phase peptide synthesis. I. The synthesis of a tetrapeptide. *Journal of the American Chemical Society* **1963**, 85 (14), 2149-2154.
32. Merrifield, R., Automated peptide synthesis. In *Hypotensive Peptides*, Springer: 1966; pp 1-13.
33. Horvath, S. J.; Firca, J. R.; Hunkapiller, T.; Hunkapiller, M. W.; Hood, L., [16] An automated DNA synthesizer employing deoxynucleoside 3'-phosphoramidites. In *Methods in enzymology*, Elsevier: 1987; Vol. 154, pp 314-326.
34. Mozziconacci, O.; Schöneich, C., Chemical degradation of proteins in the solid state with a focus on photochemical reactions. *Advanced drug delivery reviews* **2015**, 93, 2-13.
35. Vandenbergh, J.; Reekmans, G.; Adriaenssens, P.; Junkers, T., Synthesis of sequence-defined acrylate oligomers via photo-induced copper-mediated radical monomer insertions. *Chemical science* **2015**, 6 (10), 5753-5761.
36. Solleder, S. C.; Wetzel, K. S.; Meier, M. A., Dual side chain control in the synthesis of novel sequence-defined oligomers through the Ugi four-component reaction. *Polymer Chemistry* **2015**, 6 (17), 3201-3204.
37. Solleder, S. C.; Zengel, D.; Wetzel, K. S.; Meier, M. A., A Scalable and High-Yield Strategy for the Synthesis of Sequence-Defined Macromolecules. *Angewandte Chemie International Edition* **2016**, 55 (3), 1204-1207.
38. Solleder, S. C.; Martens, S.; Espeel, P.; Du Prez, F.; Meier, M. A., Combining two methods of sequence definition in a convergent approach: scalable synthesis of highly defined and multifunctionalized macromolecules. *Chemistry—A European Journal* **2017**, 23 (56), 13906-13909.
39. Kanasty, R. L.; Vegas, A. J.; Ceo, L. M.; Maier, M.; Charisse, K.; Nair, J. K.; Langer, R.; Anderson, D. G., Sequence-defined oligomers from hydroxyproline building blocks for parallel synthesis applications. *Angewandte Chemie International Edition* **2016**, 55 (33), 9529-9533.
40. Espeel, P.; Carrette, L. L.; Bury, K.; Capenberghs, S.; Martins, J. C.; Du Prez, F. E.; Madder, A., Multifunctionalized sequence-defined oligomers from a single building block. *Angewandte Chemie International Edition* **2013**, 52 (50), 13261-13264.
41. Martens, S.; Van den Begin, J.; Madder, A.; Du Prez, F. E.; Espeel, P., Automated synthesis of monodisperse oligomers, featuring sequence control and tailored functionalization. *Journal of the American Chemical Society* **2016**, 138 (43), 14182-14185.
42. Trinh, T. T.; Oswald, L.; Chan-Seng, D.; Lutz, J. F., Synthesis of molecularly encoded oligomers using a chemoselective “AB+ CD” iterative approach. *Macromolecular rapid communications* **2014**, 35 (2), 141-145.
43. Chan-Seng, D.; Lutz, J.-F. o., Primary Structure Control of Oligomers Based on Natural and Synthetic Building Blocks. *ACS Macro Letters* **2014**, 3 (3), 291-294.
44. Ding, S.; Jia, G.; Sun, J., Iridium-Catalyzed Intermolecular Azide–Alkyne Cycloaddition of Internal Thioalkynes under Mild Conditions. *Angewandte Chemie* **2014**, 126 (7), 1908-1911.
45. Zhang, X.; Gou, F.; Wang, X.; Wang, Y.; Ding, S., Easily Functionalized and Readable Sequence-Defined Polytriazoles. *ACS Macro Letters* **2021**, 10 (5), 551-557.
46. Wang, X.; Zhang, X.; Wang, Y.; Ding, S., IrAAC-based construction of dual sequence-defined polytriazoles. *Polymer Chemistry* **2021**, 12 (26), 3825-3831.
47. Marsault, E.; Peterson, M. L., Macrocycles are great cycles: applications, opportunities, and challenges of synthetic macrocycles in drug discovery. *Journal of medicinal chemistry* **2011**, 54 (7), 1961-2004.

48. Mole, T. K.; Arter, W. E.; Marques, I.; Félix, V.; Beer, P. D., Neutral bimetallic rhenium (I)-containing halogen and hydrogen bonding acyclic receptors for anion recognition. *Journal of Organometallic Chemistry* **2015**, 792, 206-210.
49. Lim, J. Y.; Marques, I.; Thompson, A. L.; Christensen, K. E.; Felix, V.; Beer, P. D., Chalcogen bonding macrocycles and [2] rotaxanes for anion recognition. *Journal of the American Chemical Society* **2017**, 139 (8), 3122-3133.
50. He, Q.; Vargas-Zúñiga, G. I.; Kim, S. H.; Kim, S. K.; Sessler, J. L., Macrocycles as ion pair receptors. *Chemical reviews* **2019**, 119 (17), 9753-9835.
51. Barendt, T. A.; Ferreira, L.; Marques, I.; Felix, V.; Beer, P. D., Anion-and solvent-induced rotary dynamics and sensing in a perylene diimide [3] catenane. *Journal of the American Chemical Society* **2017**, 139 (26), 9026-9037.
52. Mullen, K. M.; Mercurio, J.; Serpell, C. J.; Beer, P. D., Exploiting the 1, 2, 3-triazolium motif in anion-templated formation of a bromide-selective rotaxane host assembly. *Angewandte Chemie International Edition* **2009**, 48 (26), 4781-4784.
53. Spence, G. T.; Pitak, M. B.; Beer, P. D., Anion-induced shuttling of a naphthalimide triazolium rotaxane. *Chemistry—A European Journal* **2012**, 18 (23), 7100-7108.
54. Pasini, D., The click reaction as an efficient tool for the construction of macrocyclic structures. *Molecules* **2013**, 18 (8), 9512-9530.
55. Binauld, S.; Hawker, C. J.; Fleury, E.; Drockenmuller, E., A modular approach to functionalized and expanded crown ether based macrocycles using click chemistry. *Angewandte Chemie International Edition* **2009**, 48 (36), 6654-6658.
56. Peng, R.; Xu, Y.; Cao, Q., Recent advances in click-derived macrocycles for ions recognition. *Chinese Chemical Letters* **2018**, 29 (10), 1465-1474.
57. Li, Y.; Flood, A. H., Pure C \square H Hydrogen Bonding to Chloride Ions: A Preorganized and Rigid Macrocyclic Receptor. *Angewandte Chemie International Edition* **2008**, 47 (14), 2649-2652.
58. Megiatto Jr, J. D.; Schuster, D. I., Introduction of useful peripheral functional groups on [2] catenanes by combining Cu (I) template synthesis with “click” chemistry. *New Journal of Chemistry* **2010**, 34 (2), 276-286.
59. Barran, P. E.; Cole, H. L.; Goldup, S. M.; Leigh, D. A.; McGonigal, P. R.; Symes, M. D.; Wu, J.; Zengerle, M., Active-Metal Template Synthesis of a Molecular Trefoil Knot. *Angewandte Chemie* **2011**, 123 (51), 12488-12492.
60. Xiang, L.; Li, Z.; Chen, J.; Zhang, M.; Wu, Y.; Zhang, K., Periodic polymers based on a self-accelerating click reaction. *Polymer Chemistry* **2018**, 9 (29), 4036-4043.
61. Chen, J.-Q.; Xiang, L.; Liu, X.; Liu, X.; Zhang, K., Self-accelerating click reaction in step polymerization. *Macromolecules* **2017**, 50 (15), 5790-5797.
62. Meichsner, E.; Fong, D.; Ritaine, D. E.; Adronov, A., Strain-promoted azide-alkyne cycloaddition polymerization as a route toward tailored functional polymers. *Journal of Polymer Science* **2021**, 59 (1), 29-33.
63. Arnold, R. M.; McNitt, C. D.; Popik, V. V.; Locklin, J., Direct grafting of poly (pentafluorophenyl acrylate) onto oxides: versatile substrates for reactive microcapillary printing and self-sorting modification. *Chemical Communications* **2014**, 50 (40), 5307-5309.